NASA Tech Briefs

National Aeronautics and
Space Administration

February 1988
Volume 12 Number 2

NASA Technology Helps Win Run In The Sun

Thomson Saginaw Ball Screw Actuators:

NASA Tech Briefs
National Aeronautics and
Space Administration

FEBRUARY 1988
Volume 12 Number 2

ABP BPA

SPECIAL FEATURE

TECHNICAL SECTION

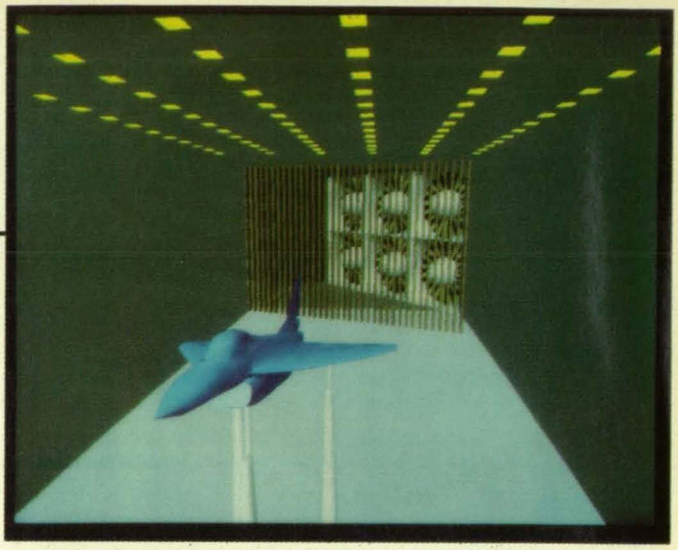

Each object in this computer-generated image was analyzed by NASA Ames Research Center aerodynamicists using the VSAERO (Vortex/Surface Aerodynamics) computer program. The design of the blue E-7 STOVL (short takeoff vertical landing) fighter model was based on VSAERO potential flow calculations. The white struts supporting the model were analyzed with the flow code to determine potential aerodynamic interference effects on the E-7. The vertical bars in front of the drive fans represent a set of flow turning vanes that were tested with the code. VSAERO also helped estimate the aerodynamic loads on the white nose cones and intake cowlings of the drive fans. *(Graphics courtesy Mark Bennett of Sterling Software, Federal Systems Div.)*

DEPARTMENTS

ON THE COVER—The Sunraycer experimental solar-powered automobile. There was a sense of deja vu down under when Sunraycer captured first place in the 1987 World Solar Challenge, for it marked the second time within a year that NASA technology had helped the United States win an international racing crown in Australia. For more on this Mission Accomplished story, turn to page 8. *(Photo courtesy Martyn Cowley of AeroVironment, Inc.)*

NASA Tech Briefs, ISSN 0145-319X, USPS 750-070, copyright © 1988 in U.S., is published monthly except July/August and November/December (10x per year) by Associated Business Publications Co., 41 E. 42nd St., New York, NY 10017-5391. The copyrighted information does not include the individual Tech Briefs which are supplied by NASA. Editorial, sales, production and circulation offices at 41 E. 42nd Street, New York, NY 10017-5391. Subscriptions for non-qualified subscribers in the U.S., Panama Canal Zone, and Puerto Rico, $75.00 for 1 year; $125.00 for 2 years; $200 for 3 years. Single copies $15.00. Remit by check, draft, postal or express orders. Other remittances at sender's risk. Address all communications for subscriptions or circulation to NASA Tech Briefs, 41 E. 42nd Street, New York, NY 10017-5391. Second-class postage paid at New York, NY and additional mailing offices.

POSTMASTER: please send address changes to NASA Tech Briefs, 41 E. 42nd Street, Suite 921, New York, NY 10017-5391.

NASA Tech Briefs

National Aeronautics and Space Administration

ABP BPA

NASA Tech Briefs:

Published by .... **Associated Business Publications**
Editor-in-Chief .... **Bill Schnirring**
Publisher .... **Thomas H. King**
Associate Publisher .... **Frank Nothaft**
Associate Publisher .... **Robin J. DuCharme**
Managing Editor .... **R. J. Laer**
Associate Editor .... **Leo D. Kluger**
Associate Editor .... **Joseph T. Pramberger**
Technical Advisor .... **Dr. Robert E. Waterman**
Production Manager .... **Rita Nothaft**
Traffic Manager .... **James E. Cobb**
Circulation Director .... **Anita Weissman**
Controller .... **Neil B. Rose**
Awards Manager .... **Evelyn Mars**
Reader Service Manager .... **Arlene Berrios**

Technical Staff:
Briefs prepared for National Aeronautics and Space Administration by **Logical Technical Services Corp.**, NY, NY
Technical/Managing Editor .... **Ted Selinsky**
Art Director .... **Ernest Gillespie**
Administrator .... **Elizabeth Texeira**
Chief Copy Editor .... **Lorne Bullen**
Staff Editors .... **Dr. James Boyd, Dr. Larry Grunberger, Jordan Randjelovich, George Watson, Oden Browne, Joseph Renzler, Dr. Theron Cole, Jr.**
Graphics .... **Luis Martinez, Vernald Gillman, Charles Sammartano**
Editorial & Production .... **Bill Little, Frank Ponce, Ivonne Valdes, Paul Marcus**

NASA:
NASA Tech Briefs are provided by the National Aeronautics and Space Administration, Technology Utilization Division, Washington, DC:
Administrator .... **Dr. James C. Fletcher**
Assistant Administrator for Commercial Programs .... **James T. Rose**
Deputy Assistant Administrator (Programs) .... **Henry J. Clarks**
Deputy Director TU Division (Publications Manager) .. **Leonard A. Ault**
Manager, Technology Utilization Office, NASA Scientific and Technology Information Facility .... **Walter M. Heiland**

Associated Business Publications
41 East 42nd Street, Suite 921, New York, NY 10017-5391
(212) 490-3999
President .... **Bill Schnirring**
Executive Vice President .... **Frank Nothaft**
Vice President Marketing .... **Mark J. Seitman**

Advertising:
New York Office: (212) 490-3999
Sales Manager .... **Robin DuCharme**
Account Executive (Mid-Atlantic) .... **Dick Soule**
Account Executive (Midwest) .... **Michelle Larsen**
Advertising Coordination Manager .... **Erving Dockery, Jr.**
Account Executives (Eastern MA, NH, ME, RI) .... **Lee Arpin** at (617) 899-5613; **Bill Doucette** at (617) 278-7792
Account Executive (Western MA, CT, VT) .... **George Watts** at (413) 596-4747
Account Executives (No. Calif., UT) ....
for Area Code 415—**Janice Richey King** and for Area Code 408—**Richard Cassidy** at (415) 656-3613
Account Executives (So. Calif., AZ, NV, NM) ....
for Area Codes 818/213/805—**Thomas Stillman** or **Dana Gindoff** and for Area Codes 619/714—**Leslie Alley** at (213) 541-4699

NTBM-Research Center
Project Director .... **Mark J. Seitman**
Account Supervisor .... **Lourdes Del Valle**

NEW CAPABILITIES

CAPTURE IT

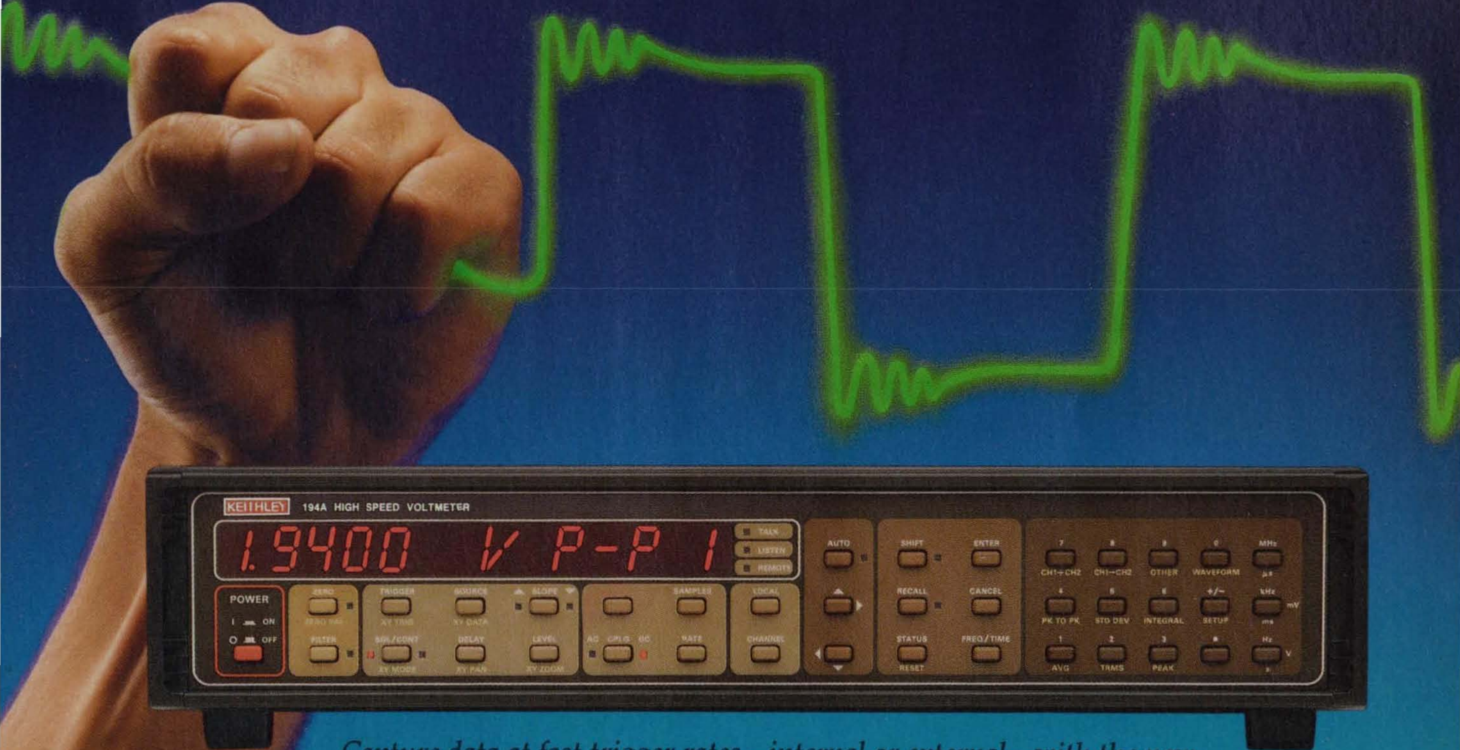

Capture data at fast trigger rates—internal or external—with the new Model 194A High Resolution Digitizer. Here are the advantages:

Faster, More Thorough Testing.

NOW—With the Model 194A High Speed Digitizer, you can acquire samples with external trigger pulses. Capture discrete samples synchronized to changes in position, distance, angle, log (time), a stimulus level, or other events. With trigger rates up to 1MHz, you can take more data in less time. That means more complete testing at lower cost.

Resolution of 16 bits. At rates up to 100kHz.

The Model 194A's 16-bit (4½-digit) resolution lets you detect 1 part in 32,000—far better than most digitizing devices. For higher frequency waveforms—up to 1MHz—the 194A samples with 8-bit resolution. And its 64k bytes of memory is up to 8 times that of other digitizers.

Add the 1944A Channel 2 option and acquire two different waveforms simultaneously, in time sync, or asynchronously. Each channel is independent, isolated, fully programmable, and has 64k bytes of memory.

The 194A provides 5 trigger options for initiating a measurement. Pre- and post-trigger data can be stored.

Analyze and Automate

The 194A directly displays key waveform parameters such as integration, RMS, average, and peak-peak. With two channels installed you can compute ratio or difference between channels.

All functions are IEEE-488 bus programmable. And our exclusive, built-in TRANSLATOR software reduces bus transfer time and simplifies documentation.

At **$4095**, you won't find better performance. And the optional second channel for just **$1995** doubles acquisition capability. For complete details contact the **Product Information Center, Keithley Instruments, Inc., 28775 Aurora Road, Cleveland, Ohio 44139, (216) 248-0400.**

KEITHLEY

Circle Reader Action No. 536

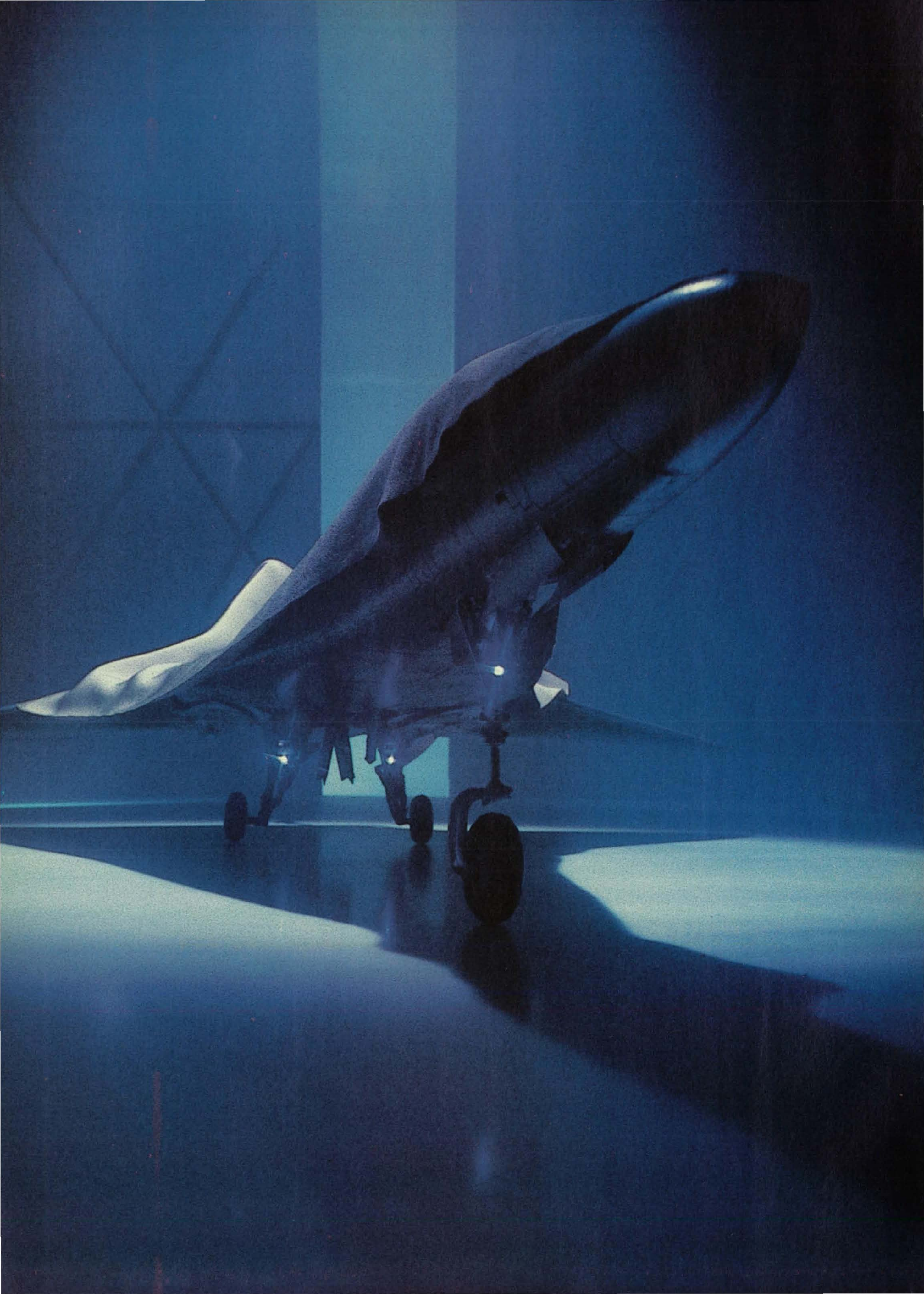

The future raced into the city of Adelaide, Australia on November 6, 1987, as a bug-shaped vehicle called the *Sunraycer* crossed the finish line of the World Solar Challenge, a first-ever transcontinental race of solar-powered automobiles.

The General Motors-built *Sunraycer* finished more than two days and 600 miles in front of the nearest challenger, averaging 41.6 miles per hour over the 1,950 mile course and setting a new world speed record for a land vehicle powered solely by sunlight.

Sunraycer's victory marked the second time within a year that NASA technology had helped the United States win an international racing championship in Australia. Last February, *Stars & Stripes* captured sailing's premier prize, the America's Cup, aided by NASA-spawned hull and keel innovations that allowed the 12-meter yacht to glide through the waters of Perth more smoothly.*

Nine months later, NASA enlightening struck again. *Sunraycer's* success depended on its aerodynamically contoured body, created by G.M. Hughes Electronics and AeroVironment Inc., of Monrovia, California. To streamline the shape, designers employed a NASA computer program called VSAERO (Vortex/Surface Aerodynamics). Originally developed for aircraft wing analysis, VSAERO calculates the aerodynamic characteristics of three-dimensional objects. The FORTRAN 77 program was written by Brian Maskew of Analytical Methods Inc., Redmond, WA, under a NASA Ames Research Center contract.

How It Works

Using VSAERO, the body surface is approximated by a finite number of surface elements, or panels. Applying a body-surface boundary condition to each panel produces a set of simultaneous linear equations. The program assembles and solves these equations, then uses the resulting singularity strengths to calculate flow quantities such as velocities and pressures.

"Since VSAERO uses integral methods for both the potential and viscous flows, calculations are relatively fast compared with differential equation methods," said Dr. Michael Summa, Senior Research Scientist for Analytical Methods. As a result, he said, "the code is extremely useful for designing complex automobile shapes like *Sunraycer's*."

Dr. John Letcher, consultant to AeroVironment on the *Sunraycer* project added, "VSAERO is an effective design tool because its geometry routines are very flexible, offering nearly complete freedom in topology and shape of the desired configurations."

By applying VSAERO calculations, designers eliminated *Sunraycer's* induced drag, enabling the car to slip smoothly through turbulent winds. Explained AeroVironment's Dr. Bart Hibbs: "We ran the flow code for ten systematically varied configurations, assessing and completely cancelling the vortex wake strength." The final design "cut through the air without a trace of wake," said AeroVironment President Dr. Paul MacCready.

In a G.M. wind tunnel test, *Sunraycer* recorded a 0.13 drag coefficient, the lowest ever registered for a land vehicle, according to G.M. spokesman Bruce McCristal.

Fighting The Wind

VSAERO also provided solutions to the design dilemma of protecting *Sunraycer's* 360 pound aluminum and honeycomb body against violent gusts caused by passing tractor-trailer trucks. Designers needed to minimize the vehicle's lift to keep *Sunraycer* from being blown off the road. Using the NASA flow code, they adjusted the camber and produced a car with neutral lift.

"The final product showed excellent crosswind stability," said Dr. Alec Brooks, Project Manager for AeroVironment. After the race, *Sunraycer* lead driver John Harvey commented: "Facing those heavy crosswinds, I'd rather be in *Sunraycer* than a standard automobile."

From Sea To Shore

Ironically, the application of flow analysis to racing design began with *Australia II*, the yacht that won the 1983 America's Cup. The Australians utilized a flow code developed by Dutch aerodynamicist Dr. Joop Sloof in designing the revolutionary winged keel which gave the vessel a major advantage over the competition.

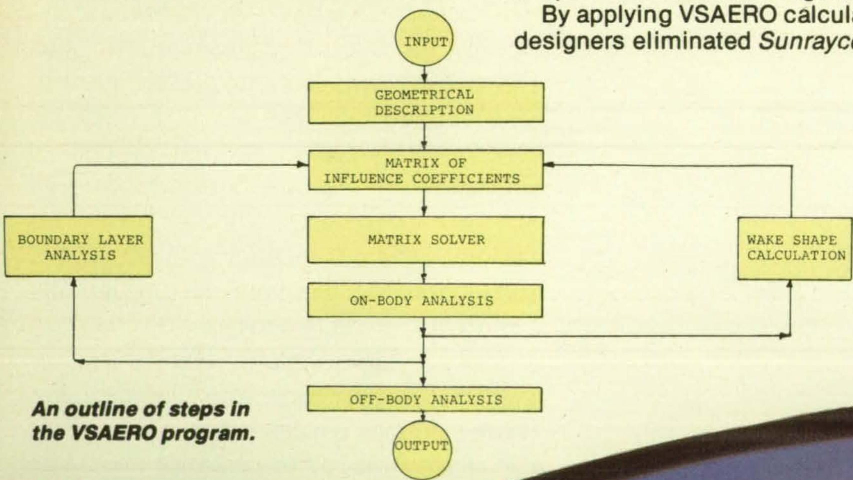

An outline of steps in the VSAERO program.

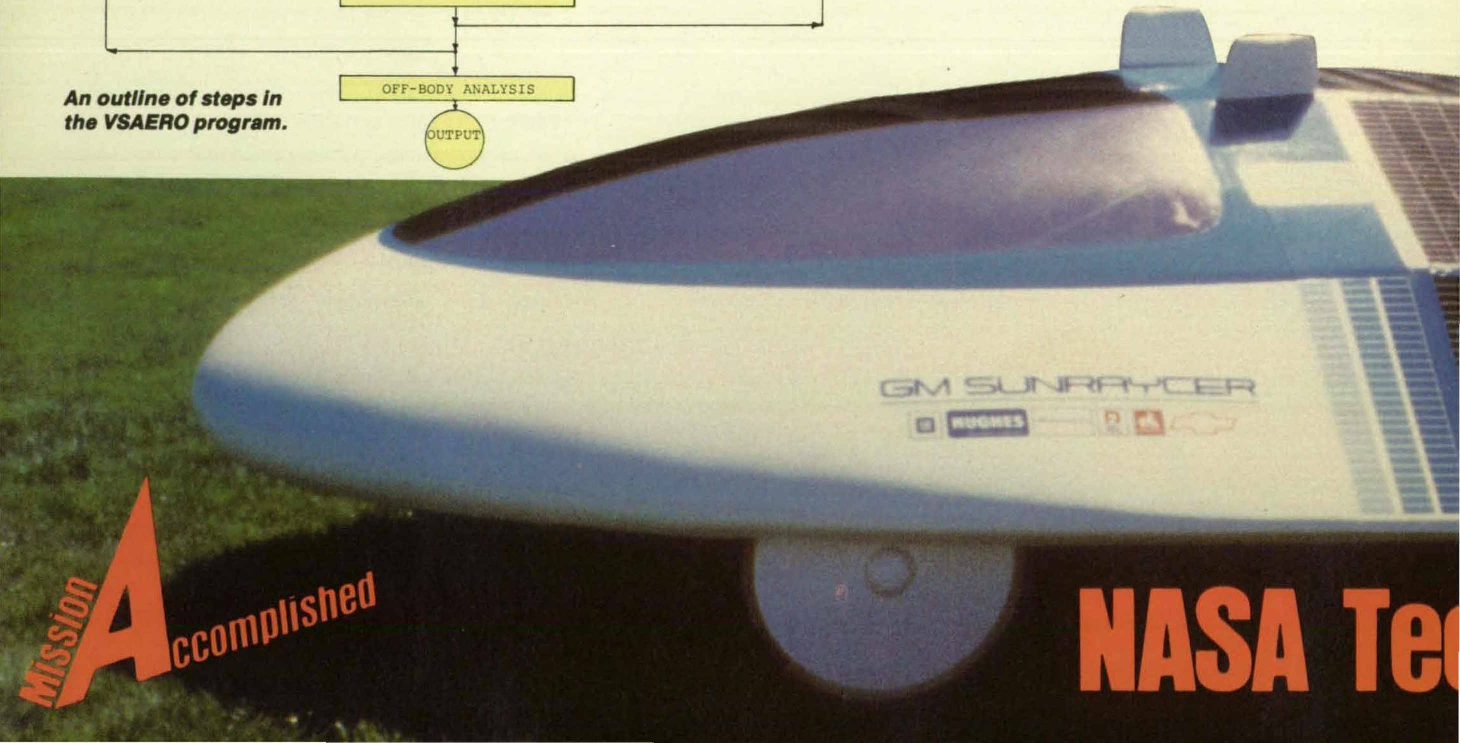

From Aerospace To Auto Race

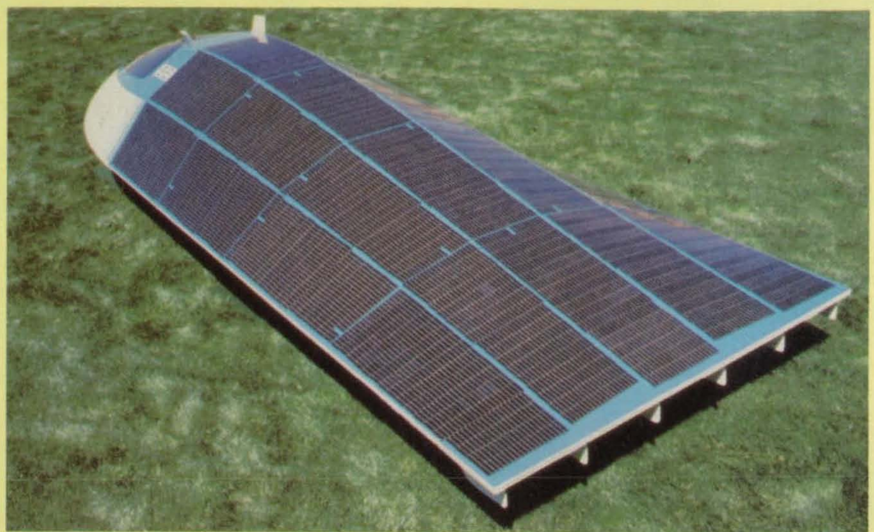

Sunraycer derives its power from 7,200 photovoltaic cells mounted in a graphite-composite frame conforming to the car's tail. The solar array consists of 80 percent gallium arsenide cells, provided by Mitsubishi and the Applied Solar Energy Corp. (ASEC), and 20 percent Spectrolab K-7 silicon cells. The cells convert 16.5 percent of the solar energy they absorb into usable electricity, and on a sunny day can produce one kilowatt of power at 150 volts—the amount consumed by a typical hair dryer.

A highly efficient electric drive motor helps *Sunraycer* make the most of its limited power supply. The car cruises at up to 45 miles per hour on solar power alone, and reaches 60 miles per hour supplemented by its rechargable silver-zinc batteries.

The solar technology developed for *Sunraycer* may one day power extraterrestrial vehicles, according to Dr. Henry Brandhorst, Chief of the Power Technology Division at NASA's Lewis Research Center. "The advanced solar cells on *Sunraycer* would be fully applicable to a Mars rover," he said. Such an application would bring the technology full circle, for the solar cell originated from space research.

NASA's Langley Reseach Center sponsored development of the first high-efficiency gallium arsenide cell, created under contract by IBM Laboratories in 1973. NASA also pioneered the aerospace application of silicon cells. Initially developed for 1950's satellites, silicon cells have provided on-board power for the majority of NASA spacecraft, and will be the primary power source for Space Station.

In some early spacecraft, solar arrays cost up to $1000 per watt. Years of research by NASA's Jet Propulsion Laboratory and Lewis Research Center, in cooperation with the Department of Energy, have reduced the price to less than $100 per watt, acceptable in space use because there is little choice, but still too expensive for widespread Earth applications. Solar arrays are presently used where no conventional power source exists, such as remote automated weather stations, sea-based navigational buoys, forest stations, and third world villages. □

"*Australia II's* domination proved that computer aided design could make a significant difference," said Dr. Letcher, who was also Senior Scientist for the team designing *Stars & Stripes*. "Probably every challenger for the 1987 America's Cup series used some form of potential flow code."

While exploring keel and hull configurations for *Stars & Stripes*, the Sail America syndicate obtained a copy of VSAERO from the Ames Center. Designers used the code to calculate the lift and drag for various keel and winglet combinations, identifying promising shapes that were then tested with models. For lift and moment calculations, said Letcher, "the program gave excellent, accurate results."

Coming Attractions

VSAERO will soon be available from COSMIC, NASA's Computer Software Management and Information Center in Athens, GA. While the NASA program contains a 1000 panel upper limit, an offshoot version with a 3000 panel ceiling is currently distributed by Analytical Methods. The expanded version aided in design of the new 40-by-80-by-120 foot wind tunnels of the National Full-Scale Aerodynamics Complex at NASA Ames. VSAERO provided aerodynamic analysis on items ranging from the contraction section of the in-draft inlet, to the turning vanes, to the acoustic linings of the test sections.

The code has also been used to design a number of new car models, including the *Mazda RX-7*, the *Isuzu Spectrum*, and the *Porche 956*. General Motors is applying VSAERO extensively in developing their 1993 passenger car line.

Though a commercially produced solar-powered car is still a long way off, the aerodynamics technology incorporated into *Sunraycer* will provide near-term benefits, according to Mr. McCristal. "We learned a lot about low-speed aerodynamics," he said, "and that knowledge will help us build better cars down the road." □

*See NASA Tech Briefs' March, 1987 issue, page 82.

nology's Day In The Sun

New Product Ideas

New Product Ideas are just a few of the many innovations described in this issue of *NASA Tech Briefs* and having promising commercial applications. Each is discussed further on the referenced page in the appropriate section in this issue. If you are interested in developing a product from these or other NASA innovations, you can receive further technical information by requesting the TSP referenced at the end of the full-length article or by writing the Technology Utilization Office of the sponsoring NASA center (see page 12). NASA's patent-licensing program to encourage commercial development is described on page 12.

High-Resolution Detector for X-Ray Diffraction

A proposed x-ray-sensitive imaging detector would offer superior spatial resolution, counting-rate capacity, and dynamic range. The new area detector would be used primarily for studying single-crystal proteins before the crystals deteriorate. The principle can be adapted to imaging detectors for electron microscopy and fluorescence spectroscopy and for general use in astronomy, engineering, and medicine. (See page 46).

Composite Cathode-Ray Tube

A proposed composite cathode-ray tube would consist of a rectangular array of cathode-ray tubes joined at the edges, sharing a common vacuum. The composite tube with its superior display would be useful for classroom presentations, conferences, and the like. For example, large detailed maps could be presented, and images from remote sensing equipment would have higher resolution. (See page 14).

Emergency-Evacuation Cart

A self-propelled cart would enable rescuers to evacuate victims from toxic, flammable, and other hazardous environments. Pressurized hydraulic fluid that would drive the cart does not require shielding in flammable or explosive surroundings. (See page 76).

Wicks for Refrigerants in Heat Pipes

An open-cell polyethylene foam used in filters is a very effective wick material for heat pipes. The only currently-known material to be physically and chemically compatible with the most efficient refrigerants, this foam features flexibility to withstand vibration and a self-lubricating surface for easy machining and insertion into pipes. (See page 56).

Fire-Resistant Polyamides Containing Phosphorus

Fire-resistant polymers have been obtained from 1-[(dialkoxyphosphonyl)methyl]-2,4- and -2,6-diaminobenzenes by their reaction with acyl or diacyl halides of higher functionality. The incorporation of the groups containing the phosphorus increases the fire resistance of the product and adds a new class of polyamides to such polymers. (See page 56).

Fire-Resistant, Plastic-Foam Airducts

Inexpensive, lightweight polyimide-foam airducts suitable for air-conditioning and heating resist the spread of flames and generate little smoke. These ducts are less expensive to manufacture than conventional fiberglass-insulated aluminum ducts and are safer than polyisocyanurate-foam ducts. (See page 58).

Newport's Programmable Motion Control System:

An easy, powerful approach to automating *all* your micropositioners

- **Simultaneous control of up to four axes**
- **Hand-held keypad/display for manual or programmed control**
- **Easy-to-use built-in programming language**
- **Standard RS-232C and IEEE-488 ports**
  Easy interfacing and remote computer control
- **Wide range of micrometer-replacement actuators**
  Easily retrofit your existing Newport mounts and stages for automated 0.1 micron/0.001° resolution positioning control

Newport's Model 855 Programmable Motion Control System is part of our comprehensive line of precision motion products. See page E-12 of our catalog or call for more information.

714/965-5406

18235 Mt. Baldy Circle
Fountain Valley, CA 92708
Europe: Newport Gmbh Ph. 06151-26116
U.K.: Newport Ltd. Ph. 05827-69995

Newport Corporation

Circle Reader Action No. 540

HOW YOU CAN BENEFIT FROM NASA's TECHNOLOGY UTILIZATION SERVICES

If you're a regular reader of TECH BRIEFS, then you're already making use of one of the low- and no-cost services provided by NASA's Technology Utilization (TU) Network. But a TECH BRIEFS subscription represents only a fraction of the technical information and applications/engineering services offered by the TU Network as a whole. In fact, when all of the components of NASA's Technology Utilization Network are considered, TECH BRIEFS represents the proverbial tip of the iceberg.

We've outlined below NASA's TU Network—named the participants, described their services, and listed the individuals you can contact for more information relating to your specific needs. We encourage you to make use of the information, access, and applications services offered by NASA's Technology Utilization Network.

How You Can Utilize **NASA's Industrial Applications Centers—**A nationwide network offering a broad range of technical services, including computerized access to over 100 million documents worldwide.

You can contact NASA's network of Industrial Applications Centers (IACs) for assistance in solving a specific technical problem or meeting your information needs. The "user friendly" IACs are staffed by technology transfer experts who provide computerized information retrieval from one of the world's largest banks of technical data. Nearly 500 computerized data bases, ranging from NASA's own data base to Chemical Abstracts and INSPEC, are accessible through the nine IACs located throughout the nation. The IACs also offer technical consultation services and/or linkage with other experts in the field. You can obtain more information about these services by calling or writing the nearest IAC. User fees are charged for IAC information services.

Aerospace Research Applications Center (ARAC)
Indianapolis Center for Advanced Research
611 N. Capitol Avenue
Indianapolis, IN 46204
Dr. F. Timothy Janis, Director
(317) 262-5036

Central Industrial Applications Center/NASA (CIAC)
Southeastern Oklahoma State U.
Station A, Box 2584
Durant, OK 74701
Dickie Deel, Acting Director
(405) 924-6822

North Carolina Science and Technology Research Center (NC/STRC)
Post Office Box 12235
Research Triangle Park, NC 27709
J. Graves Vann, Jr., Director
(919) 549-0671

NASA Industrial Applications Ctr. 823 William Pitt Union
University of Pittsburgh
Pittsburgh, PA 15260
Paul A. McWilliams, Exec Director
(412) 648-7000

NASA/Southern Technology Applications Center
P. O. Box 24
Progress Ctr., One Progress Blvd.
Alachua, FL 32615
J. Ronald Thornton, Director
(904) 462-3913
(800) 354-4832 (FL only)
(800) 225-0308 (toll-free US)

NASA/UK Technology Applications Center
University of Kentucky
109 Kinkead Hall
Lexington, KY 40506-0057
William R. Strong, Director
(606) 257-6322

NERAC, Inc.
One Technology Drive
Tolland, CT 06084
Daniel U. Wilde, President
(203) 872-7000

Technology Application Center (TAC)
University of New Mexico
Albuquerque, NM 87131
Stanley A. Morain, Director
(505) 277-3622

NASA Industrial Applications Center (WESRAC)
University of Southern California
Research Annex
3716 South Hope Street, Room 200
Los Angeles, CA 90007
Radford G. King, Acting Director
(213) 743-8988
(800) 642-2872 (CA only)
(800) 872-7477 (toll-free US)

NASA/SU Industrial Applications Center
Southern University Department of Computer Science
Baton Rouge, LA 70813
John Hubbell, Director
(504) 771-2060

If you represent a public sector organization with a particular need, you can contact NASA's Application Team for technology matching and problem solving assistance. Staffed by professional engineers from a variety of disciplines, the Application Team works with public sector organizations to identify and solve critical problems with existing NASA technology. **Technology Application Team, Research Triangle Institute, P.O. Box 12194, Research Triangle Park, NC 27709. *Doris Rouse, Director,* (919) 541-6980**

How You Can Access Technology Transfer Services At NASA Field Centers: **Technology Utilization Officers & Patent Counsels—**Each NASA Field Center has a Technology Utilization Officer (TUO) and a Patent Counsel to facilitate technology transfer between NASA and the private sector.

If you need further information about new technologies presented in *NASA Tech Briefs,* request the Technical Support Package (TSP). If a TSP is not available, you can contact the Technology Utilization Officer at the NASA Field Center that sponsored the research. He can arrange for assistance in applying the technology by putting you in touch with the people who developed it. If you want information about the patent status of a technology or are interested in licensing a NASA invention, contact the Patent Counsel at the NASA Field Center that sponsored the research. Refer to the NASA reference number at the end of the Tech Brief.

Ames Research Ctr.
Technology Utilization Officer: Laurance Milov
Mail Code 223-3
Moffett Field, CA 94035
(415) 694-6471
Patent Counsel: Darrell G. Brekke
Mail Code 200-11
Moffett Field, CA 94035
(415) 694-5104

Lewis Research Center
Technology Utilization Officer: Daniel G. Soltis
Mail Stop 7-3
21000 Brookpark Road
Cleveland, OH 44135
(216) 433-5567
Patent Counsel: Gene E. Shook
Mail Code 301-6
21000 Brookpark Road
Cleveland, OH 44135
(216) 433-5753

National Space Technology Laboratories
Technology Utilization Officer: Robert M. Barlow
Code GA-00
NSTL Station, MS 39529
(601) 688-1929

John F. Kennedy Space Center
Technology Utilization Officer: Thomas M. Hammond
Mail Stop PT-TPO-A
Kennedy Space Center, FL 32899
(305) 867-3017
Patent Counsel: James O. Harrell
Mail Code PT-PAT
Kennedy Space Center, FL 32899
(305) 867-2544

Langley Research Ctr.
Technology Utilization Officer: John Samos
Mail Stop 139A
Hampton, VA 23665
(804) 865-3281
Patent Counsel: George F. Helfrich
Mail Code 279
Hampton, VA 23665
(804) 865-3725

Goddard Space Flight Center
Technology Utilization Officer: Donald S. Friedman
Mail Code 702
Greenbelt, MD 20771
(301) 286-6242
Patent Counsel: R. Dennis Marchant
Mail Code 204
Greenbelt, MD 20771
(301) 286-7351

Jet Propulsion Lab.
NASA Resident Office
Technology Utilization Officer: Gordon S. Chapman
Mail Stop 180-801
4800 Oak Grove Drive
Pasadena, CA 91109
(818) 354-4849
Patent Counsel: Paul F. McCaul
Mail Code 180-801
4800 Oak Grove Drive
Pasadena, CA 91109
(818) 354-2734
Technology Utilization Mgr. for JPL: Norman L. Chalfin
Mail Stop 156-211
4800 Oak Grove Drive
Pasadena, CA 91109
(818) 354-2240

George C. Marshall Space Flight Center
Technology Utilization Officer: Ismail Akbay
Code AT01
Marshall Space Flight Center, AL 35812
(205) 544-2223
Patent Counsel: Leon D. Wofford, Jr.
Mail Code CC01
Marshall Space Flight Center, AL 35812
(205) 544-0024

Lyndon B. Johnson Space Center
Technology Utilization Officer: Dean C. Glenn
Mail Code EA4
Houston, TX 77058
(713) 483-3809
Patent Counsel: Edward K. Fein
Mail Code AL3
Houston, TX 77058
(713) 483-4871

NASA Headquarters
Technology Utilization Officer: Leonard A. Ault
Code IU
Washington, DC 20546
(202) 453-1920
Assistant General Counsel for Patent Matters: Robert F. Kempf, Code GP
Washington, DC 20546
(202) 453-2424

A Shortcut To Software: **COSMIC®—**For software developed with NASA funding, contact COSMIC, NASA's Computer Software Management and Information Center. New and updated programs are announced in the Computer Programs section. COSMIC publishes an annual software catalog. For more information call or write: **COSMIC®** 382 East Broad Street, Athens, GA 30602 *John A. Gibson, Dir.,* (404) 542-3265

If You Have a Question. . . **NASA Scientific & Technical Information Facility** can answer questions about NASA's Technology Utilization Network and its services and documents. The STI staff supplies documents and provides referrals. Call, write or use the feedback card in this issue to contact: **NASA Scientific and Technical Information Facility,** Technology Utilization Office, P.O. Box 8757, Baltimore, MD 21240-0757. *Walter M. Heiland, Manager,* (301) 859-5300, Ext. 242, 243

Data-Control Systems hands you a new PCM Decommutator with a unique remote display.

The DCS Model 5011 has given "state of the art" new meaning with this latest generation of microprocessor-controlled PCM Decommutators. Among its advances: a handheld terminal which is a remote word selector, enabling the operator to monitor information while moving around the test site.

Other advances: operational capability up to 10 MBPS NRZ, combined with storage of programmed formats and a six-line, 40-character-per-line plasma display. In addition, the 5011's four-mode synchronization method includes a VERIFY mode to confirm the correct pattern before entering the LOCK mode.

And, the DCS 5011 offers a decommutator, an integral bit synchronizer, a PCM simulator and a remote display in one powerful unit.

The new Model 5011 Bus structured PCM Decommutator. . .another innovative product by DCS, employing the latest in DSP, PLA and LCA technology. For information, contact us at one of the addresses below.

Quanta Systems Corporation
Data-Control Systems

1455 Research Boulevard
Rockville, MD 20850
(301) 279-8798
TWX (710) 828-9785

8295 Westminster Ave., Suite 150
Westminster, CA 92683
(714) 894-4471
TWX (910) 596-1802

CompuDyne Defense Electronics Group

Circle Reader Action No. 371

Electronic Components & Circuits

Composite Cathode-Ray Tube

The brightness and resolution of large images would be increased.

NASA's Jet Propulsion Laboratory, Pasadena, California

A proposed composite cathode-ray tube would consist of a rectangular array of cathode-ray tubes joined at the edges, sharing a common vacuum. Each electron gun would generate an independent image on its portion of the screen. The composite tube (see figure) would be operated most advantageously under digital control to make available several display modes; for example, different split-screen images of arbitrary size, one large image formed as a mosaic of the individual images, or each gun generating a separate, unrelated image in the conventional manner.

The number of picture elements available for one large composite image is the sum of elements contributed by all the component tubes. Consequently, the resolution can be greater than in a projection television picture obtained by conventional optical magnification of a standard image, which does not increase the number of picture elements.

The brightness of the composite display would be greater than that of a magnified image. This is because in the composite tube, each component tube would operate at normal brightness; whereas optical magnification spreads the light out, and the cathode-ray-tube current cannot be increased enough to compensate. Therefore, although a magnified display must be viewed in a darkroom, the composite display could be viewed in a well-lit room.

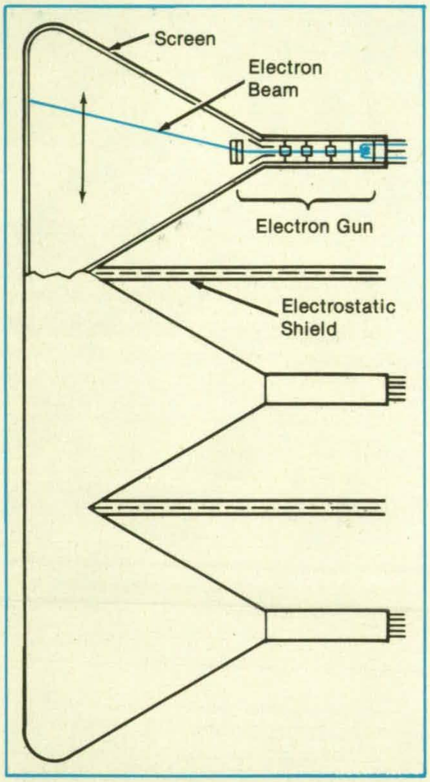

The **Composite Cathode-Ray Tube** would contain a rectangular array of electron guns aimed at a flat screen. A single large image or a split-screen display would be formed by the mosaic of the images generated by the electron guns.

When the full composite screen is used to display a conventional image, the resolution would not be increased because the input signal still contains only the conventional number of picture elements. The effect of magnified graininess could be alleviated, however, by dividing each input picture element into subelements and using digital image enhancement. The brightness of each picture element would be convolutionally processed with that of neighboring elements to produce subelements that smooth out brightness steps in regions of gradual transition. Edge-detection techniques would also be used so that sharp edges would not be smoothed out but instead confined to lines of single elements.

The composite tube would be useful for classroom presentations, conferences, and the like. For example, large, detailed maps could be presented to academic, governmental, or military audiences. Images from remote sensing equipment could be more detailed, with resolution increased by using multiple, parallel video transmission channels, one for each electron gun.

This work was done by Mukund D. Gangal of Caltech for **NASA's Jet Propulsion Laboratory**. *For further information, Circle 65 on the TSP Request Card. NPO-16549*

Addressable Inverter Matrix Tests Integrated-Circuit Wafer

Addressing elements indirectly through a shift register reduces the number of test probes.

NASA's Jet Propulsion Laboratory, Pasadena, California

With the aid of a new technique, a complex test structure on a silicon wafer can be tested with a relatively small number of test probes. The technique conserves silicon area by reduction of the area devoted to pads. At the same time, it allows thorough evaluation of test structure characteristics and of manufacturing process parameters.

This test structure consists of an inverter matrix (essentially a matrix of transistor switches and power conductors) and a shift register formed on the wafer by the same photolithography used to form the integrated circuits on the wafer. The shift register addresses each of the inverters in the matrix. The shift register, in turn, is controlled by signals from an external testing instrument.

Previously, only the inverter matrix was placed on the wafer. The elements of the matrix were addressed directly by the external instrument, and a relatively large number of pads were needed for the instrument probes. To test 100 inverters, for example, 20 pads were needed. With the addition of the shift register for addressing the

The New 4180 Plug-In

SPEED TRIALS.

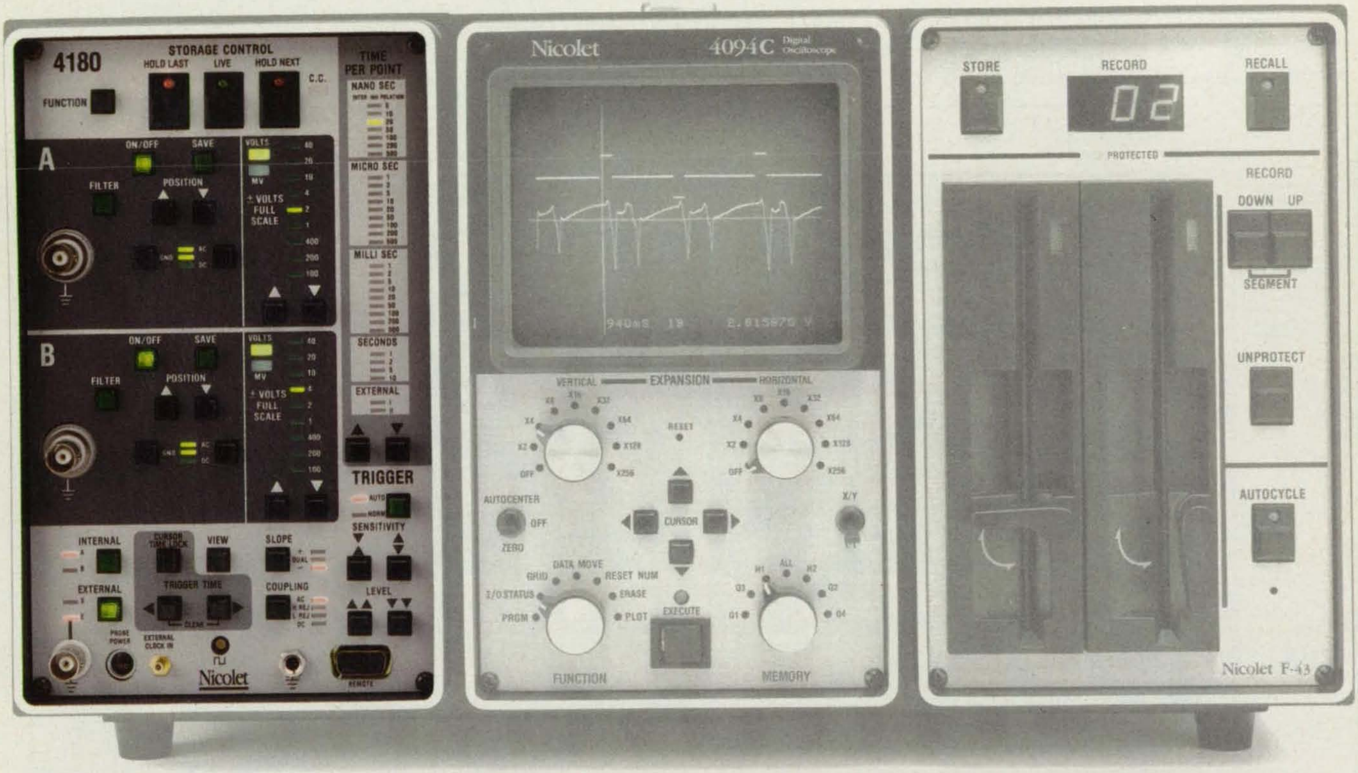

• Multi-channel: two or four channel configurations.

• Unmatched single-shot capabilities.

• High speed, 200 MHz digitizing.

• 100 MHz analog input bandwidth.

• Real-time math functions.

• For your Free Speed Trial call: 800-356-3090 or 608-273-5008

Nicolet Test Instruments Division
P.O. Box 4288
5225-2 Verona Road
Madison, WI 53711-0288

Nicolet Digital Oscilloscopes

Speed. Using the latest designs in ADC technology, your input signal can be digitized at speeds up to 200 MHz (5ns per data point) and saved for analysis. The wide band input amplifiers allow signals up to the 100 MHz Nyquist limit to be input without distortion. Sophisticated trigger setup displays allow you to accurately set the level, sensitivity, and slope to make one-shot transients easy to catch; eliminating the usual hit or miss guesswork. For multi-channel applications two 4180's can operate together in one mainframe producing a four channel scope with no degradation in speed or performance.

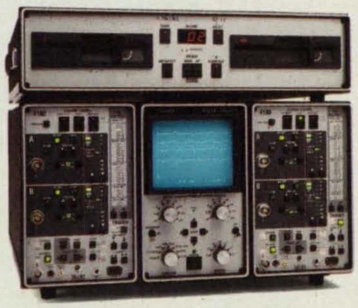

Real-Time Math. In addition to the extensive post-processing capabilities in the mainframe, the 4180 has several useful routines which present computed results as live, real-time displays: *FFT, MAX/MIN, A+B, A−B, A×B, A/B,* and *AVERAGING.*

Nicolet

INSTRUMENTS OF DISCOVERY

Circle Reader Action No. 350

inverter matrix, the number of testable circuits does not depend on the number of pads. In a demonstration wafer, for example, only 20 pads could accommodate 222 CMOS (complementary metal oxide/semiconductor) inverters.

The test structure consists of a shift register and a matrix of inverter/ transmission-gate cells connected to a two-by-ten array of probe pads (see figure). The entire pattern is contained in a square area having only 1.6-millimeter sides. The shift register is a conventional static CMOS device that uses inverters and transmission gates in a master/slave D flip-flop configuration.

A single probe pad connects to all the inverter inputs. The inverter outputs connect to row-addressable transmission gates, which connect to column buses that terminate at probe pads. The shift register applies proper biases to turn on the transmission gates row by row. Each inverter has the same low series resistance in its power line.

Of course, it is necessary to be sure that the shift register works properly before the test pattern can be evaluated reliably. Therefore three reference sites are placed in the matrix. At these sites, the inverters are absent, and the input to the transmission gate is connected to the structure input. When measurements are made at these sites, the output voltage is expected to equal the input voltage if the shift-register devices are good. In effect, the sites serve as markers that indicate that the shift register has advanced to rows 1, 8, and 15.

This work was done by Martin G. Buehler of Caltech for **NASA's Jet Propulsion Laboratory**. *For further information, Circle 64 on the TSP Request Card.*

Title to this invention has been waived under the provisions of the National Aeronautics and Space Act [42 U.S.C 2457(f)], to Caltech. Inquiries concerning licenses for its commercial development should be addressed to

Edward Ansell
Director of Patents and Licensing
Mail Stop 301-6
California Institute of Technology
1207 East California Boulevard
Pasadena, CA 91125

Refer to NPO-16612, volume and number of this NASA Tech Briefs *issue, and the page number.*

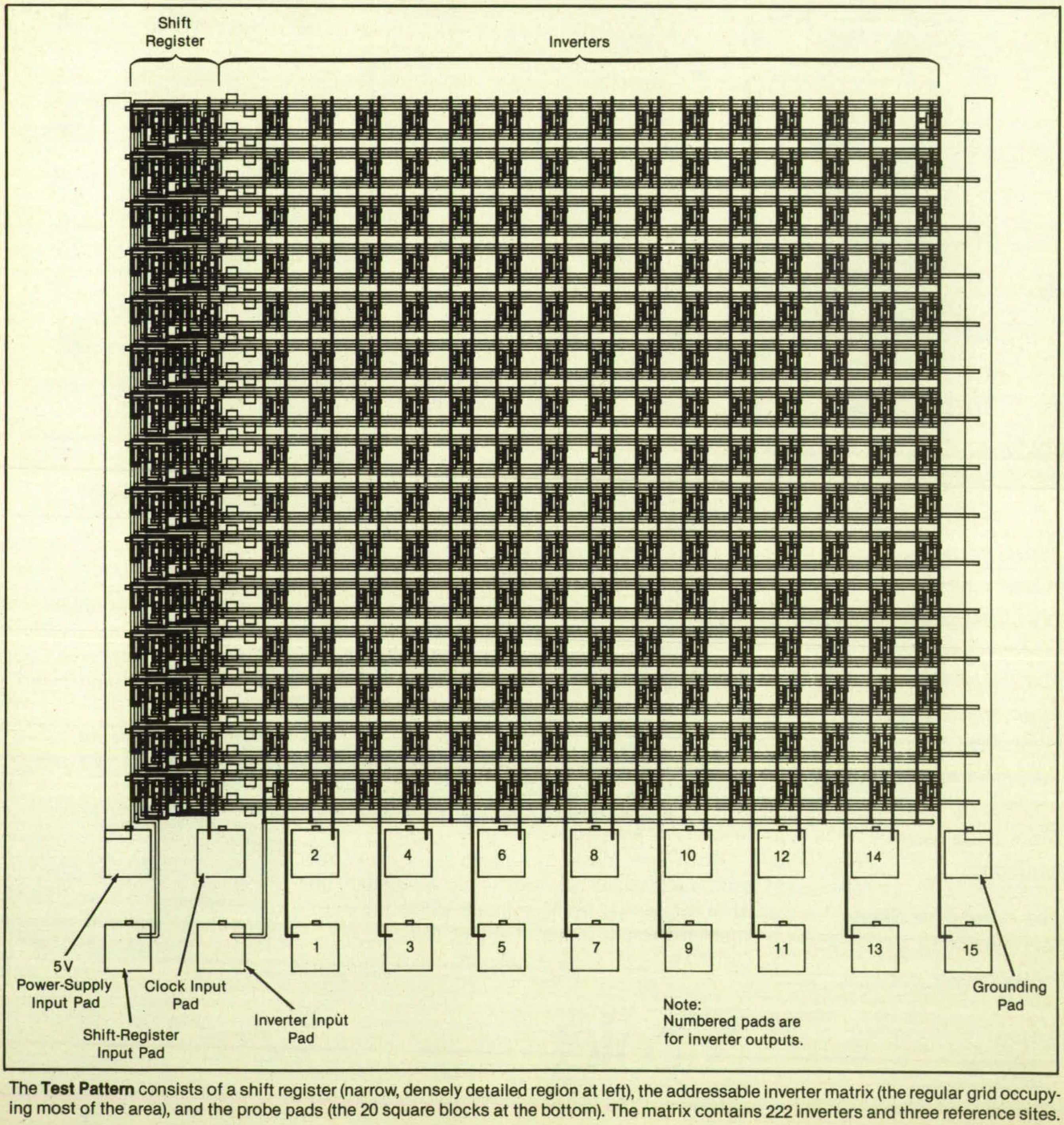

The **Test Pattern** consists of a shift register (narrow, densely detailed region at left), the addressable inverter matrix (the regular grid occupying most of the area), and the probe pads (the 20 square blocks at the bottom). The matrix contains 222 inverters and three reference sites.

Circle Reader Action No. 568

Detecting Faults in High-Voltage Transformers

A simple fixture aids the detection of faults that escape standard inspection procedures.

Marshall Space Flight Center, Alabama

A simple fixture quickly shows whether a high-voltage transformer has excessive voids in its dielectric materials and whether its high-voltage lead wires are too close to the transformer case. The fixture is a "go/no-go" indicator; a corona appears in it if the transformer contains such faults.

Voids as small as 0.01 in. (0.25 mm) or less allow internal arcs in epoxy insulating material that can destroy a transformer under high-voltage stress. Electrical breakdown can also result where a high-voltage wire is not covered with a sufficient thickness of insulation. In both cases, the faults can elude standard x-ray inspection but are readily detectable with the help of the fixture.

The fixture consists of a cap of clear epoxy resin with stainless-steel mesh lining the cavity (see figure). The inside of the cap is sized and shaped to mate with the transformer. Leads connect the mesh to ground. The high-voltage transformer is inserted in the cap, and a 15-kV potential is applied to it.

If the transformer has voids or wire-proximity faults, a glow will be visible in the mesh when it is viewed through the cap in a dark room. The position of the corona glow indicates the location of the fault in the transformer. The fixture has been used to detect several faulty transformers that had passed x-ray inspection.

This work was done by Raymond K. Blow of Rockwell International Corp. for **Marshall Space Flight Center**. *No further documentation is available.*

Inquiries concerning rights for the commercial use of this invention should be addressed to the Patent Counsel, Marshall Space Flight Center [see page 12]. Refer to MFS-29225.

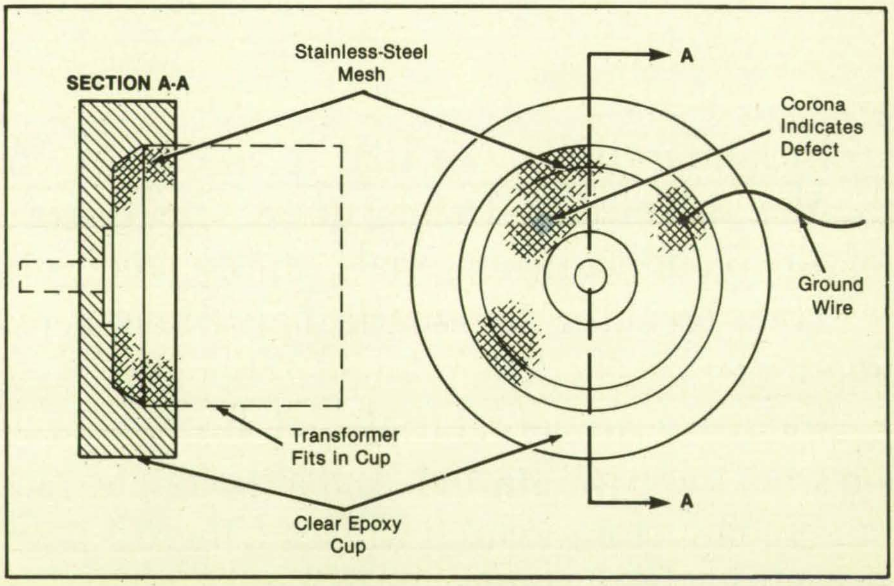

The **Transformer Nests in a Wire Mesh** supported by a cap of clear epoxy. If the transformer has defects of the type described in the text, the blue glow of a corona appears in the mesh and can be seen through the cap.

Electrically-Conductive Polyaramid Cable and Fabric

Tows coated with metal provide strength and conductance.

Marshall Space Flight Center, Alabama

A cable suitable for use underwater is made of electrically conductive tows of metal-coated polyaramid filaments surrounded by an electrically insulating jacket. The conductive tows can also be used to make conductive fabrics (see Figure 1).

Conventional underwater cables tend to rupture when released after severe

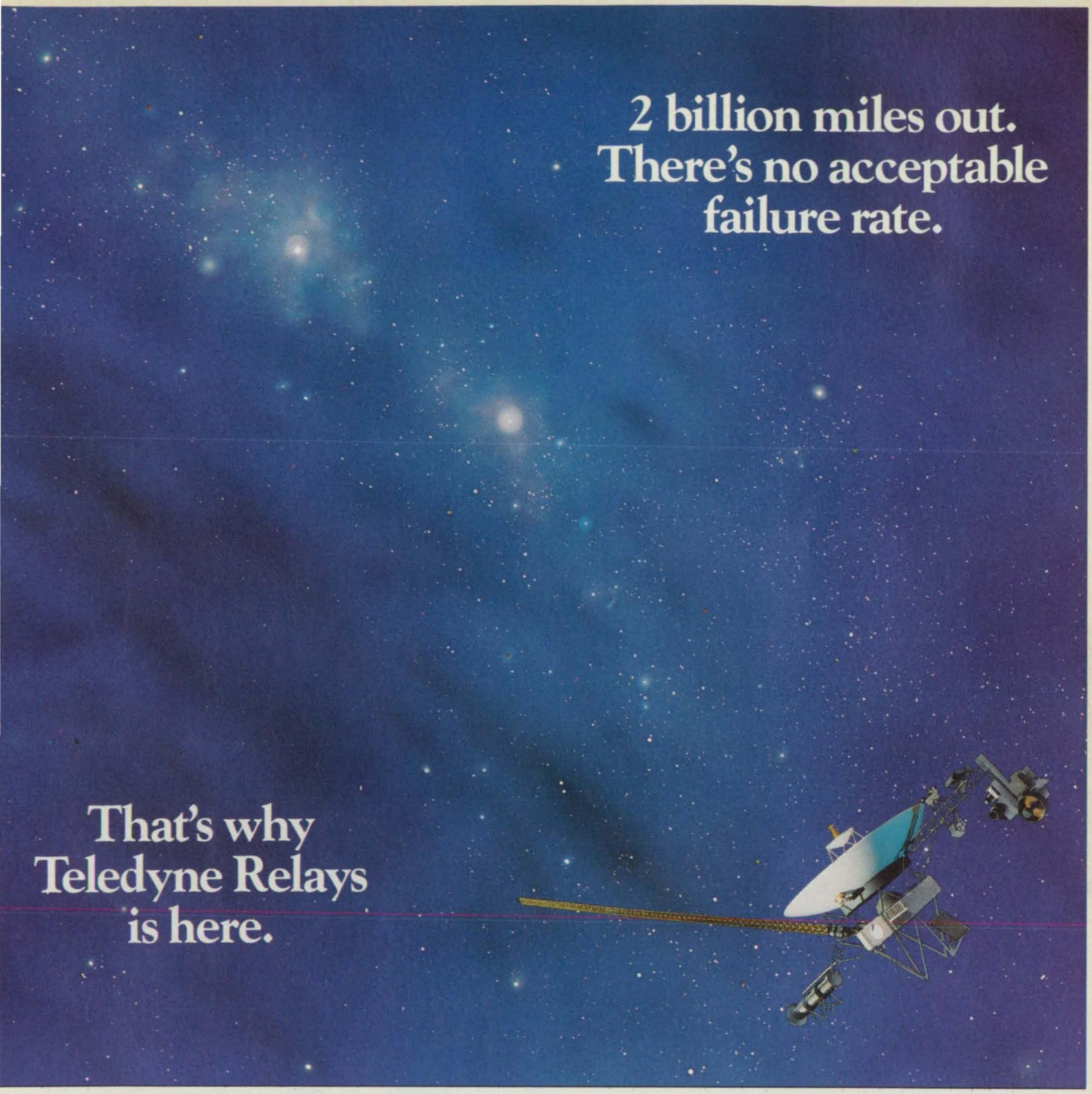

On Voyager 2, TO-5 electromechanical relays made by Teledyne Relays have spent eight years in deep space. And are still operating perfectly.

And this is only one example of the extraordinary reliability of TO-5 electromechanical relays from Teledyne Relays.

This reliability is the reason why the TO-5 has become the industry standard. And it's the reason designers keep specifying it for use in advanced technologies from space probes to weapons systems. From flight controls to test equipment.

In the 24 years since we invented the TO-5 Relay technology, we've supplied millions of relays to a very demanding market; because Teledyne's TO-5 electromechanical relays are not a compromise.

If you are working on a design which calls for unquestioned reliability, work with us. For applications on or under the sea. On or above the earth. Anywhere you need superior performance. Put our quarter century of experience to work for you.

Because—when there's no acceptable failure rate, there's only one acceptable choice—Teledyne Relays.

TELEDYNE RELAYS
Innovations In Switching Technology

12525 Daphne Ave., Hawthorne, California 90250 • (213) 777-0077
European Hqtrs: Abraham Lincoln Strasse 38-42, 6200 Wiesbaden, W. Germany • 06121-768
Belgium Sales Office: 181 Chaussee de la Hulpe, 1170 Brussels • (2) 673-99-88
U.K. Sales Office: Heathrow House, Bath Rd., Cranford, Hounslow, Middlesex, TW5 9QP • 1-897-2501
Japan Sales Office: Taikoh No. 3 Building, 2-10-7 Shibuya, Shibuya-Ku, Tokyo, 150 Japan • (3) 797-6956
France Sales Office: 85-87 Rue Anatole-France, 92300 Levallois-Perret • 1-7587160

Circle Reader Action No. 572

Figure 1. **Cable or Fabric** can be made of tows of metal-coated polyaramid filaments.

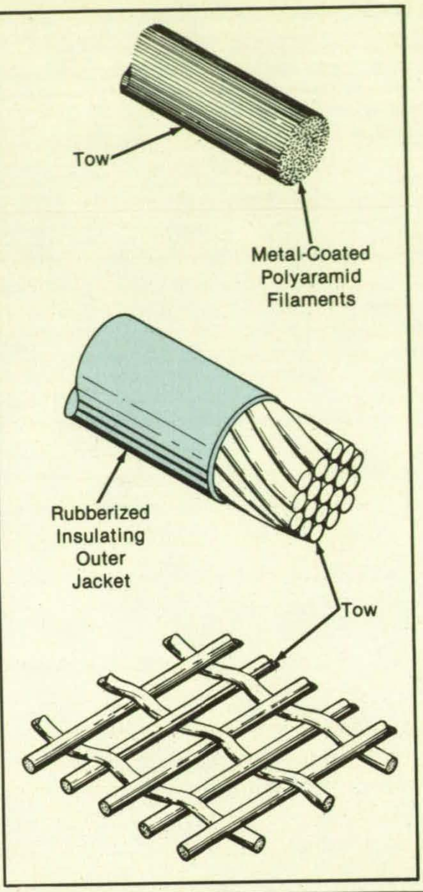

stretching because the copper conductors in them remain elongated, while the polyaramid jackets or wrappings in them spring back to nearly their original lengths. In the new cable, the tension is borne by the metal-coated filaments, so that upon release, the entire cable springs back to nearly its original length without damage.

Figure 2 illustrates the process for coating the filaments in a tow. A typical tow contains about 1,000 polyaramid fibers, each 11.9 μm thick. Some tows are manufactured with a light sizing. Upon unwinding from a spool, the tow first passes through a cleaning solution of sodium hydroxide or a chlorinated solvent or both, to remove the sizing. The cleaning solution is rinsed off with water, and the tow is then passed into an activating solution of palladium chloride and/or tin chloride with hydrochloric acid and water.

After the activating solution is rinsed off with water, the tow passes through an accelerating solution of 50 percent hydrochloric acid in water. The acid is rinsed off in water, and the tow then enters the first plating bath. (Although two baths are shown here, one or three or more could also be used.) After each plating bath, the tow is rinsed with water. After the last rinse in water, the tow is rinsed in alcohol, dried, and wound on a spool.

The metal plate of choice consists of two layers of copper for high conductance plus an outer coat of nickel to retard oxidation of the copper. Experimental tows exhibited lineal resistivities of the order of 1 Ω/ft (3 Ω/m). In one case, the breaking strength of the tow was measured and was found to have decreased by 8 to 12 percent as a result of the plating.

This work was done by Ralph F. Orban of Material Concepts, Inc., for **Marshall Space Flight Center**. *For further information, Circle 12 on the TSP Request Card.*

In accordance with Public Law 96-517, the contractor has elected to retain title to this invention, covered by U.S. Patent No. 4,634,805. Inquiries concerning rights for its commercial use should be addressed to

Ralph F. Orban
Material Concepts, Inc.
New Products Dev. Division
666 North Hague Avenue
Columbus, OH 43204.

Refer to MFS-26031, volume and number of this NASA Tech Briefs *issue, and the page number.*

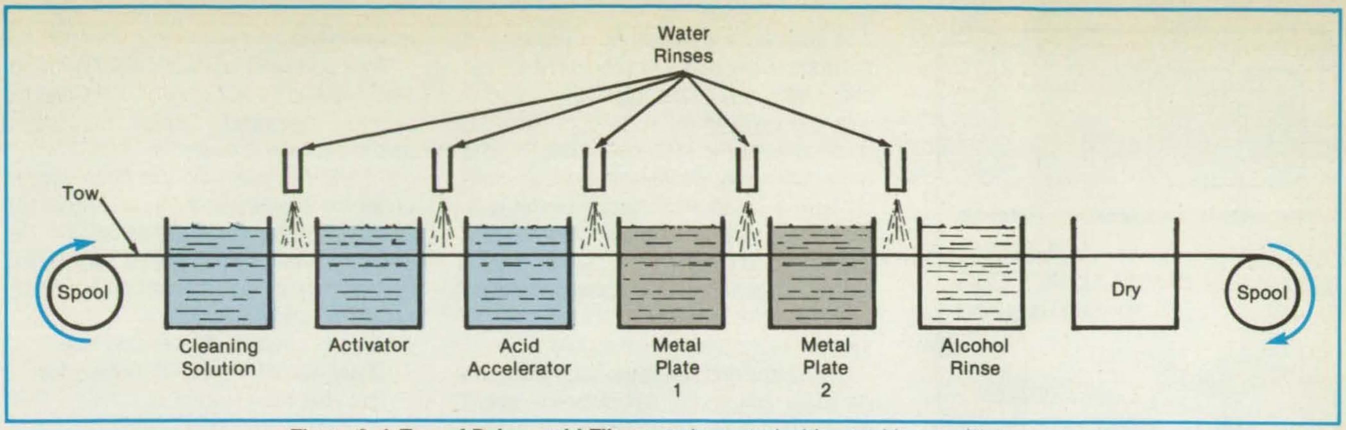

Figure 2. A **Tow of Polyaramid Filaments** is coated with metal in a multistep process.

Submounts for Laser-Diode Chips

A practical bonding method is applicable to almost all types of mounts.

Langley Research Center, Hampton, Virginia

A universal method of bonding a laser-diode chip to its mount has been developed. Previous methods for mounting laser-diode chips have presented serious problems and are not applicable to all types of mounts. The new technique is applicable to almost all of the different types of mounts used in the production of laser diodes.

In the new process, a thin sheet of conducting metal, such as copper, beryllium/copper, or silver is photoetched to give a multiple of square or rectangular pieces all electrically connected to each other and to the original metal sheet via narrow connectors (see figure). The sheet is plated with 2 μm of nickel and 2 to 4 μm of tin. The individual pieces, or submounts, are then separated manually by use of a sharp knife or are mechanically punched out. The metal sheet is generally 1 to 5 mils (0.025 to 0.13 mm) thick.

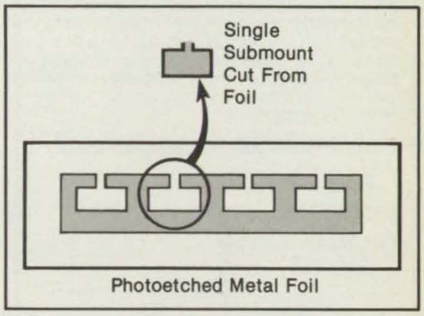

Submounts are etched, then cut from a metal foil.

A submount is placed on a mount and the edge of the submount aligned with that of the mount. A diode chip is then aligned with the edge of the submount, and the diode is soldered in place by heating the whole assembly. Because there is tin plate on both the top and bottom of the submount, the chip-to-submount bonding and submount-to-main-mount bonding take place simultaneously. Then the connecting wire is bonded from the top of the diode to the wire-bond area on the mount.

The shape and size of the submount can be easily adapted to suit different mount geometries. A big advantage of this type of submount is that the edge on which the diode is mounted is very sharp, eliminating the costly need for a sharp edge on the mount itself.

This work was done by Anil Ramniklal Dholakia and Louis Trager of RCA Corp. for **Langley Research Center**. *No further documentation is available.*

Title to this invention has been waived under the provisions of the NASA Act [42 U.S.C. 2457(f)], to the David Sarnoff Research Center, Inc. Inquiries concerning licenses for its commercial development should be addressed to

Allen L. Limberg, Patent Counsel
David Sarnoff Research Center, Inc.
P.O. Box 432
Princeton, N.J. 08540-0432

Refer to LAR-13651, volume and number of this NASA Tech Briefs *issue, and the page number.*

Improved Traveling-Wave Tube

This new design provides high power and bandwidth.

Lewis Research Center, Cleveland, Ohio

A new space traveling-wave tube (TWT) provides a coherent source of 75 watts of continuous-wave (CW) power output over a bandwidth of 5 GHz at a frequency of 65 GHz. This coupled-cavity TWT provides 50 dB of saturated gain. The TWT includes a thermionic emitter, an M-type dispenser cathode that provides a high-power electron beam. The beam is focused by permanent magnets through the center of the radio-frequency (RF) cavity structure.

The coupled cavity circuit is a slow-wave structure that supports the RF signal. Amplification takes place by an exchange of energy between the electron beam and the RF wave. The power of the signal increases until the signal leaves the RF structure. The beam is collected in a four-stage, radiation-cooled collector. The efficiency of the TWT is increased by operating the four-stage collector at increasingly higher bias voltages.

This V-band TWT represents a breakthrough in the development of a very-wide-band, high-gain 75-W CW RF amplifier. This development provides the opportunity to deploy satellite-to-satellite communications systems with capabilities for the transmission of information far exceeding present capabilities. The TWT is designed for reliable operation for 10 years. Its overall efficiency of 35 percent minimizes the prime power input and dissipation of heat. The availability of this new space TWT provides the means to meet the future requirements of very-high-data-rate transmission links between satellites.

This work was done by Art Rousseau, Ivo Tammaru, and John Vaszari of Hughes Aircraft Co. for **Lewis Research Center**. *No further documentation is available.*
LEW-14580

Books and Reports

These reports, studies, handbooks are available from NASA as Technical Support Packages (TSP's) when a Request Card number is cited; otherwise they are available from the National Technical Information Service.

Performance of Infrared-Detector Array

The noise equivalent power of each picture element is about 4×10^{-18} W/Hz$^{1/2}$.

A report describes the design, characteristics, and performance of an Si:Sb integrated array of infrared detectors, the sensitivity of which extends to a wavelength of about 31 μm, an improvement over the 28-μm limit of current Si:As impurity-band-conduction devices. The report also describes the electronics and special Dewar system developed to test the device at low temperature to reduce background noise.

The array was developed as part of a program to develop detectors for such future space-based infrared astronomy missions as the Space Infrared Telescope Facility and the Large Deployable Reflector. The use of integrated arrays in photometric, spectroscopic, and polarimetric applications should allow extended portions of the sky and their associated spectral features to be recorded with high sensitivity and superior positional accuracy.

The array is constructed in a hybrid configuration, with separately-optimized

detector and readout substrates mated together via an array of indium bump contacts, one for each 76- by 76-μm picture element of the 58-by 62-element array. The silicon detector substrate is doped with Sb at a concentration of about 4×10^{15} atoms/cm^3; to achieve optimum responsivity, heavier doping would have been required. A quantum efficiency of about 20 percent is expected. Nearly all of the surface of the array is optically active. Both surfaces of the 0.5-mm-thick detector substrate are covered with implanted transparent electrodes. The rear surface is aluminized to provide a reflection that increses the length of the optical path through the detector.

The direct-readout multiplexer chip contains switching metal oxide/semiconductor field-effect transistors that provide both random access and nondestructive read-out of the charges accumulated in individual picture elements. This feature is particularly useful in astronomical applications where bright and faint objects commonly appear in the same scene and is also useful for monitoring the effects of hits by energetic cosmic rays.

During testing, the detector array is mounted in a sealed aluminum chamber in a liquid-helium Dewar. A double-leaved shutter assembly at the upper end of the helium-cooled workspace has provisions for mounting filters and apertures; the maximum beam size is f/180. When the external aperture is blocked off, the background reading is 10^9 photons/cm^{2}s; with neutral-density filters in place, the room-temperature background flux viewed by the array has an estimated density of about 2×10^7 photons/cm^{2}s. Modifications are planned to reduce the background to about 2×10^5 photons/cm^2, the level expected in a cooled space telescope.

The test-system electronics comprise three sections: (1) the Dewar electronics, (2) the "front-end" equipment, and (3) the host computer. Mounted on the Dewar are an electronically-isolated level-shifting unit that translates the transistor/transistor-logic-level array-address signals to the metal oxide/semiconductor levels required by the array; adjustable dc bias supplies; and the two-channel preamplifiers that filter and amplify the low-level analog output signals of the array for transmission to the "front-end" equipment.

The "front-end" equipment, which is housed in a 19-in. (48-cm) chassis, uses a single-board computer based on a 68000 microprocessor to address the array and acquire the data. A readout rate of 30 frames/s (107 kilopixels/s) is possible; higher rates could be achieved by the use of timing circuitry on the interface board of the array. The transmission of a full image to the 68010 microprocessor-based host computer takes 10 ms.

The host computer, based on a 68010 microprocessor, provides the computing power and graphical capability to display and store the image data generated by the array. The computer work station can also serve as a general-purpose terminal in a high-speed local-area network.

In tests at a temperature of 7 K, the multiplexer worked well both in a fast-reading mode (several frames per second) and in an integrating mode (integration times up to 6 s). Based on measurements made at a wavelength of 2μm and scaled to the peak-response wavelength of 30 μm, the responsivity is between 1 and 6 A/W. Each well in the multiplexer has a capacity of about 2×10^5 electrons. The noise and electronic interference total 600 electrons per reading or less in a bandwidth of 0.5 Hz; the resulting noise-equivalent power for an average detector element is about 4×10^{-18}W/Hz$^{1/2}$.

This work was done by J. H. Goebel, M. E. McKelvey, C.R. McCreight, and G. M. Anderson of **Ames Research Center.** *To obtain a copy of the report, "Low-Background Direct Readout Array Performance," Circle 165 on the TSP Request Card.*

Inquiries concerning rights for the commercial use of this invention should be addressed to the Patent Counsel, Ames Research Center, [see page 12]. Refer to ARC-11735.

Books and Reports

Computer Programs

Adaptive Bandwidth Compression for Moving Images

Data would be compressed in images with fast motion and expanded when the motion slows.

Lyndon B. Johnson Space Center, Houston, Texas

A proposed data-compression scheme would adapt the transmission rate for a moving image to the speed of motion of the image. The scheme exploits the fact that the resolution of a human eye decreases as the apparent speed of a viewed object increases. High resolution of the transmitted image of a rapidly moving object is unnecessary to the eye because the eye will still view it at reduced resolution. The resolution and consequently the transmission bandwidth of a television image can therefore be reduced to the observer's resolution limits as the speed of the observed object increases. The system could adapt itself automatically, or its transmission rate could be altered manually. The compression technique can be used with almost any type of scanning image sensor to reduce the bandwidth of transmitted signals.

The system would include a television camera and laser rangefinder, both of which would be aimed in the same direction. The camera and rangefinder would feed video signals to an adaptive sampler (see figure). The sampler would encode the video and drive the television transmitter.

A remote control station would receive the video signal and decode it into a serial data stream. A multiple-field adaptive decommutator would store the serial data and use them to drive a television monitor. A manual or automatic control circuit in the remote control station would send command signals to the decoder and to the adaptive sampler at the camera according to the capacity of the video channel and the motion of the image as determined by the rangefinder.

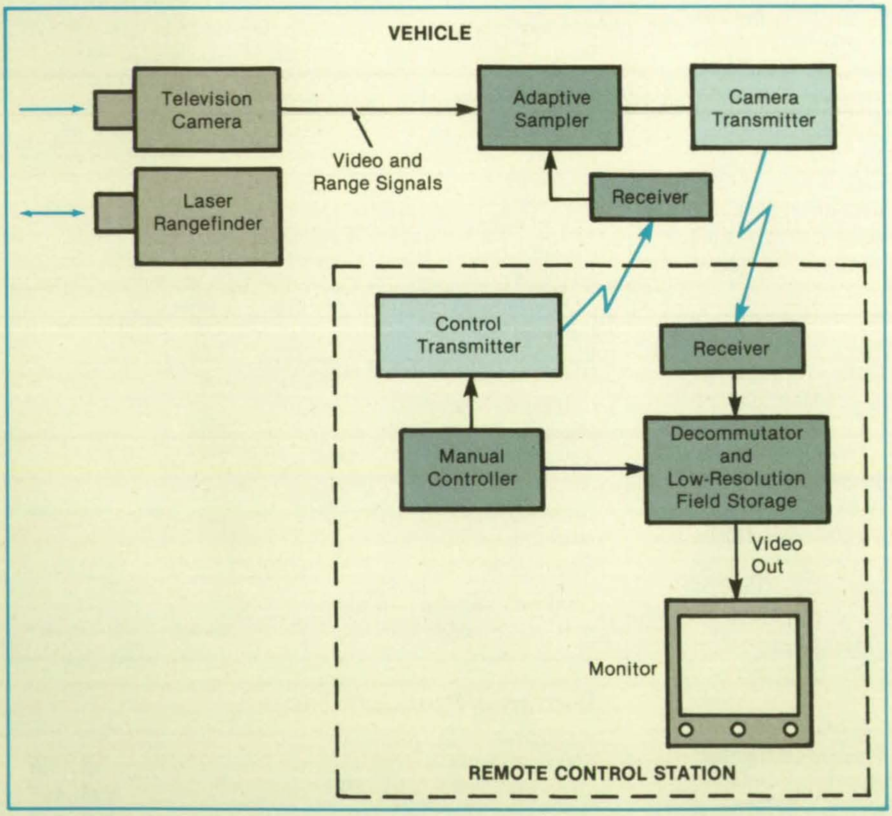

A Laser Rangefinder Would Measure the Speed of a target. An adaptive sampler could determine the required resolution of the target image on the basis of the measured speed and would provide a decommutator at the control station with more or fewer partial image fields per unit time. When the monitor displays the maximum number of fields simultaneously, the resolution is the highest.

The sampling rate per pixel would be set equal to the channel capacity. The display simultaneous-refresh rate would be set to present the optimum resolution in motion as a function of the speed of motion. Each horizontal line scanned by the camera would be sampled at a rate fast enough to equal the video channel capacity. For example, a 500 kb/s channel would allow sampling every 16th pixel of a 60-Hz, 525-line, positive-interlace camera having 400 pixels per line.

The first encoded field would then consist of 250 lines of 25 encoded pixels each. (Of the 262½ lines in a field, 12½ are used for the vertical retrace.) Each additional field would consist of a different set of 25 by 250 pixels until 32 fields — a full-resolution frame — are accumulated. The individual low-resolution fields would be stored in the adaptive decommutator at the control station. On command, the decommutator would play back all fields simultaneously or any combination of fields, as determined by the motion in a scene.

The rangefinder data would be encoded into the vertical-blanking interval to control the number of fields played back simultaneously. Increased motion would allow fewer simultaneous playbacks. The available channel capacity determines the number of fields that are available for full resolution. The channel capacity and the compression ratio could be determined by the camera or by the control-station circuitry.

This work was done by Olin L. Graham of **Johnson Space Center**. *No further documentation is available.*

This invention is owned by NASA, and a patent application has been filed. Inquiries concerning nonexclusive or exclusive license for its commercial development should be addressed to the Patent Counsel, Johnson Space Center [see page 12]. Refer to MSC-20821.

Where do you find good Ada programmers?

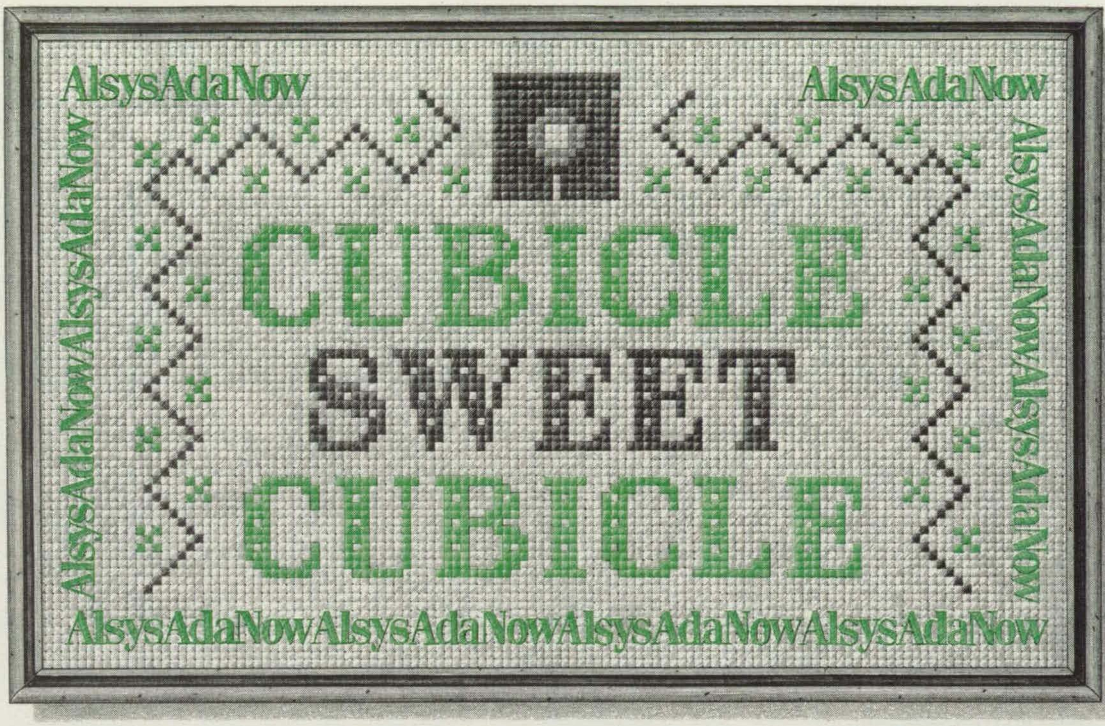

Free Poster: see coupon.

You could spend and spend trying to hire good Ada programmers and still not find what you need. Big demand; short supply. The irony is, your best Ada people may be the programmers you already have; all they need is good training.

Alsys offers a full range of quality Ada training products for growing your own programmers. For example . . .

■ A 27 video tape seminar covering the entire Ada language – 18 hours of authoritative instruction by the principal designer of the language itself. Benefit? Understanding Ada's architecture and scope should be the foundation for all further work or study. It will help develop that most elusive skill: the Ada programming intuition to guess right.

■ For programmers ready for hands-on skills development, a comprehensive CAI course on a PC, running 50–60 hours, with exercises and progress tracking. Multiple users. Licenses for 5 machines. The course is also excellent for brushing up, or extra work on one subject, or for new employees.

■ For practicing, and then moving directly to serious Ada programming, Alsys offers a full-featured, production quality Ada compiler, with tools, for the PC AT. This same compiler is used to build some of the largest Ada programs in existence!

Alsys offers more training products. A CAI course for programmers familiar with Fortran . . . a searchable, on-line version of the Reference Manual . . . a (limited) offering of live training courses.

Good Ada training for your own people. For Ada now. Write or call.

alsys

Ada Programmers Are Made – Not Hired.

In the US: Alsys Inc., 1432 Main St., Waltham, MA 02154 Tel: (617) 890-0030
In the UK: Alsys Ltd., Partridge House, Newtown Rd., Henley-on-Thames, Oxon RG9 1EN Tel: 44 (491) 579090
In the rest of the world: Alsys SA, 29 Avenue de Versailles, 78170 La Celle St., Cloud, France Tel: 33 (1) 3918.12.44

Send me POSTER and more information on:

____ *Ichbiah, Barnes & Firth on Ada* 27-tape Video Series.
____ *Lessons on Ada* CAI Course. ____ Live Training.
____ *PC AT Compiler and Tools.* ____ *AdaQuery* On-Line Reference.
____ *You Know Fortran, Ada is Simple* CAI Course.
____ *Ada Immersion* Combination Package.

Name ________
Company ________
Address ________
City ____ State ____ Zip ____
Phone ( ) ____ Ext. ____
Mail to: Alsys, Inc. 1432 Main St., Waltham, MA 02154

*Ada is a registered trademark of the U.S. Government (AJPO).

Circle Reader Action No. 341

Stereoscopic Optical Signal Processor

Correlation of optical signals indicates the identity, distance, or movement of an object.

Marshall Space Flight Center, Alabama

An optical signal processor produces a two-dimensional cross correlation of images from a stereoscopic video camera in real time. The cross correlation is used to identify an object, determine its distance, or measure its movement.

Video images from a pair of monochrome television cameras are transmitted over separate lines to separate cathode-ray tubes, where the two images are displayed. The light from each cathode-ray tube is collected and collimated by a lens and directed onto the input plane of an associated liquid-crystal light valve (see figure). Simultaneously, part of the light from a diffuse, extended source (a laser, tungsten filament, or arc lamp) is linearly polarized, collimated, and directed through one of the polarization-sensitive beam splitters onto the output plane of one of the light valves. Part of this light is also directed through the other polarization-selective beam splitter and onto the output plane of the other liquid-crystal light valve.

The linearly polarized light falling on the output planes of the two light valves is modulated by the images projected on the input planes. These modulated beams are reflected from the output planes back into the optical system and are selectively directed by the beam splitters to a video detector.

With the video switch in position 1, the composite modulated beams on the video detector produce range information. When the object is at a predetermined optimum range, a peak correlation signal is produced at the center of the detector by the beams from the left and right channels. The distance of the correlation signal from the center indicates the range of the object.

With the switch in position 2, the system indicates whether the object has moved with respect to the cameras. The image from the right camera is stored in a video-frame memory. At a specified time later, the stored image is displayed on the left cathode-ray tube for modulation and comparison with the modulated beam from the right channel. A reference image is thus correlated with the current image in the video detector. If the target has moved, the correlation peak will have shifted.

With the switch in position 3, the signal produced by the right camera is correlated with a signal from a video playback unit. In this position, the system can identify an unknown object. In a trial-and-error procedure under computer control, the playback unit generates a series of images of known objects for correlation with the unknown object viewed by the right camera.

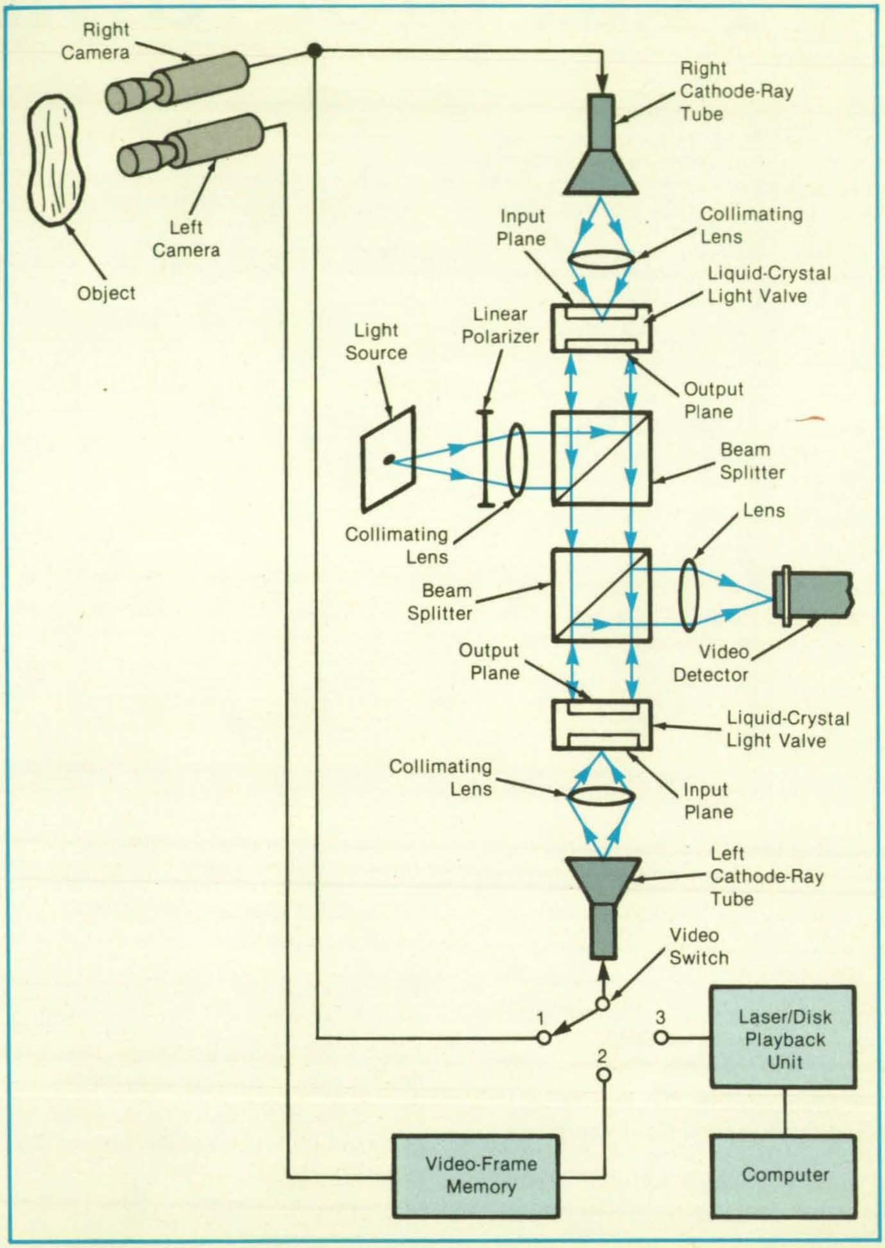

Left and Right Cameras Modulate Beams from a light source for correlation in a video detector. The switch in position 1 produces information about the range of an object viewed by the cameras. Position 2 gives information about movement. Position 3 helps to identify the object.

This work was done by Glenn D. Graig of **Marshall Space Flight Center**. *For further information, Circle 157 on the TSP Request Card.*

This invention has been patented by NASA (U.S. Patent No. 4,556,986). Inquiries concerning nonexclusive or exclusive license for its commercial development should be addressed to the Patent Counsel, Marshall Space Flight Center [see page 12]. Refer to MFS-25752.

DATAWATCH 150
The world's most portable TEMPEST printer...
And lowest cost, too

The DATAWATCH 150 Ink-Jet Printer is the smallest, lightest, battery operated portable TEMPEST printer . . . and the least expensive, too. Weighing only 8 pounds and no bigger than a cereal box, you can carry it easily. Since the DATAWATCH 150 runs on rechargeable batteries, you can use it anywhere. And its rugged construction makes it as reliable in the field as it is on your desk top.

Although small in size, the fully functional 150 prints just about anything you can write in text, script, or near letter quality type. It even creates graphics, addresses envelopes and prints directly on transparencies. And the speed is exceptional for a printer of this type, handling up to 240 CPS in condensed mode. Plus, ink-jet technology means no ribbon to protect.

DATAWATCH

Datawatch Corporation
317 New Boston Street • Wilmington, MA 01887
Telephone: (617) 932-0550 Fax: (617) 932-9203
In Washington, DC area call (703) 476-2249
In Canada call Ahearn & Soper Inc. (613) 226-4520

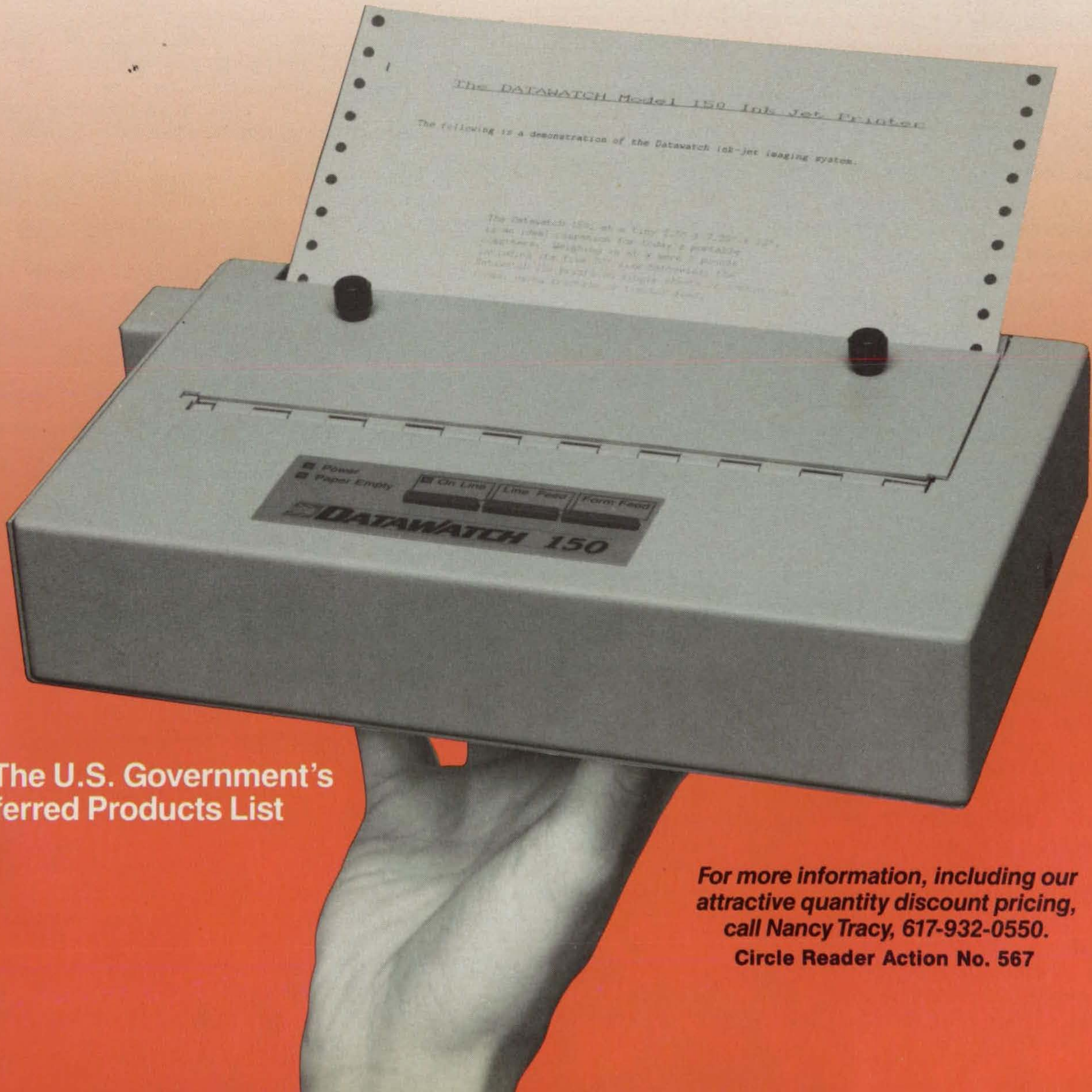

On The U.S. Government's Preferred Products List

For more information, including our attractive quantity discount pricing, call Nancy Tracy, 617-932-0550.

Circle Reader Action No. 567

A Work Station for Control of Changing Systems

A touch screen and microcomputer enable flexible control of complicated systems.

Goddard Space Flight Center, Greenbelt, Maryland

A computer work station equipped to produce graphical displays is used as a command panel and status indicator for a command-and-control system. The work-station operator uses the images of control buttons displayed on a touch screen to send prestored commands. The use of a prestored library of commands reduces the incidence of errors that are likely if each command were entered individually on a keyboard in real time. If necessary, however, the operator can use a conventional keyboard to enter commands in real time to handle unforeseeable situations.

The work station was developed for control of the Earth Radiation Budget Satellite (ERBS), in which faulty commands caused by erroneous manual keying could have dire consequences. A potential industrial application is controlling a "just-in-time" production line in which units are to be assembled to different specifications — for example, an automobile assembly line where body types and factory options vary from car to car along the line. With a repertory of commands on the touch screen, an operator could readily command the appropriate parts and assembly operations.

The station includes a color video-display unit with the touch screen, the keyboard, and a video generator controlled by a microcomputer with floppy-disk drive (see figure). The microcomputer is connected to another microcomputer, which serves as the application processor, and to a printer.

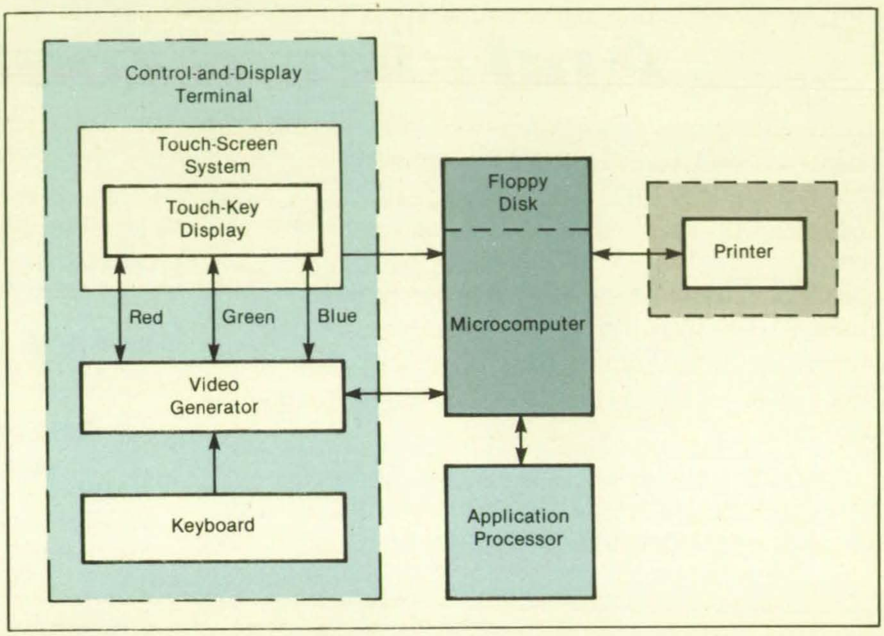

A **Work Station** offers a selection of touch-screen buttons for issuing commands and displays information on the status of the commanded system. The operator can change the display of buttons at will. Usually, only those buttons needed at a given time are displayed. The buttons are labeled with the time at which they should be pressed and are usually laid out in order of use.

Some ideas suggested by operators will be incorporated into a future version of the station. The layout of button images, for example, will be changed to make frequently used buttons larger than others so that they are more likely to be hit accurately. Unused buttons will be eliminated. Windows can be displayed on the screen to show interactive-dialog boxes and to combine related commands into sections. In addition, it will be possible to write and store commands at the station, rather than at another terminal.

This work was done by Daniel J. Mandl of **Goddard Space Flight Center**. *For further information, Circle 150 on the TSP Request Card.*
GSC-13106

Computer Interface for a Spectroreflectometer

A FORTRAN program controls stepping motors and signal-processing electronics via an S-100 computer bus.

Marshall Space Flight Center, Alabama

A group of spectroreflectometers have been modified to provide computer-controlled operation and data collection. In their original form, these instruments included vacuum-tube electronics, strip-chart output, and related mechanical parts, but no provision for connection to computers. In the modification, the original high-quality optical and most of the mechanical parts were retained, thus allowing continued use of an extensive collection of accessories and adapters already purchased.

Solid-state digital electronic circuitry was added to allow data transfer and control signals to be handled via an S-100 computer bus. The computer programs were written in FORTRAN IV to enable modification by the user to fit special configurations and test procedures. New signal-processing electronics provide improved performance at low light levels by integrating readings over longer periods when necessary.

The continuous-control motors and the associated circuitry are replaced with two computer-controlled stepping motors: one motor moves the prism or diffraction grating of the monochromator to select the wavelength of the beam; the other motor operates the slit-width mechanism to control the beam intensity. A chopper modulates the monochromator output by turning it on and off at a rate of 480 Hz. A second optical chopping system switches the light beam back and forth between sample and reference paths at a rate of 15 Hz.

The photodetector signal and the chopper and sample/reference timing signals are passed on to signal-processing and computer-interface circuits (see figure) mounted on cards that plug into the S-100 bus. The timing signals control the gating and switching of the photodetector signal so that the sample and reference portions of the signal are fed to the correct channels and sampled during the appropriate intervals.

Band-pass filters remove harmonics

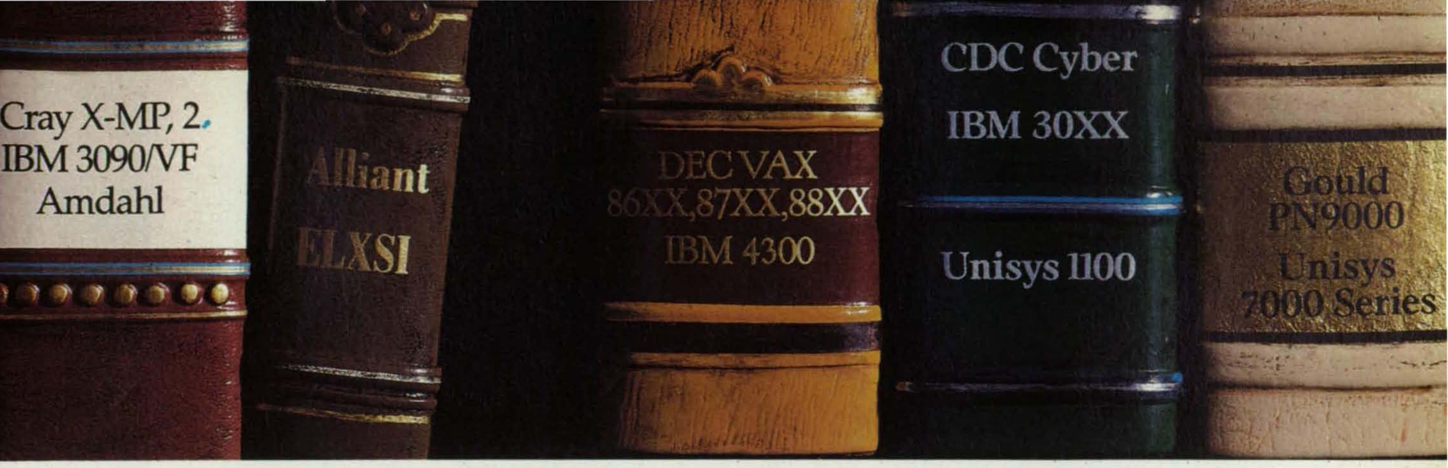

ONLY ONE MATHEMATICS LIBRARY GIVES YOU ACCESS TO THE GREAT WORKS AND THE BEST SELLERS.

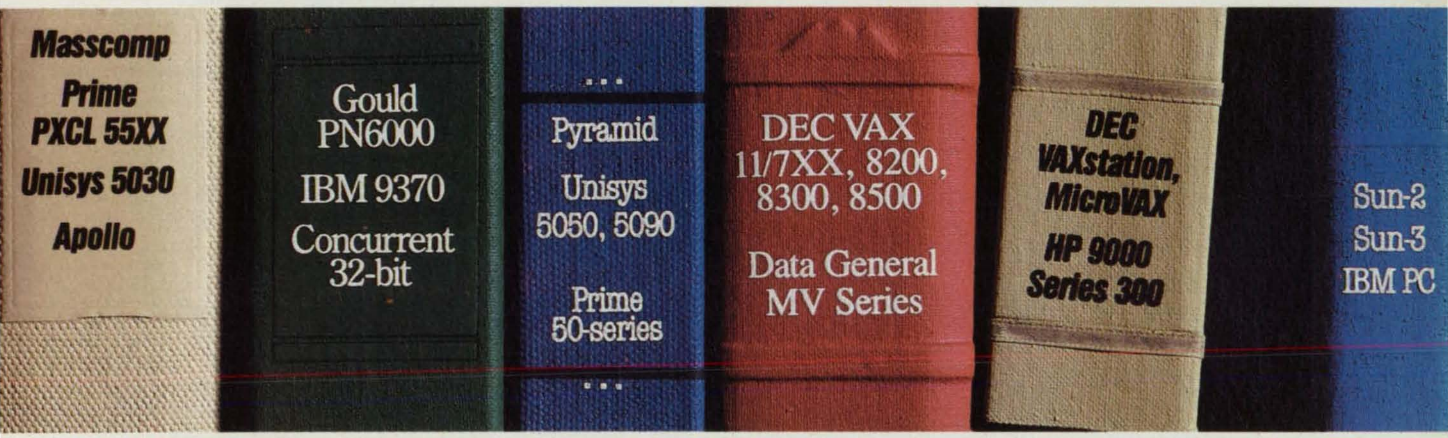

Only Math Advantage® runs the same 260 hard-math subroutines on supercomputers, minicomputers, and workstations. Including Cray,™ Cyber,™ IBM™ Vector Facility,™ VAX,™ Apollo,™ Sun,™ IBM PC/AT,™ and more. Only Math Advantage is *optimized* for so many high-performance systems, and is so compatible.

The Math Advantage library is identical across hosts. So you can develop on a workstation and execute on a supercomputer, with no recoding. And enjoy a single, consistent user interface.

Math Advantage is optimized for both vector and parallel architectures. It's designed for high-performance applications—signal, seismic, and image processing, simulation—where CPU time is at a premium. Development is faster too, with its ready-to-use vector operations, eigensolvers, BLAS, matrix operations, and FFTs. And it's available in FORTRAN, C, and Ada.

Now in version 3.0, Math Advantage gives you more compatibility than any other math library. It's compatible with the FPS™ and Numerix™ array processor libraries, as well as the SEG seismic subroutine standard. And, for Vector Facility users, it complements and builds upon the content of ESSL.

Math Advantage is from the experts in high-performance development tools—Quantitative Technology Corporation. So you can count on unmatched documentation, support, and technical excellence. Over a dozen computer equipment manufacturers offering Math Advantage on their systems do just that. For more information, contact QTC at (503) 626-3081 or Telex 910 240 2827.

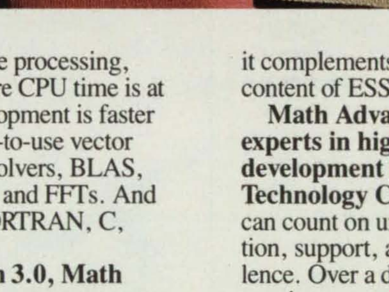

Toolsmith Series®

QTC
Quantitative Technology Corporation

Quantitative Technology Corporation, 8700 Creekside Place, Beaverton, Oregon 97005.

Circle Reader Action No. 570

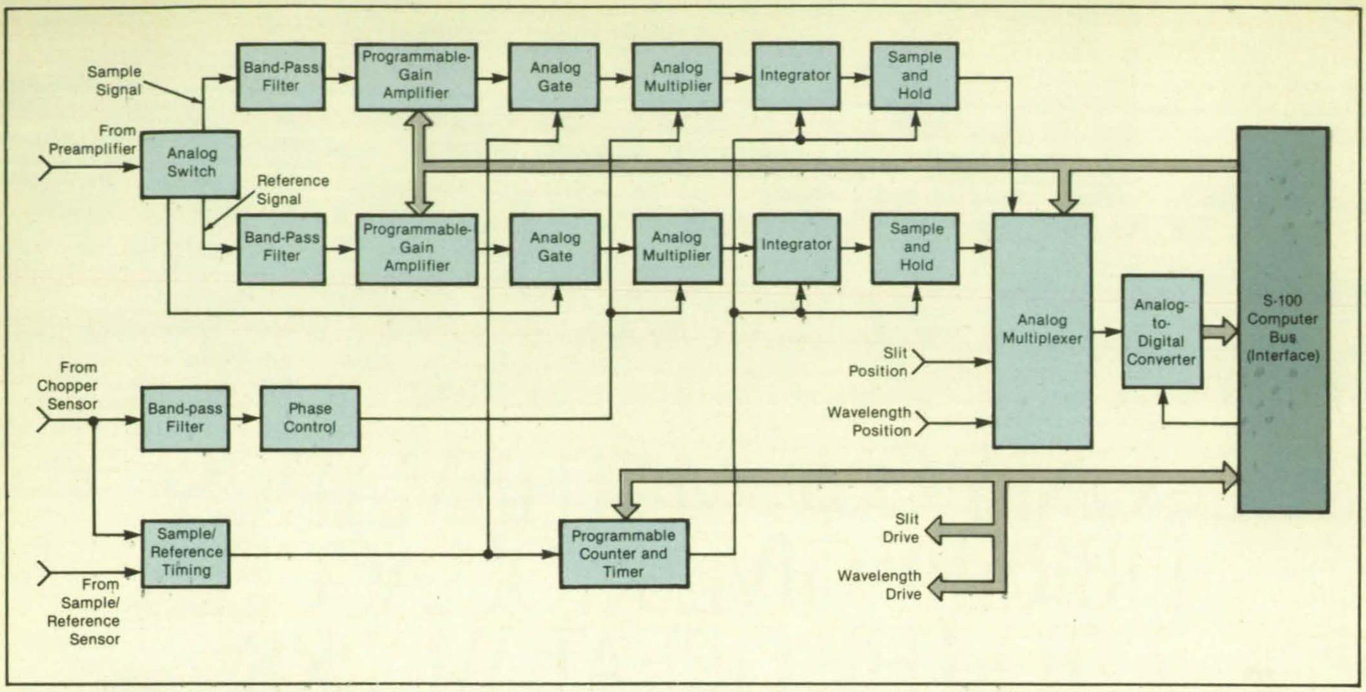

Analog and Digital Signal-Processing Circuits enable the use of computerized automatic data collection and analysis. Previously, the spectroreflectometer data were recorded on strip charts.

from the chopper-sensor signal. Synchronous detection with analog multipliers further enhances the signal-to-noise ratio. A computer-controlled programmable counter allows the signals from 1 to 64 half chopper cycles to be integrated before digitization of the signals.

This work was done by William A. Hurd and Glenn B. Shelton of Radiometrics, Inc., for **Marshall Space Flight Center**. *For further information, Circle 131 on the TSP Request Card. MFS-26021*

Robot Gripper With Signal Processing

A single-chip computer and sensor-circuit chips preprocess sensor data.

NASA's Jet Propulsion Laboratory, Pasadena, California

A gripping pad for a robot arm contains its own sensors and signal-processing circuits. It communicates with the robot controller through a pair of wires or optical fibers. The self-contained circuitry combines the sensor signals for serial digital transmission so that large, heavy, vulnerable, multiple-wire cable is unnecessary. Housed within the gripper, the circuitry is protected from damage and from electromagnetic interference.

The gripper is a pair of hollow boxlike pads with orthogonal V-shaped grooves in the gripping faces (see Figure 1). It can grasp round, oval, square, or flat objects in either of two orientations with respect to the gripper axis. The flat faces accommodate flat pieces like sheet-metal parts; the grooves can hold such objects as a screwdriver on a bar.

Sensing devices are positioned in cavities in the grooves, on the flat pads, and on the edges of the gripper. Optical proximity sensors in the grooves yield information for centering the object and guiding the gripper in its final approach and closure. Additional sensors in the groove detect slippage of the object so that the robot can tighten its grip if necessary. Proximity sen-

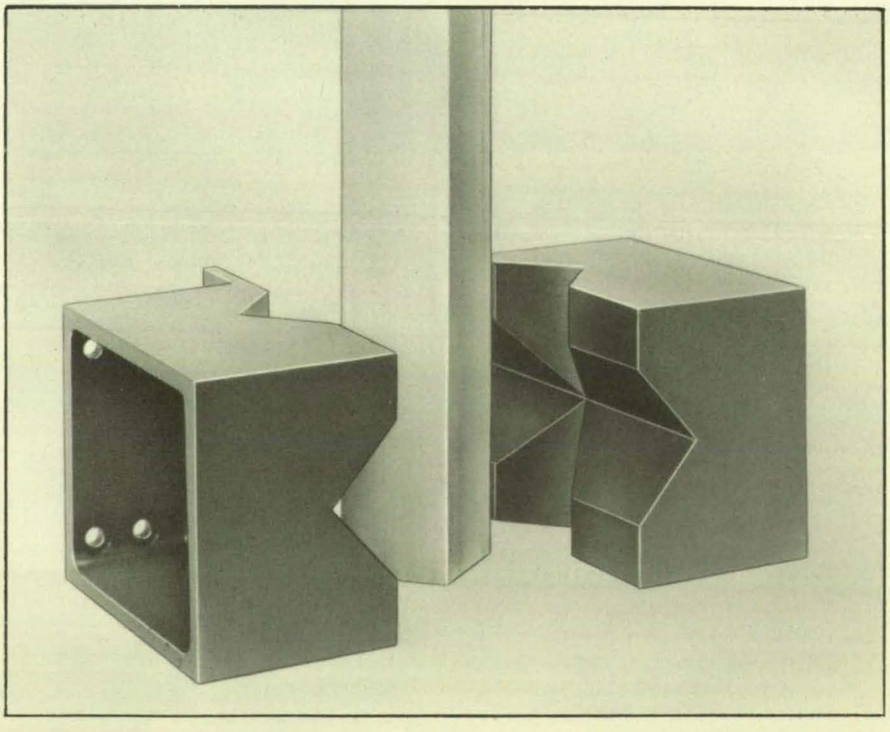

Figure 1. **Gripping Surfaces Are Crossed With Grooves** for grasping differently shaped objects. The gripper cavities, one of which is visible in the left member, will house the sensors and preprocessing circuitry.

sors on the gripper edges look outward, sensing obstacles around the hand. The sensors yield signals to prevent collisions and guide the gripper in channels or recesses. Touch sensors on the grooves and flats indicate when the gripper has made contact with the object.

A single-chip programmable computer and integrated-circuit chips in the gripper cavities filter, condition, and process the sensor data (see Figure 2). Because sensor signals travel only a few centimeters to the chips rather than the length of the robot arm, they are subjected to little delay and interference. Preprocessing in the gripper reduces the load on the main robot computer. Sensor data are sent to the main robot computer on a single digital serial communication line from the single-chip computer. Provided with programs and sensor-calibration data from the main computer, the gripper could do simple tasks on its own or with only a little supervision. The gripper could also maintain a constant slip-free grip on an object without crushing it.

The gripper cavity can be designed so that when circuit boards are inserted in its sockets sensors would simultaneously be positioned in sockets. A removable protective plate covers the cavity. These features simplify the assembly of the gripper and make it easy to remove and replace circuit modules.

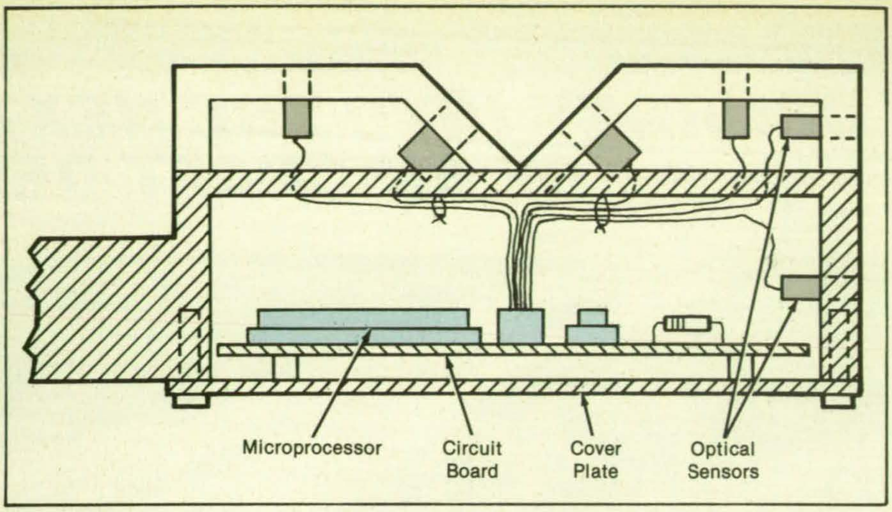

Figure 2. The **Sensors and Preprocessing Circuitry** in the robot gripper reduce the amount of data that must be transmitted between the robot controller and the gripper. Placement in the gripper also reduces signal delays and vulnerability to electromagnetic interference.

This work was done by Richard R. Killion of Caltech for **NASA's Jet Propulsion Laboratory**. *For further information, Circle 38 on the TSP Request Card.*
NPO-16977

Books and Reports

These reports, studies, handbooks are available from NASA as Technical Support Packages (TSP's) when a Request Card number is cited; otherwise they are available from the National Technical Information Service.

Trends in Satellite Communication

Personal communications, orbiting switchboards, and videophones are foreseen.

A report assesses trends in satellite communication from the present to the year 2010. The report, prepared to provide background for long-range recommendations for NASA activities, assesses current applications, possible future applications, and the effects of such new developments as optical-fiber networks, the Integrated Services Digital Network standard, and very-small-aperture terminals (VSAT's). It examines the restrictions imposed by the limited spectrum resource and the technology needs created by trends.

The following major developments are predicted:

- Large satellites for personal communication, by which a user wearing a small radiotelephone will be able to dial virtually any other telephone;
- VSAT-compatible satellites with onboard switching of voice messages;
- Large satellites providing pervasive videophone service; and
- Large geostationary communication facilities used by several carriers, perhaps from several nations.

For each of these developments, frequency reuse will be needed and will require large and complex multibeam antennas. Phased-array feeds will be needed to minimize weight and power consumption and to enhance reliability. Methods for generating and isolating hundreds of beams should be studied and integrated with the feed developments.

Onboard processing is a recurring theme in future systems, although it varies in complexity. A baseband processor will serve as an appropriate start and can be extended to serve the needs of several systems. For example, communication links between satellites will enable domestic satellites to connect to international satellites; with onboard switching, international calls could readily be routed by direct dialing. For personal communication, however, an order-of-magnitude increase in circuit capacity will be needed.

For personal communication and one version of an "orbiting-switchboard" VSAT satellite, narrow-band uplinks will be necessary to minimize the complexity and the effective isotropic radiated power of used transmitters. Therefore bulk demodulation will be needed to avoid the weight and power consumption of thousands of discrete demodulators.

This work was done by William A. Poley, Grady H. Stevens, Steven M. Stevenson, Jack Lekan, Clifford H. Arth, James E. Hollansworth, and Edward F. Miller of **Lewis Research Center.** *Further information may be found in NASA TM-88867 [N87-16300/NSP], "An Assessment of the Status and Trends in Satellite Communications 1986-2000."*

Copies may be purchased [prepayment required] from the National Technical Information Service, Springfield, Virginia 22161, Telephone No. (703) 487-4650. Rush orders may be placed for an extra fee by calling (800) 336-4700. LEW-14548

Studies of Single-Event-Upset Models

Experimental data are correlated with computer simulations.

A report presents the latest in a series of investigations of "soft" (nonpermanent) bit errors known as single-event upsets (SEU), which are induced in logic circuits by ionizing radiation. In this investigation, the SEU response of a low-power, Schottky-diode-clamped, transistor/transistor-logic (TTL) static random-access memory (RAM) was observed during irradiation by Br and O ions in the energy ranges of 100 to 240 and 20 to 100 MeV, respectively. The experimental data complete the verification of the computer model used to simulate SEU in this circuit.

The objective of this research is a method for the computer simulation of the susceptibilities of integrated circuits to SEU, for use by the designers of such circuits. Computer models of the TTL RAM circuit in question and of other circuits had been developed with the SPICE computer program. Previous experiments had begun the verification of the TTL RAM model. According to this model, each event is represented by current injection in the macromodel of the device struck by the ionizing particle. The charge collected from each ion track is estimated by consideration of the geometrical features of the device and the range-versus-energy characteristics of the ion species in question.

The Br and O ion beams for the experiments were generated in a Van de Graaff accelerator, filtered, and aimed at the circuit to probe the SEU response at various beam energies, angles of incidence, and points of incidence. The resulting data show that SEU behavior depends strongly on both the location of an ion track in a bipolar transistor and the voltage applied to the transistor during irradiation (i.e., whether it represents an addressed or unaddressed memory element).

The data show that for purposes of the computer simulation model, the threshold for SEU is best described by a critical charge, rather than by a threshold value of the linear energy transfer (a measure of loss of energy by the ion along its track in the device). The calculation of soft-error rates of a given RAM in a given radiation environment must take account of multiple thresholds for different sensitive regions and the bias voltages of the bipolar transistors in the RAM.

The SPICE model accurately predicts the critical-charge values and is slightly conservative when used to predict SEU for design purposes. To afford the best protec-

tion against and to make accurate predictions of SEU, circuit designers must know the diffusion profiles and the sizes and shapes of circuit features.

Future circuits and devices will probably not be examined as thoroughly as this one was. In many cases, it may be more productive to evaluate new types by computer modeling and verifying the models indirectly by testing standard circuits made by specified design rules and fabrication processes.

This work was done by J. A. Zoutendyk, L. S. Smith, and G. A. Soli of Caltech for **NASA's Jet Propulsion Laboratory.** *To obtain a copy of the report, "Single-Event Upset (SEU) Model Verification and Threshold Determination Using Heavy Ions in a Bipolar Static RAM." Circle 15 on the TSP Request Card. NPO-16735*

Adaptive Control for Flexible Structures

Measurement noise would be filtered without introducing instability.

A paper discusses ways to cope with measurement noise in an adaptive control system for a large, flexible structure in outer space. The system would generate control signals for the torque and thrust actuators to turn all or parts of the structure to desired orientations while suppressing torsional and other vibrations that would arise from controlled and uncontrolled motions. The main result of the paper is a general theory for the introduction of filters to suppress measurement noise while preserving stability.

A typical adaptive control law for a flexible structure includes proportional and integral components of the control gain. The integral control law acts to integrate, over time, a quantity proportional to the square of the measurement noise. Because this quantity is zero or positive, the integration inevitably creates an undesired drift in the integral component of the gain. In addition, the direct feedback of the measurement noise degrades the adaptive performance.

Earlier research showed that leakage terms can be appended to the adaptive control law to eliminate drifts in the adaptive gain, but the control demand remains unrealistically high. Filters can be introduced at critical positions in the adaptive configuration to reduce the control demand, but the arbitrary choice and placement of filters can give rise to instabilities via the filter lags.

To overcome the inadequacies of the previous approaches, the authors present a new algorithm and the new concept of branch filtering. The most natural solution is to insert a measurement-noise filter in the output—directly after the point in the signal-flow path at which the noise is generated—and to use the filtered measurement-error signal as a component of feedback. In practice, the requirement of global stability of the adaptive algorithm is very difficult to satisfy because the phase lag of the output filter adds to that of the controlled structure. However, both the phase lag and the noise-squaring bias are avoided by filtering only a single branch of the output error that feeds into the adaptive control law. This approach is called "branch filtering."

Versions of an adaptive control algorithm were tested by numerical simulation of its effects on a four-panel planar space station. The system was represented by a simplified mathematical model of 19 degrees of freedom. Also for simplicity, the actuators and sensors were treated as co-located pairs, and the sensor bandwidths and actuator dynamics were not considered. The algorithm performed better when augmented with branch filtering than it did when augmented with prior techniques for coping with noise and instability.

This work was done by David S. Bayard, Che-Hang Charles Ih, and Shyh Jong Wang of Caltech for **NASA's Jet Propulsion Laboratory**. *To obtain a copy of the report, "Adaptive Control for Flexible Space Structures With Measurement Noise," Circle 71 on the TSP Request Card. NPO-17115*

It's what you can't see...

...that makes Rantec standard power supplies FULL-MIL qualified.

☐ **FACT:** The development of a custom "military" power supply has high risk and a long lead time.

☐ **FACT:** "Quasi-Mil" standard products are filling the time constraint needs of FULL-MIL schedules and are often misapplied to production runs.

☐ **FACT:** Long on the drawing boards, the military has finally taken steps to eliminate gross design and specification negligence (i.e. NAVMAT P4855-1, NAVSO P3641).

Looking at the surface of a power supply, it's hard to tell if it's qualified to FULL-MIL specs.

Lots of manufacturers can meet some MIL-SPECS but not FULL-MIL. The specs may even mislead you by including a few JAN components to semi-qualify to published standards. Some even encapsulate the unit so you can't see its weaknesses.

With Rantec, you are assured a standard, FULL-MIL, JAN type, tri-service qualified power supply that meets MIL-Q-9858A for reliability systems and MIL-STD-454 for workmanship standards—without the lengthy lead times, costly non-recurring engineering charges and disappointments associated with customs. We've done it on the ANUYQ-21, TRIDENT, SSN688, EF111, A6 and TRQ-32 programs, to name a few.

Don't sacrifice the integrity of your system with HALF-a-MIL™ power supplies. Insure power supply reliability with Rantec.

Contact us today.

GET THE FACTS

As a guide to optimizing power in your system design ask for your **FREE** copy of Rantec's "How to Specify FULL-MIL Spec Power Supplies: A Guide for Getting Around the Traps of HALF-a-MIL Specifications."

rantec®

EMERSON

Rantec/Power Systems • Division of Emerson Electric Co. • Department FS
9401 Oso Avenue, Chatsworth, CA 91311 • TEL: (818) 885-8223 • TWX: 910-493-1247 • FAX: 8189937780

Circle Reader Action No. 571

Sectioning Coated Specimens Without Edge Rounding

A mounting method combines rigidity for polishing with conductivity for electron microscopy.

Marshall Space Flight Center, Alabama

A new method has been devised for the preparation of cross sections of coated specimens for scanning electron microscopy (SEM) or energy-dispersive analysis (EDAX) without rounding of the edges of the coatings. After cutting and polishing, a specimen section remains smooth and flat so that it can be examined under high magnification out to the edge of the coating.

The method was developed for examining the microstructure of low-pressure-plasma-sprayed coatings on turbine blades. The cross section of the blade must be mounted in a conductive material for SEM or EDAX. Previously, the section was fully encapsulated in conductive material. However, the coating, sandwiched between the hard blade substrate and the soft encapsulant, became rounded when it was polished.

In the new method, the sectioned blade is first electroplated with hard nickel 0.003 in. (76 μm) thick. It is then encapsulated in two layers of material: the soft conductive material at the bottom and 0.25 in. (6.4 mm) of hard diallyl phthalate at the top (see figure). The surface of the section can then be polished without danger of rounding because the outer edge of the coating is supported by the nickel plate and the hard compound. The nickel plate provides an electrical path from the surface of the section to the conductive material below.

Two sections can be encapsulated and polished together to speed up specimen preparation. Moreover, less conductive material is needed in the two-layer mounting, so costs are reduced.

This work was done by Timothy N. McKechnie of Rockwell International Corp. for **Marshall Space Flight Center**. *For further information, Circle 144 on the TSP Request Card.*

Inquiries concerning rights for the commercial use of this invention should be addressed to the Patent Counsel, Marshall Space Flight Center [see page 12]. Refer to MFS-29228.

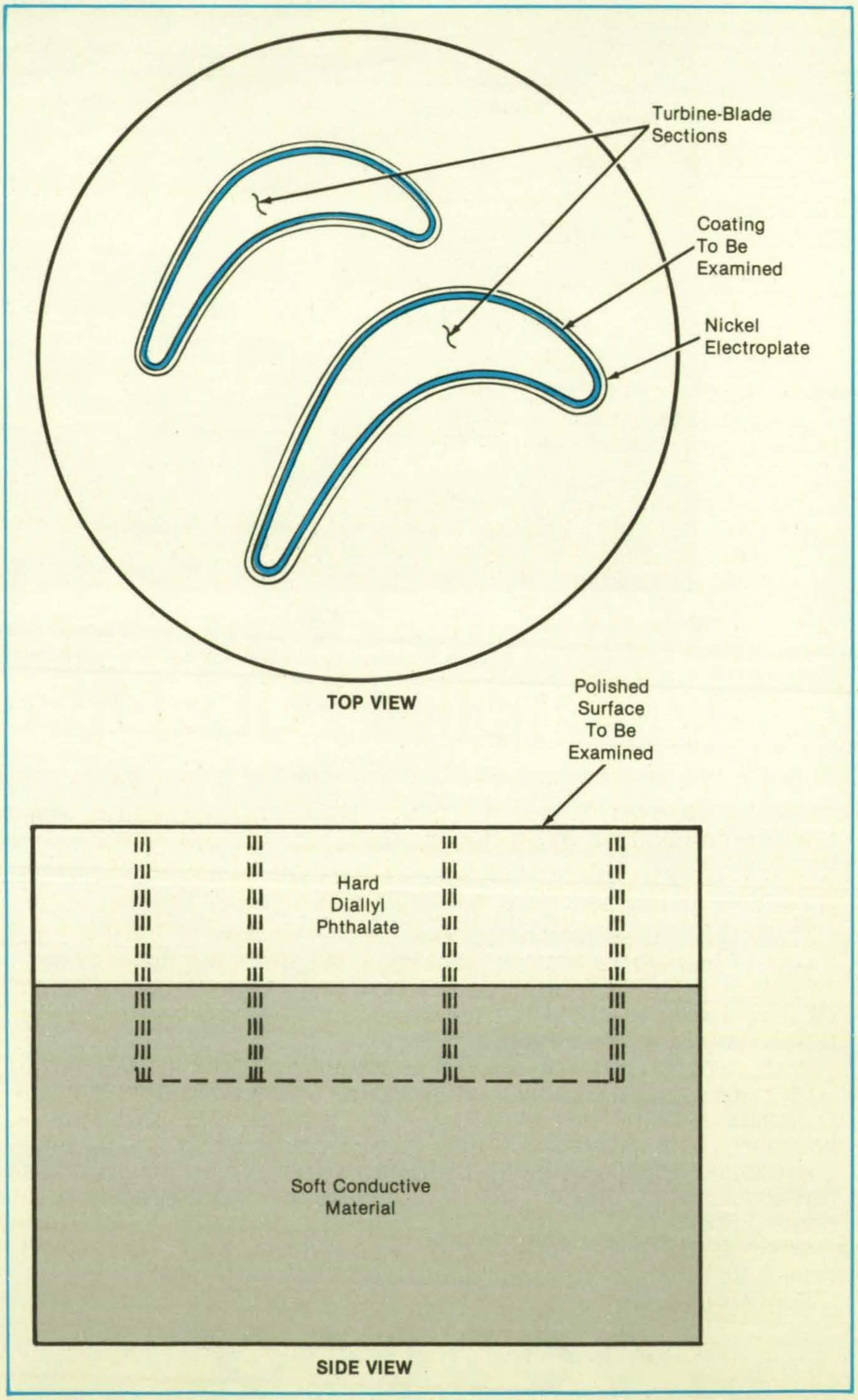

Embedded in a Hard Plastic, a pair of coated turbine-blade sections are ready for electron microscopy. A thin layer of nickel joins the blade coating electrically to a conductive layer at the base of the specimen.

SCHOTT GLASS... HELPING OUR WORLD SEE OTHER WORLDS

Precision Optical Glass of uncommon dimensions.

When the University of Pittsburgh's Allegheny Observatory was developed around the turn of the century, Schott was the only company capable of making the lens blanks for the Observatory's refracting telescope. Three quarters of a century later, that telescope is still the third largest in the world.

Today, as the lenses of that refracting telescope are being replaced, glass from Schott Glass Technologies — a United States company — is the choice.

In fact, Dr. George Gatewood, director of the llegheny Observatory, said that there wasn't uch of a choice at all. "Schott is the only comany in the world capable of producing the glass e need for our refracting telescope lenses."

He's not alone in his thinking. Becau Schott's world-wide involvement and a winning Research and Development de ment, Schott glass has been chosen for many of the most advanced optical system has ever known. Including some of the w biggest stargazers; like the University of burgh's Allegheny Observatory.

Schott Glass Technologies is a United manufacturer of many types of glass. If involved in astronomy, space exploration, space, precision measurements or optics, can help you with the right glass for thes many other fields.

SCHOTT
GLASS TECHNOLOGIES INC

400 York Avenue
Duryea, Pennsylvania 18642
(717) 457-7485 TWX 510-671-4535
Telefax (717) 457-6960

Circle Reade

Computer-Aided Goniophotometer

Repetitive measurements are made more rapidly, with greater accuracy.

Goddard Space Flight Center, Greenbelt, Maryland

A computer-compatible scanning goniophotometer enables the semiautomatic measurement of the angular uniformity of an integrating hemisphere or other large-aperture light source. The scanning mechanism eliminates the need to locate the photometer manually at each different viewing angle, using squares, protractors, and other gauges; the manual procedure was both tedious and prone to error.

The photometer has a 1° circular field of view. It is held by a parallelogram linkage (see Figure 1) that keeps it pointed at the center of the aperture of the light source while it is moved to different viewing angles. The parallelogram linkage is connected to an x-y plotter through a drive arm. The outer end of the parallelogram is scanned in x by the horizontal motion of the x arm of the plotter and in y by the vertical motion of the plotter. The drive arm slides in sleeve bearings to allow the photometer to move freely and remain at a constant radius from the center of the aperture (which is also the center of rotation).

Under the control of a computer, the photometer takes measurements at many angular positions along the raster generated by the motion of the x-y plotter. While the vertical position is held constant, the linkage is scanned horizontally over the interval of ±32° from the perpendicular to the aperture. The y position is then changed by one interval and the x scan repeated.

Altogether, the televisionlike raster generated by the plotter motion contains 50 horizontal lines (see Figure 2) corresponding to 50 different vertical positions. During the analysis of the measurements, the angular coordinates are easily recovered from x and y coordinates by calculating the projection of the flat x-y raster onto a sphere along the radius from the photometer to the center of rotation.

The scanning goniophotometer is not only less cumbersome than a manual one to set up: it is more precise, provides more data in less time, and requires a minimum of time to change to a different light source. There is no physical connection between axis of rotation of the sensor and the position of the source. Automatic operation and computer control enable the variation of the raster size, scanning speed, sampling rate, and the type of data displayed.

This work was done by Richard G. Holt of **Goddard Space Flight Center**. *For further information, Circle 141 on the TSP Request Card.*
GSC-12991

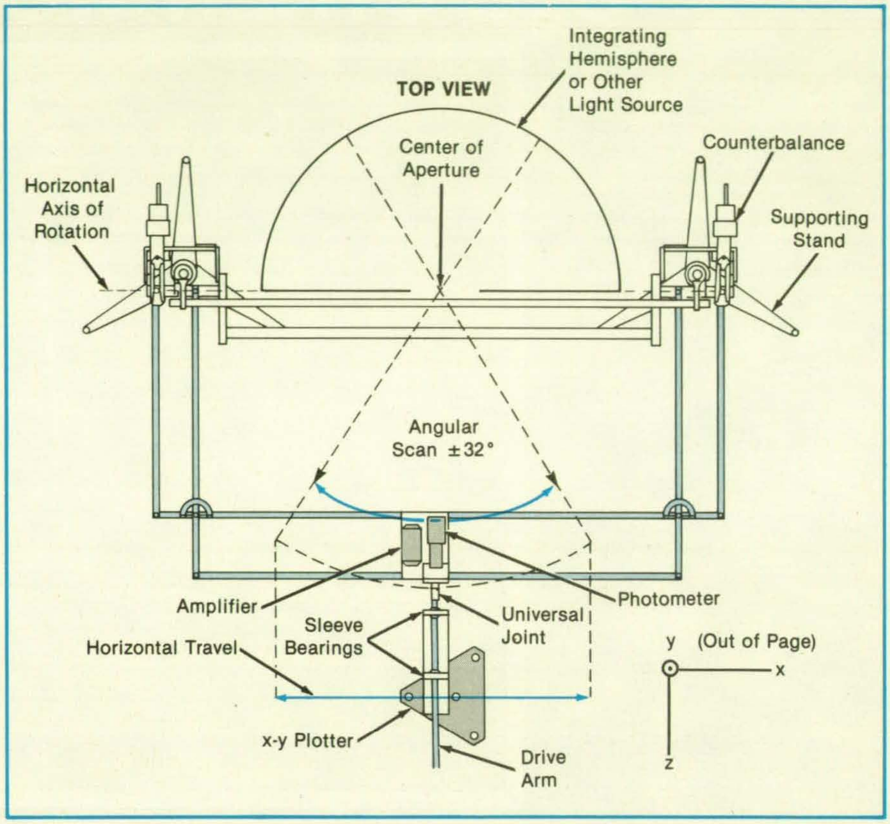

Figure 1. The **Scanning Mechanism** keeps the photometer pointed at the center of the aperture while moving it to different viewing positions.

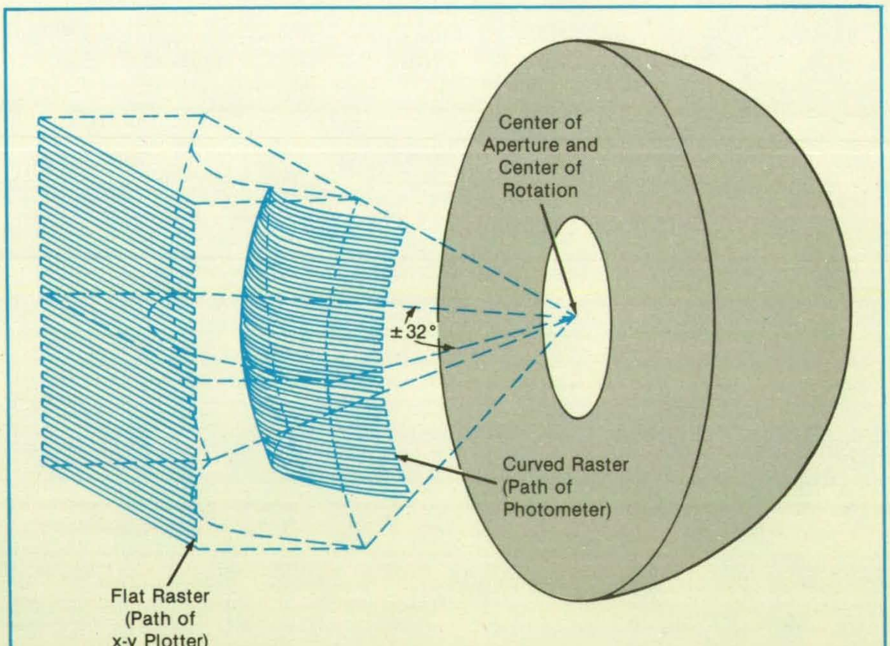

Figure 2. The **Scanning Motion** of the x-y plotter forms a raster in a vertical plane. The viewing angles represented by the raster can be visualized by simply drawing a line from a desired point on the raster to the center of the aperture.

Optical Alignment Device for Laser Communication

Alignment can be performed continuously during operation.

NASA's Jet Propulsion Laboratory, Pasadena, California

An optical alignment device under development should enable the continuous tracking and coalignment of two beams of light. It is intended primarily for a laser-communication station, in which the transmitted beam must be aligned with the received beam to ensure that the transmitted beam falls on the receiver at the other station. The device is expected to consume less power and to be smaller and less complicated than the alignment shutter and drive previously used. The shutter-type system did not permit reception during the alignment periods.

The transmitted and received beams can be distinguished by different polarizations, different wavelengths, or both. The overlapping collimated beams pass through a prism (see figure). One of the beams emerges from the prism at the output end, and one is reflected back toward a mirror near the input end. This separation of the beams can be accomplished either by a dichroic filter (in the case of wavelength distinction) or by a polarization beam-splitting cube or filter (in the case of polarization distinction).

The internally reflected beam emerges from the output end of the prism displaced laterally from the beam that passes through directly. Both emerging beams are focused by a lens onto a charge-coupled imaging device (CCD). Associated electronic circuits extract the coordinates of the two beam points on the CCD and use them as control signals for the laser-beam-aiming mirrors.

The device is expected to work even when the transmitted and received beams differ in wavelength by as little as 20 Å. It should also be possible to use the device to align a wide-band light source with a narrow-band light source embedded in it.

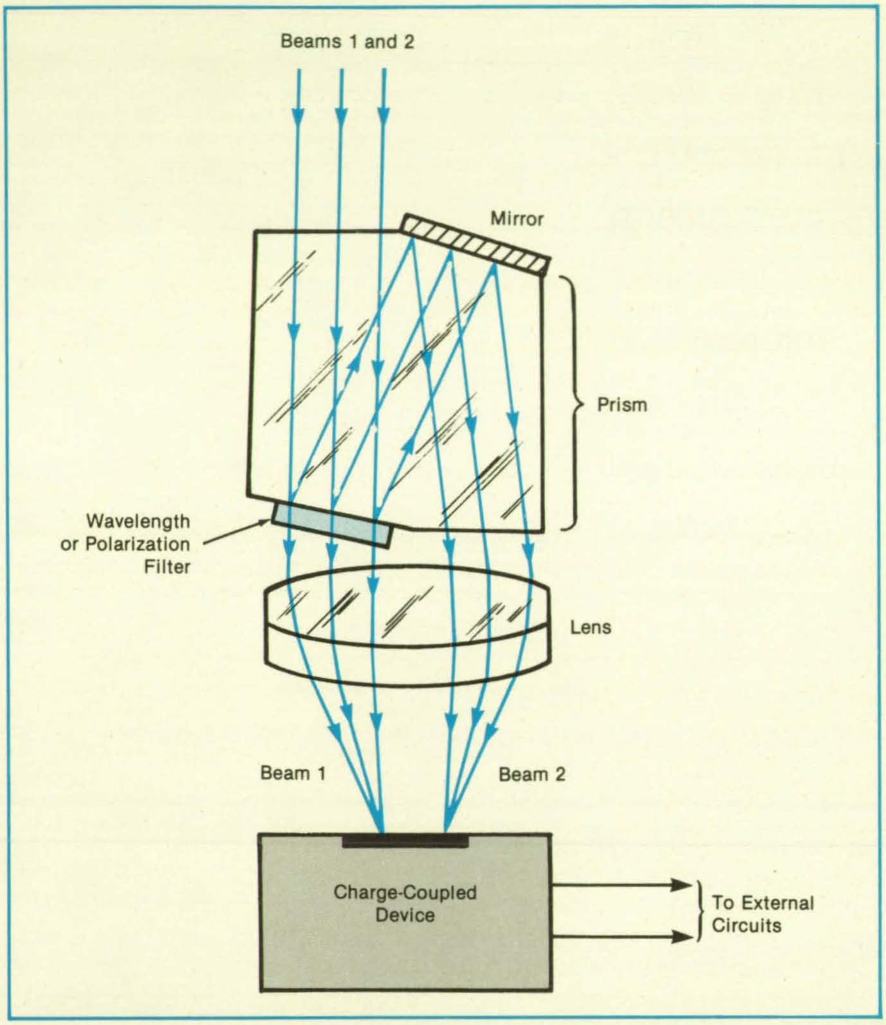

A **Prism and Filter** separate two overlapping collimated light beams of different wavelength or polarization. The coordinates of the two beams are tracked on the charge-coupled device to determine the degree of directional misalignment between the two beams.

This work was done by William L. Casey of McDonnell Douglas Corp. for **NASA's Jet Propulsion Laboratory**. *For further information, Circle 123 on the TSP Request Card. NPO-16774*

Calibration of Oxygen Monitors

Readings are corrected for the temperature, pressure, and humidity of the air.

Langley Research Center, Hampton, Virginia

A program for a handheld computer has been developed to ensure the accuracy of oxygen monitors in the National Transonic Facility (NTF), where liquid nitrogen is stored. Calibration values, determined daily, are based on entries of data on the barometric pressure, temperature, and relative humidity. The output is provided directly in millivolts.

Operations at the NTF require the storage and pumping of large volumes of liquid nitrogen. To protect against the possibility of a fault resulting in a local oxygen-deficient atmosphere, the facility is equipped with a monitoring system with an array of sensors. The system is designed to provide a local alarm at a first-level oxygen-deficiency indication and a general alarm if the deficiency progresses to a second level.

During the early operational stages, the system produced recurrent alarms, none of which could be traced to a true oxygen deficiency. A thorough analysis of the system was made with emphasis on the sensor units. These units sense the partial pressure of oxygen, which, after signal conditioning, is presented as a percent-by-volume indication at the system output. It was determined that many of the errone-

What the PC did for computing, GoldWorks™ now does for expert system building.

Remember computing before the PC?

Climate-controlled rooms behind "Restricted Area" signs. DP gurus speaking a language nobody else knew. Mystified end-users. Then technology evolved, the PC emerged and serious desktop computing became affordable. The economics of computing changed forever.

Now, GoldWorks uses PCs to transform the economics of expert system building.

On your 286- or 386-based PC, **GoldWorks** offers the functionality and power of high-end expert system tools, plus the ease of use and low cost of PC shells. With **GoldWorks**, you can *develop and deliver* serious expert systems *cost-effectively.*

"...allows us to leverage thousands of installed PCs..." –Dr. David Shpilberg, Coopers & Lybrand

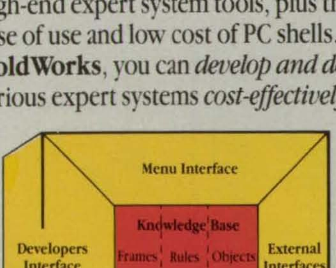

GoldWorks is the most powerful expert system tool available on PCs.

With GoldWorks, you don't have to compromise.

Easy-to-use shells run on PCs, but lack real functionality. Powerful high-end tools can't integrate with existing PC applications or deliver expert systems on PCs. GoldWorks combines the best features of both.

"...a powerful combination of expert system development and end-user support." –Bruce M. Gras, Arthur D. Little, Inc.

It's as easy to use as a shell...

The Menu Interface lets you prototype and build expert system applications fast, without knowing the underlying programming environment. On-line help and tutorials make you productive quickly.

...and as function-rich as a high-end tool.

GoldWorks offers frames, rules, object programming and powerful control mechanisms, just like the high-end tools. And GoldWorks runs on advanced PCs, so expert systems you build can be *delivered* cost-effectively to end-users.

"...power comparable to ART or KEE..." –Kenneth Levine, Lekton, Inc.

GoldWorks lets you integrate with existing PC programs.

You can integrate expert systems with dBASE III, Lotus 1-2-3 and C...plus build and deliver expert systems in network environments.

See this powerful, flexible tool for yourself. Order the GoldWorks Demonstration Kit.

You'll get an 18-minute videotape, showcasing many GoldWorks features in a sample application. You'll also receive a copy of the actual 282-page Expert System User's Guide that comes with **GoldWorks**. We'll credit your $49 to your **GoldWorks** purchase.

"Any Fortune 1000 organization can easily cost-justify...this tool." –Randy Reiter, Athena Group

For more information, or to order, call toll-free:

1-800-242-5477.

In Mass., call (617) 492-2071.

GoldWorks from Gold Hill. The expert in AI on PCs.

GOLD HILL™

Gold Hill Computers, Inc.
163 Harvard Street
Cambridge, MA 02139

Circle Reader Action No. 465

ous indications were due primarily to a lack of proper accounting for the relationship between the partial pressure and the percent by volume and were due secondarily to premature failure of the sensors.

The technology developed in response to these findings consists mostly of a method for properly accounting for those atmospheric variables, primarily the barometric pressure and the relative humidity, that influence the output of the sensors. In addition, techniques for rebuilding sensors were examined, and those elements contributing to the failure of pressure sensors were identified.

To simplify the daily routine of determination of the actual percent oxygen by volume as affected by the barometric pressure and water-vapor content, the necessary calculations were committed to a computer program. Persons responsible for the calibration of the system use a handheld computer that requires entries of the barometric pressure, temperature, and relative humidity. The computer output is presented directly in terms of the sensor output in millivolts, requiring no further conversion to arrive at the true daily calibration value. This effort has essentially eliminated false alarms, and the system now operates with a high degree of confidence and reliability.

This work was done by M. A. Zalenski, E. L. Rowe, and J. R. McPhee of Wyle Laboratories for **Langley Research Center**. *Further information may be found in NASA CR-3953 [N86-17359/NSP], "Operational Considerations in Monitoring Oxygen Levels at the National Transonic Facility".*

Copies may be purchased [prepayment required] from the National Technical Information Service, Springfield, Virginia 22161, Telephone No. (703) 487-4650. Rush orders may be placed for an extra fee by calling (800) 336-4700.
LAR-13619

Imaging of Directional-Solidification Interfaces

The movements and shapes of interfaces are revealed during crystal growth.

Langley Research Center, Hampton, Virginia

An x-ray and gamma-ray technique developed at NASA Langley Research Center enables the melt/solid interface to be observed visually during crystal growth by directional solidification in a Bridgman furnace. This technique has been used to observe the movement and shape of the interface in germanium and in lead tin telluride.

It is known that the shape of the interface during the solidification of a semiconductor crystal significantly alters such final properties of the crystal as the impurity distribution, stress, and defect density. Heretofore, the correlation between interface shapes and crystal properties has been limited to only a few semiconductor materials and by the necessity of performing all analyses after the growth was over. Therefore, there is a need for a general in situ method of determining the shape of the interface.

Two experimental semiconductor materials were used as test substances during the development of the new experimental procedure. Germanium was selected primarily because it is representative of semiconductor elements of relatively low molecular weight and low atomic number and thus is penetrated by x rays. Lead tin telluride was selected as the second test material primarily because it is representative of ternary-compound semiconductors that contain elements, especially lead, that are high in molecular weight and atomic number and thus require gamma rays to penetrate the material.

The figure shows the apparatus used in this technique. By the adjustment of the temperature field between the upper and lower isothermal regions of the furnace, the interface is moved but is kept within the insulation zone of the furnace. The difference in densities between the transmitted-x-ray images of the liquid and solid phases is greater than 2 percent, and therefore the position of the interface can be detected. Observations of the germanium and lead tin telluride samples track the interface through new positions as a consequence of increasing the temperature in the lower isothermal region, which produces meltback at the interface. When lead tin telluride is grown vertically downward, i.e., hot-on-the-bottom, it develops a central void along its length, which also has been followed by the use of this gamma-ray technique.

This new experimental technique now makes melt/solid interfaces visible to researchers during crystal growth. It should prove to be a valuable tool in efforts to grow seeded semiconductor materials in Bridgman furnaces.

This work was done by Archibald L. Fripp, Jr., William J. Debnam, Jr., and Robert F. Berry of **Langley Research Center**; *Roger K. Crouch of NASA Headquarters; Patrick G. Barber of Longwood College; and Richard Simchick of PRC Kentron, Inc. For further information, Circle 4 on the TSP Request Card.*

Inquiries concerning rights for the commercial use of this invention should be addressed to the Patent Counsel, Langley Research Center [see page 12]. Refer to LAR-13597.

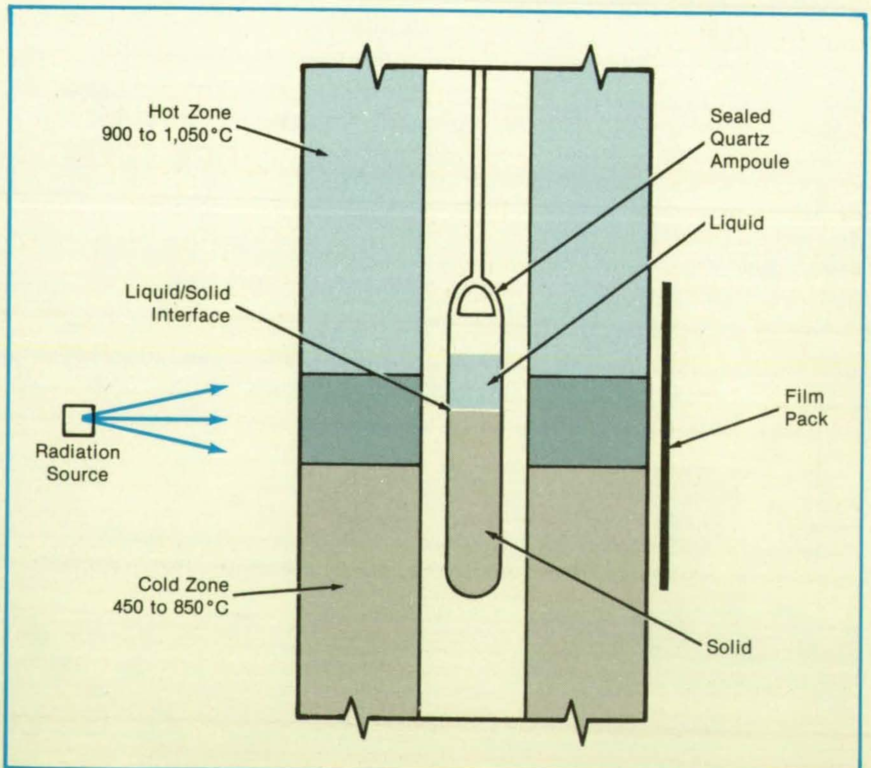

The **Interface Between the Liquid and the Solid** can be seen in an x-ray photograph because the liquid and solid have different x-ray-attenuation densities.

Loss-Compensated Optical Sensor Systems

Variations in fiber losses have little effect on outputs.

Lewis Research Center, Cleveland, Ohio

A fiber-optic sensing system that is conceptually related to the electrical bridge circuit is scarcely affected by variations in the losses of optical fibers and connectors. Versions of the system have been investigated for use as linear- and angular-position sensors for advanced aircraft controls. Position accuracies of 8 to 10 bits may eventually be achieved.

The heart of the generic system (see Figure 1) is a beam-splitting transducer, the splitting ratio of which varies as a function of magnitude of the sensed parameter. The light from two light-emitting diodes (LED's) is carried by two optical fibers to the opposite faces of the transducer. The light transmitted and reflected by the transducer is carried through another two optical fibers to two photodiodes.

The LED's are switched on and off alternately, and the resulting photodiode outputs are time-demultiplexed to obtain the transmission and reflection measurements. These measurements are digitized and processed to obtain the ratio Y:

$$Y = (T_A T_B / R_A R_B)^{1/2}$$

where $T_{A(\text{or } B)}$ is the output of photodiode U (or V) when receiving light transmitted through the transducer from LED A (or B), and $R_{A(\text{or } B)}$ is the output of photodiode U (or V) when receiving light from LED A (or B) by reflection from the transducer.

With suitable assumptions regarding the insensitivity of the system to the modal distribution of the light, the ratio is also given by

$$Y = (t_A t_B / r_A r_B)$$

where t_A, t_B, r_A, and r_B denote the transmission (t) and reflection (r) coefficients of the transducer for the corresponding measurements T_A, T_B, R_A, and R_B, respectively. Because the loss coefficients of the optical fibers and fiber connectors do not appear in this equation, Y is unaffected by changes in these losses; for example, changes due to the reconnection, bending, or replacement of fibers.

The transmission and reflection coefficients are known functions of the magnitude of the sensed parameter, either by design or by calibration. Thus, the system output signal Y can be interpreted in terms of this physical variable. Measurements on an angle sensor like that of Figure 2 confirm the assumption that Y is a highly stable function of position; for example, the disconnection and reconnection of fibers before each of 50 measurements caused a standard deviation of 0.2° in the angle measurement, representing about 0.7 percent of full scale.

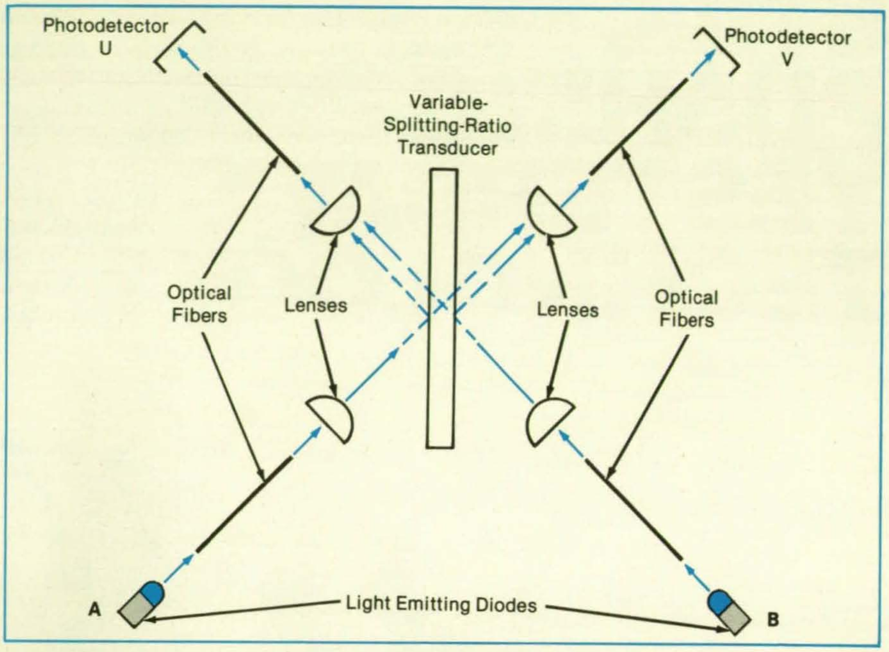

Figure 1. In the **Generic Loss-Compensated Optical Sensor**, light is generated alternately by two LED's. Two photodiodes measure the light reflected from, and transmitted through, the transducer.

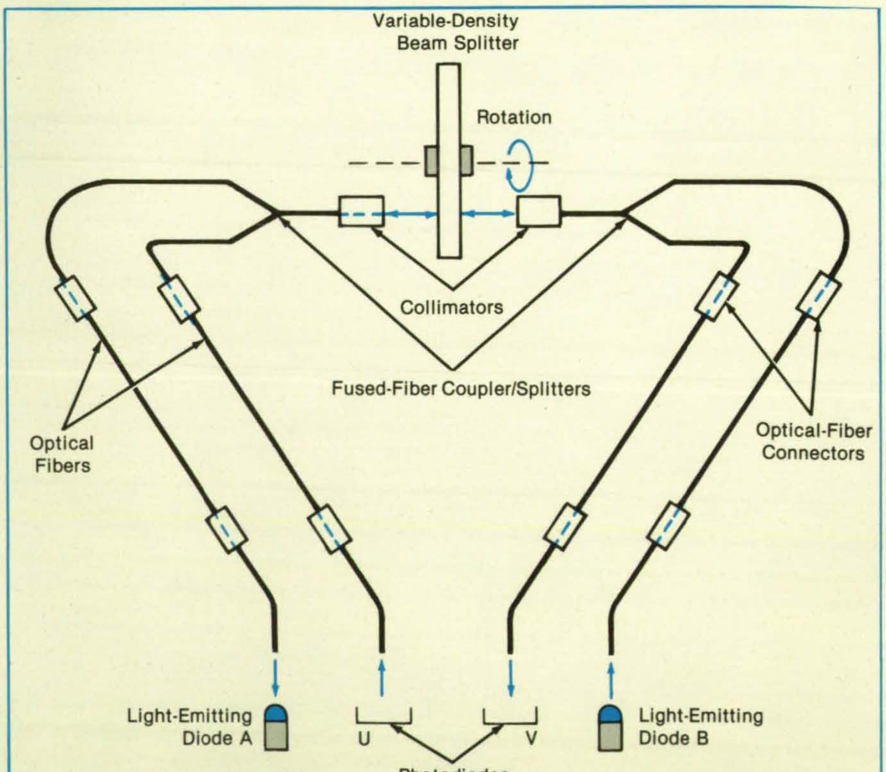

Figure 2. The **Loss-Compensated Optical Angle Sensor** operates on the principle of the generic sensor shown in Figure 1. The transducer is a rotating beam splitter, the optical density of which varies from 0 to 2.0 as a monotonic function of its angle of rotation.

This work was done by Glenn Beheim of **Lewis Research Center** *and Donald J. Anthan of Cleveland State University. Further information may be found in NASA TM-88825 [N87-13637/NSP], "Loss-Compensation of Intensity-Modulating Fiber-*

Optic Sensors."

Copies may be purchased [prepayment required] from the National Technical Information Service, Springfield, Virginia 22161, Telephone No. (703) 487-4650. Rush orders may be placed for an extra fee by calling (800) 336-4700.
LEW-14547

High-Resolution Detector for X-Ray Diffraction

A conceptual unit would have scientific, medical, and engineering uses.

Marshall Space Flight Center, Alabama

A proposed x-ray-sensitive imaging detector would offer superior spatial resolution, counting-rate capacity, and dynamic range. Unlike the multiwire xenon-filled detectors and television detectors currently used, the proposed instrument would be based on laser-stimulated luminescence and reusable x-ray-sensitive film.

The new area detector would be used primarily for protein crystallography. Its small size and convenience would enable the determination of the three-dimensional structure of single-crystal proteins immediately after growth, before the crystals deteriorate. The principle can be adapted to imaging detectors for electron microscopy and fluorescence spectroscopy and for general use in astronomy, engineering, and medicine.

The principal elements of the proposed detector are a recently-developed, reusable x-ray-sensitive film and a scanning assembly (see figure). The film contains BaFBr:Eu^{+3} phosphor, which stores a latent image for several hours after exposure to x rays. When the film is illuminated by visible light, the phosphor gives up its stored image by glowing at a wavelength of 390 nm with an intensity proportional to the x-ray energy absorbed.

According to the concept, the detector would scan the exposed film with light from a helium/neon laser and simultaneously collect the laser-induced luminescence with a linear array of charge-coupled devices. The scanning assembly would be moved across the film by a stepping motor in increments of 10 μm. The signal from the charge-coupled devices would be processed by a counter, digitized, and displayed on a high-resolution graphical system. The digitized signal would also be stored on magnetic tape as a quantized image. After the film had been scanned, it would be ready for a new exposure.

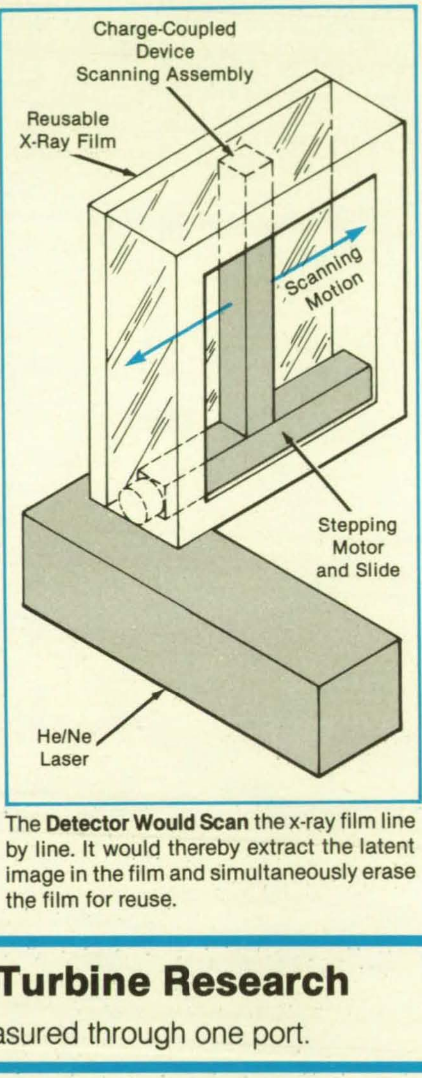

The **Detector Would Scan** the x-ray film line by line. It would thereby extract the latent image in the film and simultaneously erase the film for reuse.

The detector would have a spatial resolution about equal to the scanning step of 10 μm — adequate for the examination of macromolecular crystals formed by assemblies of enzyme complexes and virus particles. It could be placed close to the diffracting crystal so that the data could be collected in a short time, and the overall size of the diffraction apparatus could be reduced.

This work was done by Daniel C. Carter, William K. Withrow, Marc L. Pusey, and Vaughn H. Yost of **Marshall Space Flight Center**. *For further information, Circle 145 on the TSP Request Card.*

Inquiries concerning rights for the commercial use of this invention should be addressed to the Patent Counsel, Marshall Space Flight Center [see page 12]. Refer to MFS-28232.

Laser Anemometer for Turbine Research

Three velocity components are measured through one port.

Lewis Research Center, Cleveland, Ohio

A laser anemometer measures radial, axial, and circumferential gas-velocity components in a turbine stator. The measurements are made through a small cylindrical window that is typical of the restrictions on access to the flow passages of working turbomachinery.

The anemometer uses the standard intersecting-beam, laser-fringe anemometer configuration with fluorescent aerosol seed particles entrained in the flow to measure the axial and/or circumferential components of velocity in the plane defined by the intersecting beams. The radial component (along the optical axis, which is radially oriented and bisects the two beams) is measured via the Doppler shift by a confocal Fabry-Perot interferometer.

The source of the probing light beams (see figure) is an argon-ion laser operating at a wavelength of 514.5 nm. A portion of the laser beam is split off and sent to an acousto-optic modulator (Bragg cell), which is used to generate a 400-MHz reference offset from the laser frequency. The remainder of the laser beam is send to a beam divider, which splits the beam into two equally intense parallel beams about 10 mm apart.

The divider is placed in a motor-driven rotary mount so that the plane defined by the two beams and, therefore, the orientation of the interference fringes and consequently the velocity components measured in the probe volume can be controlled. A half-wave-retardation plate, gear-driven by the rotary mount at half the rotation of the divider, maintains the proper linear polarization at the beam-divider input.

Lens 3 brings the beams together in the probe volume. Light from the beams is scattered by the seed particles, both elastically at the laser wavelength and inelastically by fluorescence at a longer wavelength. The scattered light is collimated by lens 3, then passes through an aperture mask with a central stop to reduce the effective radial length of the probe volume. Lenses 4 and 5 reduce the diameter of the collimated scattered light.

A dichroic beam splitter separates the elastically scattered and fluorescent portions of the collimated scattered light. The elastically scattered beam is passed

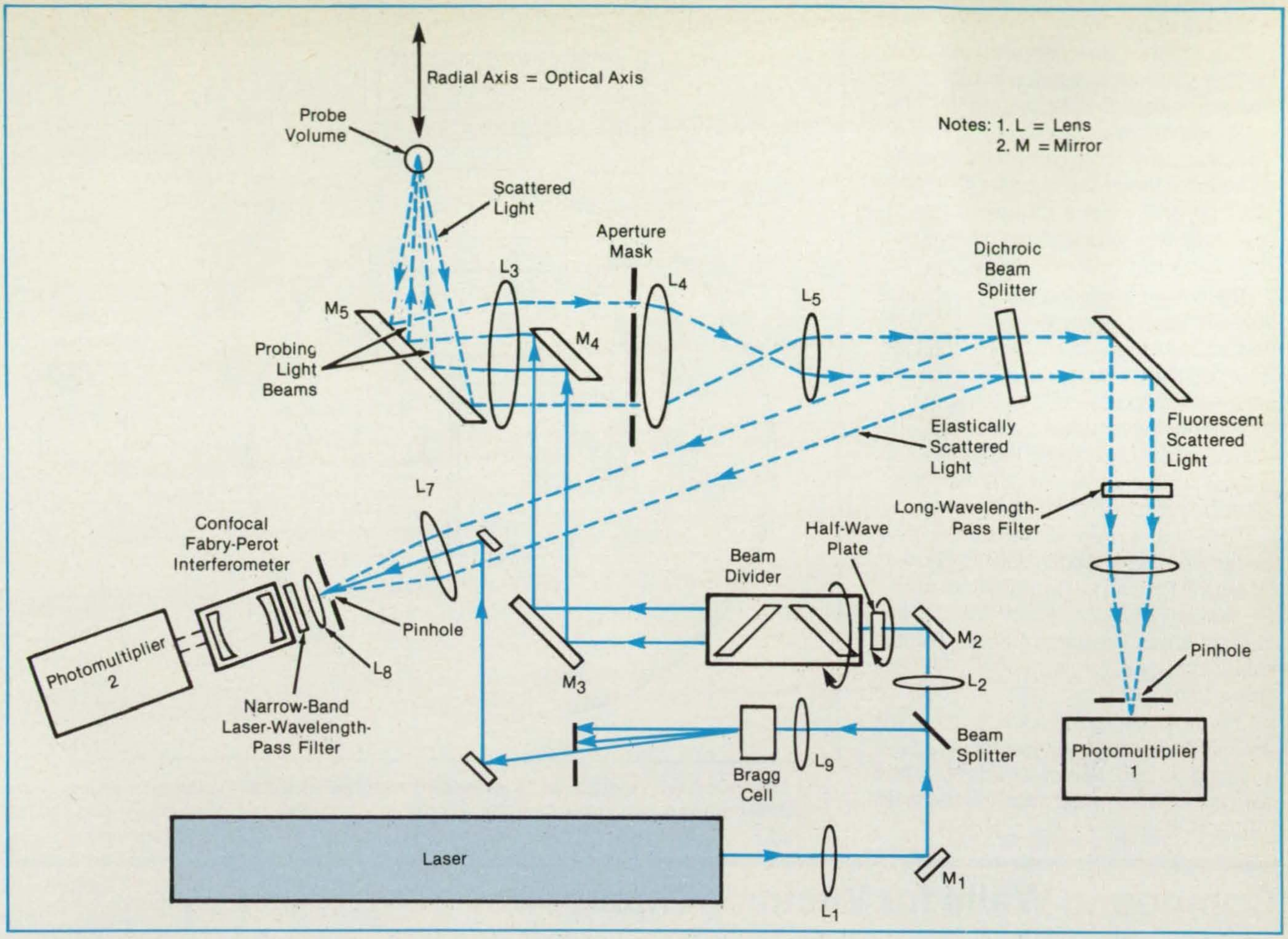

The **Laser Anemometer** combines a conventional interference-fringe anemometer configuration with a Fabry-Perot interferometer to enable the simultaneous measurement of radial and transverse velocities. The transverse-velocity axis can be rotated, thereby enabling the measurement of both transverse-velocity components. Unlike prior systems, this one does not require a large optical-access port for the measurement of the radial velocity.

through a narrow-band filter at the laser wavelength and fed to the confocal Fabry-Perot interferometer and photomultiplier.

The fluorescent light is sent through a long-wavelength-pass filter to suppress the remaining 514.5 nm light. The filtered fluorescent light is focused through a pinhole into a photomultiplier for the measurement of the transverse velocity component.

This work was done by Richard G. Seasholtz and Louis J. Goldman of **Lewis Research Center**. *Further information may be found in NASA TM-87322 [N86-24967/NSP], "Combined Fringe and Fabry-Perot Laser Anemometer for Three Component Velocity Measurements in Turbine Stator Cascade Facility."*

Copies may be purchased [prepayment required] from the National Technical Information Service, Springfield, Virginia 22161, Telephone No. (703) 487-4650. Rush orders may be placed for an extra fee by calling (800) 336-4700. LEW-14513

Laser Doppler Velocimeter System

Seeded flows are measured optically.

Ames Research Center, Mofftett Field, California

A laser Doppler velocimeter measures the seeded airflow in the Ames High Reynolds Channel No. II wind tunnel. Because the wind-tunnel test section must be placed inside a pressure vessel, the velocimeter and the affected portion of the wind tunnel are designed as an integrated system.

The optical system of the velocimeter consists of two groups of components (see figure). The outer group, mounted on top of the tunnel outside the pressure vessel, includes a 5-W, all-spectral-line argon-ion laser and associated optics to form four parallel light beams. Each pair of beams constitutes a channel and one beam in each pair is Bragg-shifted 40 MHz to eliminate the directional ambiguity. The inner group consists of a three-dimensional, computer-controlled scanning mechanism with mirrors, a focusing lens, and receiving optics to collect the light scattered from seed particles entrained in the flow.

The optical Doppler signals from both channels are spatially filtered, then transmitted through a multimode optical fiber 10 m long to receiving equipment outside the pressure vessel. There, the signals are separated by colors and detected by photomultipliers.

The optical system is designed for immunity to the effects of noise, vibration, thermal strain, and pressure strain inherent in wind-tunnel operation. A welded steel frame is mounted on six welded supports on top of the pressure vessel. Brass pads permit relative motion between the pressure vessel and the frame to relieve thermal and pressure strains. A honeycomb optical table 4 by 8 by 1 ft (1.2 by 2.4 by 0.3 m) is placed on the frame. A felt pad 0.5 in. (1.3 cm) thick between the frame and the table decouples and damps high-frequency vibrations. The table and optics are enclosed by a rigid aluminum cover

that serves as a safety shield against the laser beams and protects the optics against dust and noise.

The scanning mechanism is mounted on two rails inside the upper wall of the pressure vessel. One rail locates the inner optics with a V-track and grooved wheels. The other rail is flat to permit lateral sliding for relief of thermal and pressure strains. The inner and outer optical assemblies are fixed relatively by one of the honeycomb-table supports.

The airflow is seeded with polystyrene spheres having diameters between 0.35 and 0.55 μm. The particles are suspended in a solution of water and alcohol and sprayed into the tunnel through a row of atomizers. The sprays are directed to provide adequate coverage of the test volume without contaminating the boundary-layer suction system.

This work was done by H. Lee Seegmiller, Jon B. Bader, John P. Cooney, Anemarie De Young, Ralph W. Donaldson, Jr., William D. Gunter, Jr., and Dean R. Harrison of **Ames Research Center**. *For further information, Circle 13 on the TSP Request Card.*

Inquiries concerning rights for the commercial use of this invention should be addressed to the Patent Counsel, Ames Research Center [see page 12]. Refer to ARC-11679.

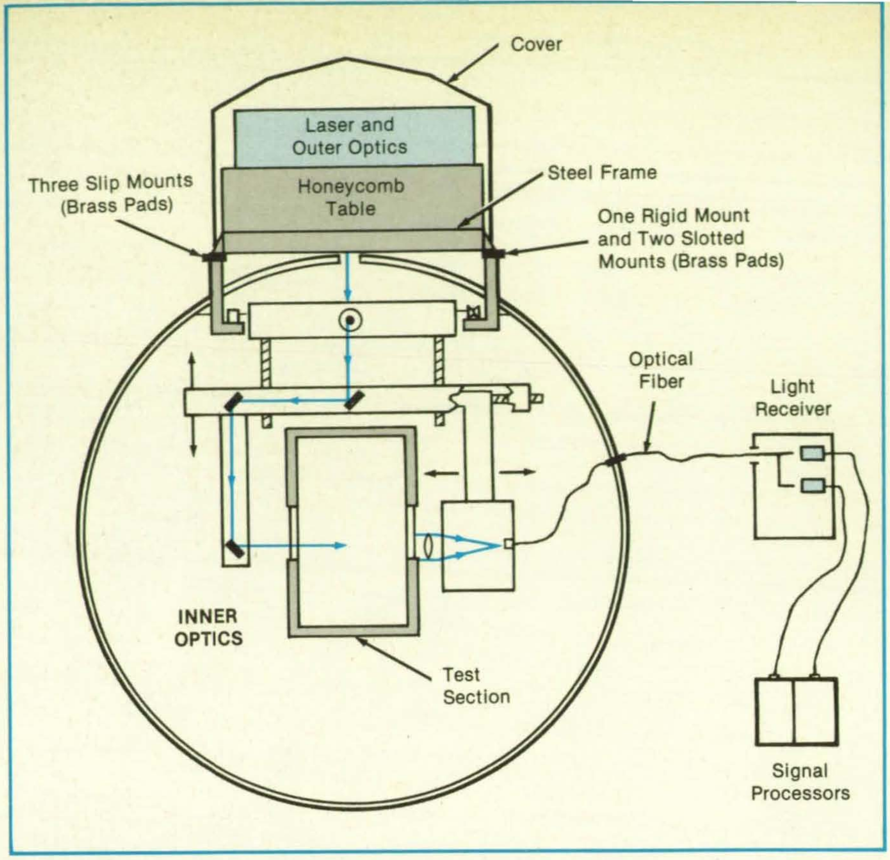

The **Laser Doppler Velocimeter** is integrated with the wind-tunnel pressure vessel with a mounting system that minimizes the effects of vibrations and of pressure and thermal strains.

Compound Walls for Vacuum Chambers

Large chambers would be built relatively cheaply.

NASA's Jet Propulsion Laboratory, Pasadena, California

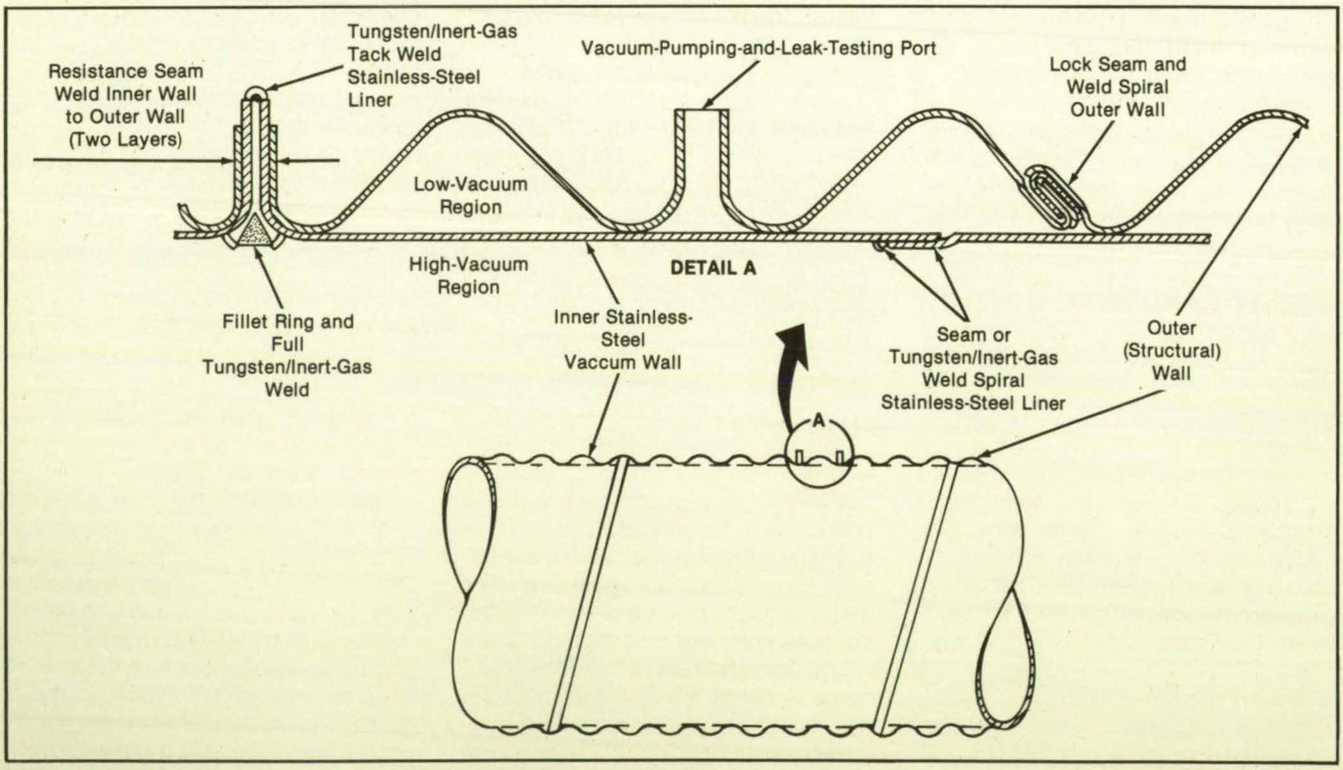

The **Compound Wall** would be made of a strong outer layer of structural-steel culvert pipe welded to a thin layer of high-quality, low-outgassing stainless steel.

A proposed compound-wall configuration would enable the construction of large high-vacuum chambers without having to use thick layers of expensive material to obtain the necessary strength. Such walls could enclose chambers more than 1 m in diameter and several kilometers long; for example, the vacuum pipes of particle accelerators for research in high-energy physics.

The structural strength to resist crushing by the atmospheric pressure of 14.7 psi (101 kPa) would be provided by an outer wall of spiral corrugated steel pipe ordinarily used to make culverts. The inner wall of the vacuum chamber would be made of a 300-series stainless steel, which is weldable, nonmagnetic, and relatively free of gas-sequestering imperfections (see figure). The inner and outer walls would be welded together. Sections of the double-wall pipe would be welded together at their ends; corrugated heavy single-wall stainless-steel segments could be used to accommodate thermal expansion during bakeout or to absorb vibrations from pumps.

The space between the two walls would be pumped to a relatively low vacuum of about 10^{-2} torr (~1 Pa), while the inner chamber would be pumped to a typical high vacuum of 10^{-8} torr (~1 μPa). Because the inner wall would have to sustain only a minuscule differential pressure, it could be made quite thin. The differential pumping of the corrugations would also serve as insurance against leaks in the inner wall: The flow through a small hole between the low vacuum and the high vacuum would be much less than the flow through the same hole from the atmosphere to the high vacuum.

If properly terminated at its ends, each section of pipe could be tested for leaks without having to evacuate the inner volume. Instead, the space between the outer walls could be evacuated through a helium leak detector while the helium is applied at various points on the inner surface.

The wall could be baked out by electrical resistance heating while both sections are evacuated as in normal operation. A strong electrical current would flow along the pipe, dividing between the inner and outer walls according to the dimensions, thicknesses, and electrical resistivities of the two walls. Because the outer wall would be cooled by air and the inner wall would be insulated by the vacuum, the inner wall would tend to run hotter, other things being equal.

This work was done by Robert E. Frazer of Caltech for **NASA's Jet Propulsion Laboratory.** *For further information, Circle 50 on the TSP Request Card.* *NPO-17039*

Ultraviolet Lidar Would Measure Wind Velocity

Incoherent Doppler-shifted scattering from aerosols will reveal important weather data.

NASA's Jet Propulsion Laboratory, Pasadena, California

A remote-sensing system now in an early stage of development could make global measurements of wind velocities along a probing beam of ultraviolet light. The ability to measure wind velocities remotely is necessary for a better understanding of atmospheric physics and to improve weather prediction. In aviation, a remote wind-measuring system could promote safety through the detection of wind shears and clear-air turbulence.

The system under development will include a range-gated (pulsed) ultraviolet-excimer laser operating at 308 or 353 nm. From an orbit around the Earth, the laser would illuminate the portion of the atmosphere to be probed. A portion of the incident radiation would undergo Mie scattering from aerosol particles entrained in the wind and would be reflected back to the orbiting station with a Doppler-shifted spectrum representative of the distribution of aerosol-particle velocities along the line of sight.

An earlier proposal for such a system was based on the use of infrared radiation from a CO_2 laser. The ultraviolet system was proposed subsequently because the ultraviolet radiation is scattered more effectively by the aerosol particles — an important consideration in measurements at high altitudes and in the southern hemisphere where aerosol concentrations are low.

The processing of the scattered light in the receiving portion of the system will be complicated somewhat by the strong component of thermally broadened Rayleigh scattering from nitrogen and oxygen molecules. In the developmental system, the receiver will contain a wavelength filter composed of multiple Fabry-Perot etalons to discriminate between the broad air spectrum and the relatively narrow aerosol spectrum (see figure).

A small fraction of the transmitted laser pulse will be diverted to the wavelength meter in the receiver to provide a measurement of the output wavelength and the wavelength reference with which the re-

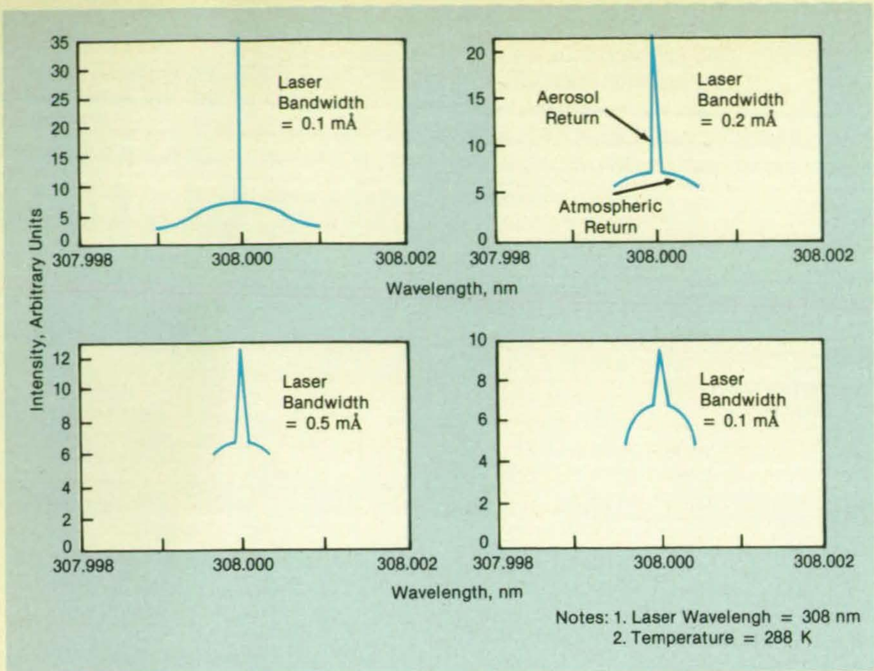

Backscattering Spectra were calculated for air based on a standard atmosphere and continental haze-type aerosol distribution. These spectra show that it is advantageous to operate at the minimum possible laser bandwidth to increase the height of the narrow aerosol return above the broad molecular return.

turn pulse is compared. Because the comparison will be made for each transmitted/received pulse pair, mode hops between laser pulses will not affect the measurement of the wind velocity. Furthermore, even in the presence of mode hopping, the differential-wavelength measurements can still be averaged to increase the accuracy.

Several experimental units have demonstrated the feasibility of the XeCl excimer type of laser that will be used. One distinct advantage of the incoherent Doppler lidar is that on account of the differential measurement at each pulse, the absolute laser frequency does not have to be controlled: it is necessary only to keep the bandwidth narrow. This places the emphasis in the stabilization of frequency on the passive wavemeter and the multiple Fabry-Perot filter, which are easier to control than is the laser.

This work was done by Iain Stuart McDermid and James B. Laudenslager for **NASA's Jet Propulsion Laboratory** *and David Rees of University College London. For further information, Circle 25 on the TSP Request Card.* *NPO-16756*

Books and Reports

These reports, studies, handbooks are available from NASA as Technical Support Packages (TSP's) when a Request Card number is cited; otherwise they are available from the National Technical Information Service.

Computational Fluid Dynamics: Past, Present, and Future

The numerical simulation of fluid flow has become routine, but improvements are needed.

A paper reviews the development of computational fluid dynamics (CFD) and explores the future prospects of the technology. The report covers such topics as computer technology, turbulence, the development of solution methodology, the development of algorithms, the definition of flow geometries, the generation of computational grids, and pre- and post-data processing.

Fifteen years ago, the elements that compose CFD — algorithm development, grid definition, geometry definition, establishing boundary and initial conditions, turbulence modeling, pre- and post-data processing, and computer technology, for example — were ripe for advances. Today, CFD is maturing and has reached a stage in which it is routinely applied to complicated problems. It is being used to design aerospace vehicles and components.

In the future, aerospace manufacturers will rely increasingly on the numerical solutions that CFD provides because of the following:
- The capability of CFD has been demonstrated.
- The number of supercomputers available for CFD is increasing.
- Not enough ground-based facilities are available for experiments.
- Ground-based facilities cannot generate data in some of the pertinent flow regimes.

An advantage of CFD over wind tunnels is that CFD software and hardware can be continually upgraded at low cost. Computing centers are cheaper to build and modify. They can take much of the load off wind-tunnel experimentation so that experimental facilities can be used more effectively and efficiently.

The physics of turbulence remains a subject of intense study. The data generated by numerical solutions can be used to create turbulence models. The data derived from such models yield more information than do data from experiments.

The report notes, however, that it is important for fluid dynamicists to work closely together, whether they use computational or experimental tools. Computer codes require experiments for validation, and experiments require supplemental computations. Research laboratories with facilities for experiments, computation, and flight testing offer the best possibility for interdisciplinary synergy and will produce the most valuable technology.

For the future, the report predicts that two areas of particular importance — unsteady flows and interdisciplinary physics — will benefit from CFD. Unsteady-flow problems result from the instability of separated flow regions or from the relative motion of one body with respect to another, in helicopters and turbomachinery, for example. Formidable efforts are underway and will eventually lead to numerical simulation.

In interdisciplinary physics, flow codes will be linked with other codes, such as those for propulsion and control. As the need grows for high-speed flight, the gasdynamic equations will increase in complexity because of strong shocks and thermal and chemical nonequilibrium phenomena. Fluid dynamicists and chemists will begin working together to study problems involving dissociation and ionization, reaction rates, radiation, and equilibrium.

This work was done by Paul Kutler of **Ames Research Center**. *Further information may be found in NASA TM-88246 [N86-28057/NSP], "A Perspective of Computational Fluid Dynamics."*

Copies may be purchased [prepayment required] from the National Technical Information Service, Springfield, Virginia 22161, Telephone No. (703) 487-4650. Rush orders may be placed for an additional fee by calling (800) 336-4700.

Inquiries concerning rights for the commercial use of this invention should be addressed to the Patent Counsel, Ames Research Center [see page 12]. Refer to ARC-11738.

Technology Developed in Two Space Projects

Two projects are examined for their influences on commercial products and future space missions.

A three-volume report presents a study of technological benefits of two spaceflight projects: Galileo, a mission to study the environment of Jupiter, and the Hubble space telescope, an astronomy mission to place a large telescope above the atmosphere of the Earth. The study focused on equipment and computer programs developed between the initial approval of projects and the integration and testing of the systems.

The study was intended to yield a better understanding of the flight-technology-development process and to create an awareness among Government officials and the general public of the achievements and ramifications of the project. The study identified 97 unique technology developments through personal interviews with 37 people on the Galileo project and 49 people on the Hubble space telescope project. Technology-development assessment sheets were written on 21 of the most important developments of the Hubble project and 20 such developments of the Galileo project.

Some of the developments have been adapted to commercial use. For example, the Galileo project yielded a miniature turbine pump, charge-coupled devices for automatic cameras, an improved photomultiplier tube, "smart" brushless dc motors with only two wires for an infinite number of operational modes, and improved rotary transformers.

Some developments also contributed to future scientific space missions. Examples are a computerized catalog of guide stars, advancement in the fabrication of large, high-resolution optics, thermal balancing of detector assemblies for operation at low temperatures, a detector-array multiplexer for greater data resolution, and improved gravity-assistance software for more-productive scientific observations at a minimum expenditure of propellant.

Volume 1 of the report presents an overview of the study, discusses the methods of collection and evaluation of data, and offers conclusions and recommendations. Volume 2 describes the interview process and summarizes the raw data. Volume 3 contains technology-assessment sheets for the developments.

This work was done by Carlton H. Joseph of Optimum Services & Systems, Inc., for **Marshall Space Flight Center**. *To obtain a copy of the report, "Galileo and Hubble Space Telescope Technology Development Study," Circle 19 on the TSP Request Card. MFS-27185*

Materials

Fluidized-Bed Deposition of Single-Crystal Silicon

A chemical-vapor-deposition technique is proposed for production of uniformly thin films.

NASA's Jet Propulsion Laboratory, Pasadena, California

Uniformly thin single-crystal films of silicon can be produced by a modification of the fluidized-bed-reactor technique that now produces polysilicon by chemical vapor deposition. The modified technique is proposed for silicon wafers for flat-plate solar arrays and may result in different structural and electronic properties in the deposition layer that would be desirable for specific microelectronic or solar-cell processing.

Currently, single-crystal sheets of silicon are drawn from melted polycrystalline silicon particles. The particles are produced in a vigorously agitated, uniformly heated fluidized bed of silicon particles heated to 650 °C in a high concentration (up to 100 percent) of silane. The reaction mechanism involves heterogeneous chemical-vapor deposition and incorporation of fine silicon particles by scavenging. In this case, the main purpose of the fluidized-bed reactor is to increase the silicon deposition rate and thus decrease cost.

In the proposed process (see figure), deposition would occur on silicon wafers, kept individually at temperatures above 1,000 °C. The heated wafers would be held in an unheated and minimally-agitated-fluidized bed of silicon particles and in a low concentration of silane (less than 1 percent in He).

In this case, the primary purpose of the fluidized-bed reactor is to provide uniform mass and heat transfer for the coating reaction. With good mixing and smoothing action of the mildly bubbling particles, a uniform thickness should be obtained. Because of the low silane concentration, the formation of fine silicon particles is not expected; consequently, the reaction mechanism would be solely that of a heterogeneous deposition.

The high substrate temperature and the use of a single-crystal substrate would ensure single-crystal epitaxial deposition. Other advantages would lie in the more efficient use of chemicals and in higher deposition rates than are possible in a conventional chemical-vapor-deposition reactor.

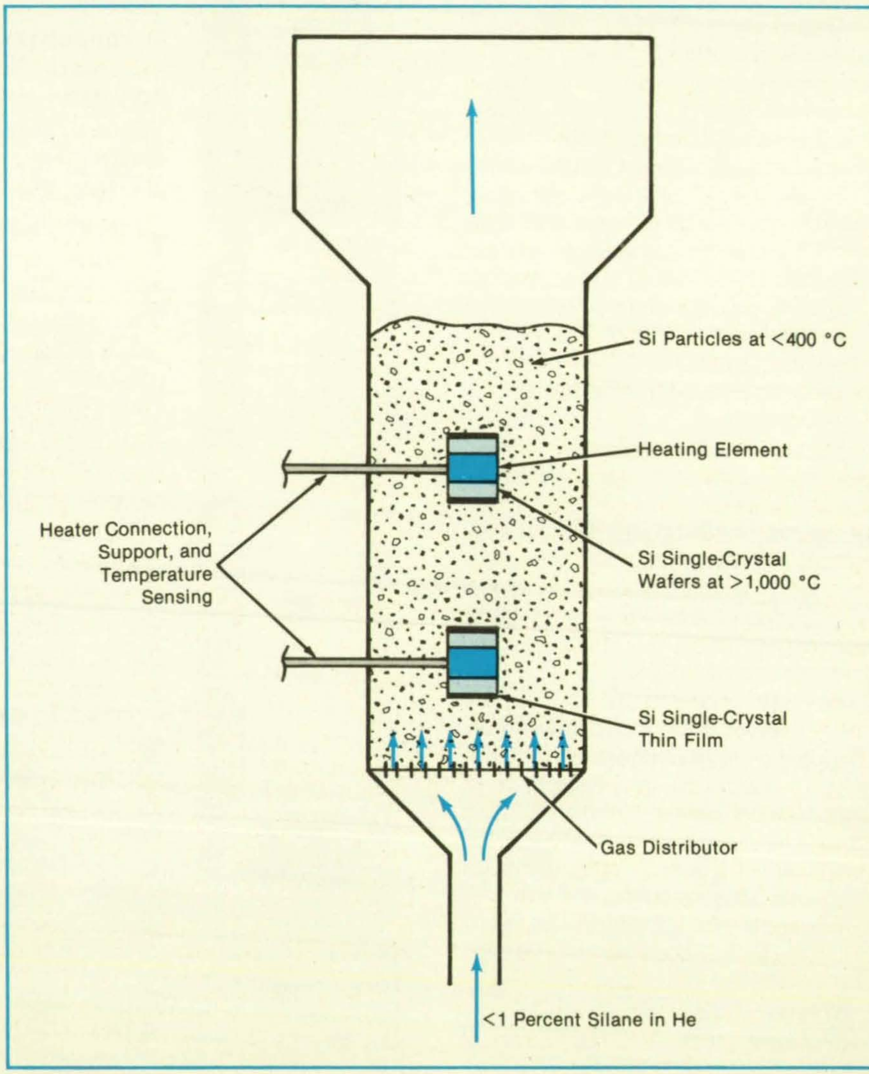

Uniformly Thin Silicon Single-Crystal Films would be deposited from silane onto silicon single-crystal wafers heated above 1,000 °C in a minimally fluidized bed of silicon particles.

If successful, this deposition scheme could be used as an alternative to the conventional chemical-vapor-deposition technique widely used in microelectronic diffusion steps or solar-cell preparations. Depending on the deposition thickness, the product could be either a thin film for direct device fabrication or a thick wafer for advanced single-crystal sheet. This deposition scheme may also be applicable to GaAs or other materials, both as deposition materials and as substrates.

This work was done by George C. Hsu and Naresh K. Rohatgi for **NASA's Jet Propulsion Laboratory**. *For further information, Circle 34 on the TSP Request Card. NPO-16608*

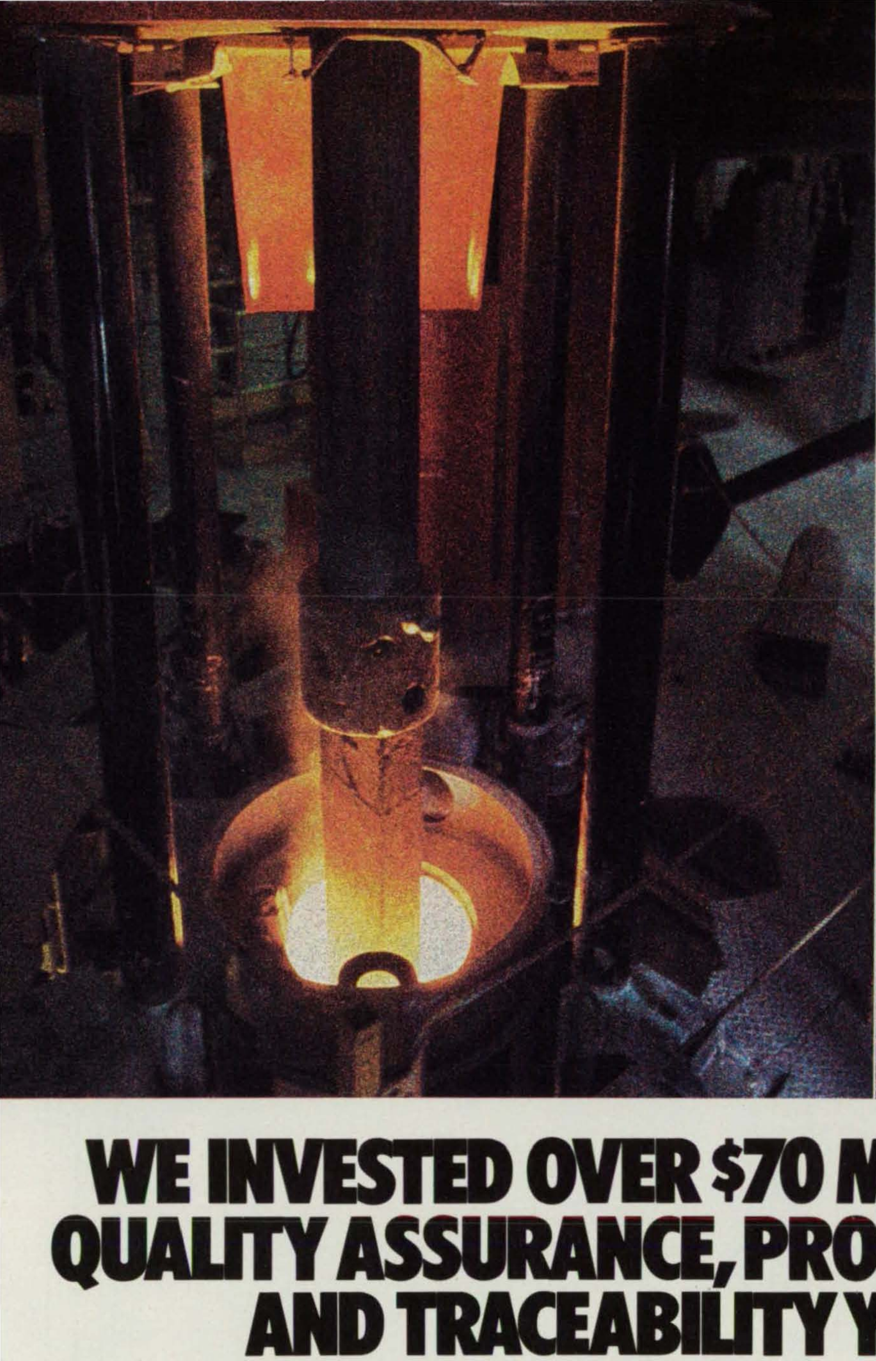

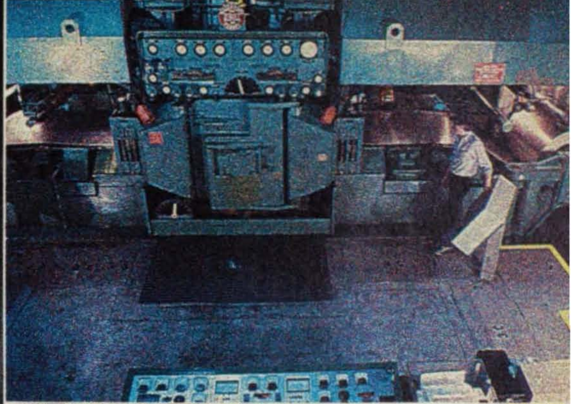

Wicks for Refrigerants in Heat Pipes

An ultra-high-molecular-weight material is compatible with efficient heat-transfer fluids.

Goddard Space Flight Center, Greenbelt, Maryland

A new wick material for heat pipes is the first to be physically and chemically compatible with the chlorofluoromethanes, the chlorofluoroethanes, and ammonia — the most-efficient refrigerant fluids. The new material allows one of these refrigerants to be used as the working fluid in a capillary-pump heat-pipe loop for cooling electronic equipment, for example.

The wick material is a uniformly-porous, permeable, open-cell polyethylene foam. It has an ultrahigh molecular weight — 1 to 5 million — and a very small pore size — 10 to 12 μm. This material has previously been used in filters but not in wicks.

The ultrahigh molecular weight of the material makes it resistant to heat. It can withstand a continuous temperature of 82 °C or temperatures up to 116 °C intermittently. It also withstands cold down to −70 °C.

The material is flexible and not fragile and thus withstands vibration. Moreover, its surface is self-lubricating so that it is easy to machine and to insert into heat pipes. Its high molecular weight also contributes to its machinability. With its uniform porosity and small interconnecting pores, the material is highly permeable to the flow of refrigerant through it and generates a large capillary pressure. A hollow tube of the material 1 in. (2.5 cm) in diameter and with walls ¼ in. (6 mm) thick draws up to 19 in. (48 cm) of water or methanol in a static height test that uses a manometer at a pressure of 1 atm (about 0.1 MPa). The material does not contaminate the refrigerant chemically nor does it release particles into the heat pipe.

The foam is machined into the form of a can with one open end and is inserted into the heat exchanger of the capillary-pump system with its open end toward the section that contains the liquid (see figure). The liquid refrigerant saturates the pores of the wick, and heat entering the heat exchanger from an external source vaporizes the liquid continuously as it emerges from the porous wick. Liquid diffuses through the wick to replenish the evaporated refrigerant.

The vapor flows through the heat pipe to a condenser, from which it returns to the heat exchanger as a liquid. The capillary pressure difference across the wick ensures continuous circulation of the refrigerant.

This work was done by Benjamin Seidenberg of **Goddard Space Flight Center**. *For further information, Circle 113 on the TSP Request Card.*

This invention is owned by NASA, and a patent application has been filed. Inquiries concerning nonexclusive or exclusive license for its commercial development should be addressed to the Patent Counsel, Goddard Space Flight Center *[see page 12]**. Refer to GSC-13019.*

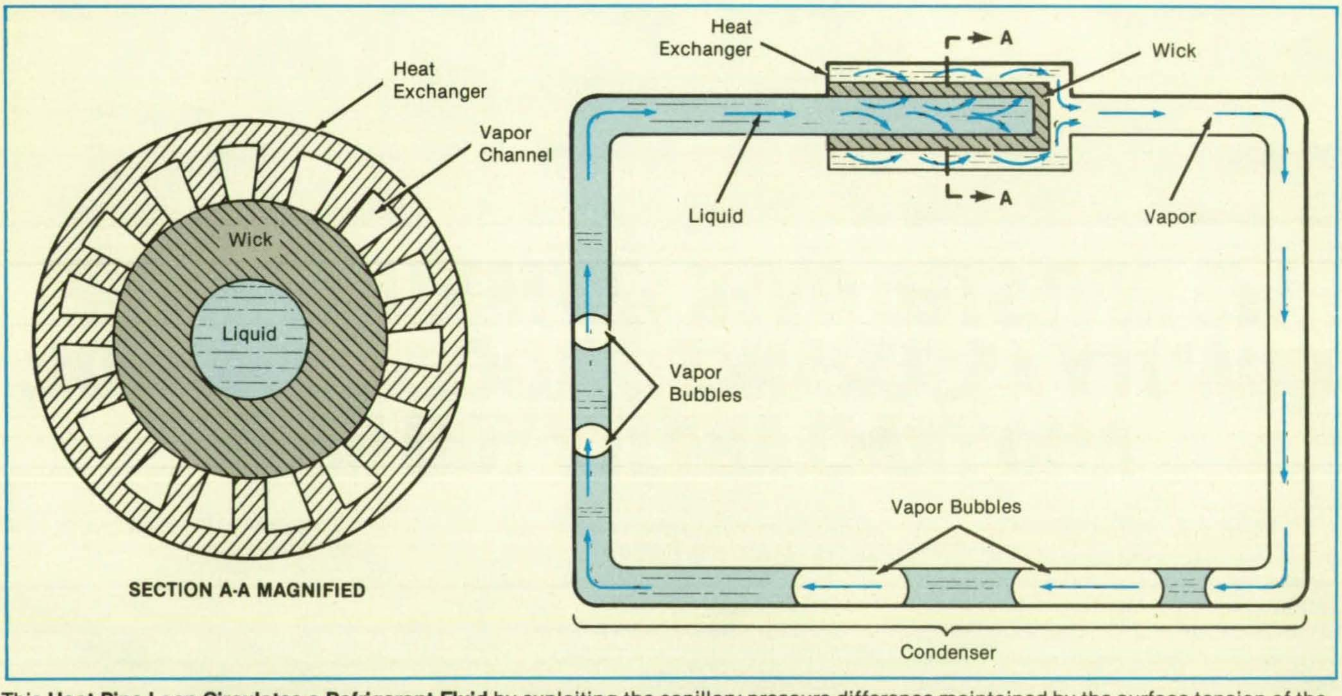

This **Heat-Pipe Loop Circulates a Refrigerant Fluid** by exploiting the capillary pressure difference maintained by the surface tension of the liquid in the wick. Channels along the outer surface of the wick carry vaporized refrigerant away from the wick surface.

Fire-Resistant Polyamides Containing Phosphorus

Flammability and weight loss are reduced.

Ames Research Center, Moffett Field, California

Fire-resistant polymers have been obtained from 1-[(dialkoxyphosphonyl) methyl]-2,4- and -2,6-diaminobenzenes by their reaction with acyl or diacyl halides of higher functionality. The incorporation of compounds containing phosphorus into certain polymers had been shown previously to increase fire retardance. This discovery adds a new class of polyamides to the group of such polymers.

The generic reactions are illustrated in the figure. First, a phosphonylmethyl benzene is nitrated, then reduced by hydrogenation to obtain the diamino compound I. The diacyl compound II is then reacted with

compound I to form the polymer with repeating units shown as compound III. Compound I can also be reacted with such other diamines as m-phenylenediamine to obtain a polymer with properties intermediate between those of a more conventional polymer and one of the new type.

In the figure, R represents an aromatic, alkyl, or haloalkyl group. Examples of R include methyl, ethyl, n-propyl, isopropyl, chloroethyl, and phenyl. R′ represents any of a variety of multivalent, essentially hydrocarbon groups; for example, $-(CH_2)_4-$.

Thermogravimetric (weight-loss) and limiting-oxygen-index (a measure of resistance to ignition) tests were performed on several of the new types of polymers and on similar polymers without the phosphorus-containing groups. The char yields or limiting oxygen indices, or both, of the new polymers were greater than those of the conventional polymers. For example, a polymer prepared from 1-[(diethoxyphosphonyl) methyl]-2,4- and -2,6-diaminobenzenes and isophthaloyl dichloride sustained a weight loss of 60 percent in air at 700 °C; the related polymer without phosphorus, prepared from m-phenylenediamine and isophthaloyl dichloride, lost 94 percent of its weight under the same conditions.

This work was done by Demetrius A. Kourtides of **Ames Research Center** *and John A. Mikroyannidis of the National Research Council. For further information, Circle 10 on the TSP Request Card.*

Inquiries concerning rights for the commercial use of this invention should be addressed to the Patent Counsel, Ames Research Center [see page 12]. Refer to ARC-11512.

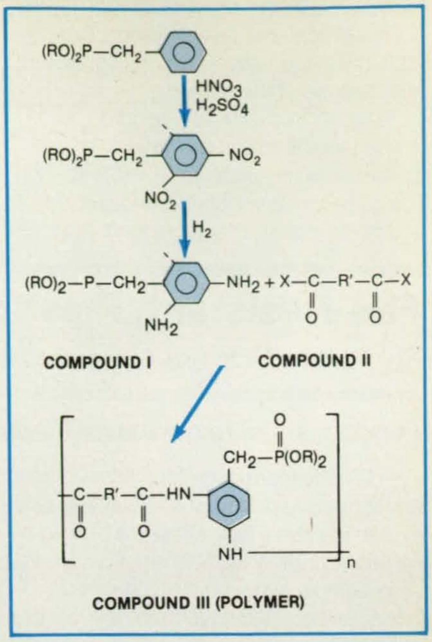

A Polyamide Containing Phosphorus (compound III) is formed by the reaction of diamino compound I and a diacyl halide, compound II. The incorporation of the groups containing the phosphorus increases the fire resistance of the product. The dashed line signifies that the second amino group can be in the fourth or sixth position.

Synthesis of B, B′, B″-Trichloroborazine

This useful compound can be made easily in a laboratory.

Ames Research Center, Moffett Field, California

A simplified, relatively safe, and economical synthesis of B,B′,B″-trichloroborazine $(BClNH)_3$ is easily practiced in a standard organic-chemistry laboratory. The yield is 20 to 30 percent — a fairly acceptable value in view of the inherent difficulty of synthesizing borazines. Because $(BClNH)_3$ is widely used as the starting material for cyclic B/N compounds, the new synthesis has potential for use in industry.

An experiment was performed to demonstrate the synthesis, the chemical reactions of which are shown in the figure. Boron trichloride was condensed in toluene and reacted with ammonia to form dichloroboramine and ammonium chloride.

$$BCl_3 + 2NH_3 \longrightarrow (BCl_2\,NH_2) + NH_4Cl$$

$$3BCl_2NH_2 \longrightarrow (BClNH)_3 + 2HCl$$

B,B′,B″-Trichloroborazine is produced in the new, simplified process.

After the excess of NH_3 was condensed into the toluene solution, the mixture was refluxed for 2 to 3 hours. The solution was cooled to room temperature, and the white ammonium chloride precipitate was removed on a filter. The toluene was distilled off, leaving white $(BClNH)_3$.

This work was done by Salvatore R. Riccitiello of **Ames Research Center** *and Timothy S. Chen and Ming-ta S. Hsu of HC Chem Research. No further documentation is available.*

Inquiries concerning rights for the commercial use of this invention should be addressed to the Patent Counsel, Ames Research Center [see page 12]. Refer to ARC-11643.

Slow Release of Reagent Chemicals From Gel Matrices

A simple technique enables the slow diffusion of chemicals into solutions.

Langley Research Center, Hampton, Virginia

A procedure has been developed for the slow release of reagent chemicals into solutions. In a particular situation it was necessary to regulate the concentration of a reagent and to have it slowly released into the reaction solution over a period of days since too rapid an addition would have caused precipitation. The standard procedure for the slow, controlled addition of reagents involves expensive and sophisticated titration equipment, which requires operator attention and which may malfunction. The new procedure is simple and inexpensive and is not subject to failure of equipment.

A gel is prepared, and the desired amount of reagent is added to the gel while it is still fluid. Gelatin was used in this situation, but other gels are equally suitable; these include agar, carboxymethyl cellulose, and silica gel. While still fluid, the gel/reagent solution is poured into an ordinary plastic drinking straw that is sealed at one end. The gel is allowed to set and can keep for days or weeks.

For use, the gelled contents of the plastic straw are squeezed out into the reaction solution. The reagent slowly diffuses out of the gel matrix, which sits in the solution looking much like a transparent snake. The rate of diffusion can be regulated by control of the density of the gel; stiffer gels allow slower diffusion than do thinner gels. The use of a toothpaste-type tube or pump dispenser could conceivably provide a more controlled technique for the

storage and dispensation of the gel matrix.

This simple and flexible procedure has many possible uses including controlled, slow release of the following:

1. Reagents in chemical reactions;
2. Reagents in crystal growth;
3. Reagents in space-flight experiments; e.g., on the Space Shuttle and Space Station, in which this technique may be especially important for the controlled addition of hazardous chemicals with minimum human attention; and
4. Preformed gel medications from packets, which may be sealed to prolong shelf life, for the dressing of wounds and burns, and for other medical treatments.

This work was done by William J. Debnam of **Langley Research Center** *and Patrick G. Barber and James Coleman of Longwood College. No further documentation is available.*

Inquiries concerning rights for the commercial use of this invention should be addressed to the Patent Counsel. Langley Research Center [see page 12]. Refer to LAR-13607.

Fire-Resistant, Plastic-Foam Airducts

Polyimide ducts are lighter and cheaper than aluminum ducts.

Lyndon B. Johnson Space Center, Houston, Texas

Polyimide-foam airducts are low in cost and light in weight. They are relatively safe in fires because they resist the spread of flames and generate little smoke.

In comparison with the conventional fiberglass-insulated aluminum ducts, the polyimide-foam ducts are less expensive to manufacture. They are made by a continuous casting process, whereas aluminum ducts require a labor-intensive process of metal forming, welding, and wrapping with a fiberglass blanket containing a Tedlar (or equivalent) polyvinyl fluoride-film vapor barrier.

In comparison with polyisocyanurate-foam ducts, which are also low in cost and lightweight, polyimide ducts produce little heat and smoke in a fire. Furthermore, the new duct material forms a protective layer of char that impedes flames.

The polyimide ducts are suitable for heating and air-conditioning in airplanes, ships, trains, and buildings. A duct for a DC-10 airplane was made on the same production tool used for polyisocyanurate-foam ducts.

This work was done by Souzane H. Tacawy and Edward L. Trabold of McDonnel Douglas Corp. for **Johnson Space Center**. *No further documentation is available.*
MSC-21186

Books and Reports

These reports, studies, handbooks are available from NASA as Technical Support Packages (TSP's) when a Request Card number is cited; otherwise they are available from the National Technical Information Service.

Boron Carbides as Thermoelectric Materials

Progress toward high performance at high temperature is reported.

A report reviews recent theoretical and experimental research on thermoelectric materials. Though the development of thermoelectric materials had languished after the considerable progress made about 30 years ago, recent work with narrow-band semiconductors has demonstrated the possibility of relatively high thermoelectric energy-conversion efficiencies in materials that can withstand the high temperatures needed to attain such efficiencies. Among these promising semiconductors are the boron-rich borides, especially the boron carbides.

For comparison with other thermoelectric materials, a given material is usually characterized by the thermoelectric figure of merit, Z, which is given by $Z = S^2\sigma/\kappa$, where S = the Seebeck coefficient, σ = the electrical conductivity, and κ = the thermal conductivity. Another useful quantity is ZT, where T = the absolute temperature. As ZT increases, so does the efficiency of thermoelectric energy conversion.

According to the theory, charge transport in a narrow-band semiconductor can occur by the hopping of small polarons between lattice sites, with the assistance of multiple phonons. The resulting charge mobilities, and therefore, the electrical conductivities, increase with temperature. If the polarons hop between sites that are roughly equivalent in energy, the Seebeck coefficient should remain approximately independent of temperature.

In a disordered small-polaron material with charge carriers hopping between inequivalent sites, the charge carriers can transport vibrational energy, which would give rise to an increase in the Seebeck coefficient with temperature. Since the electrical conductivity also increases with temperature, Z may increase dramatically with temperature. However, this increase may be restrained somewhat by an increase in the thermal conductivity from the charge-carrier contribution to the heat flow.

The materials of particular interest are the boron carbides B_xC in the composition range of $4 \leqslant x \leqslant 9$, for which S, σ, and κ have been measured. Together with the Hall data, the thermoelectric coefficients indicate that charge transport in these materials involves the hopping of small hole bipolarons. The thermoelectric properties are not determined by the composition alone; they depend somewhat on the method of preparation and the previous thermal history.

At present, the best of these materials exhibit $ZT \approx 1$. It may be possible to achieve $ZT \gg 1$ by attention to impurities, doping, process temperatures, and other manufacturing conditions. Current theory is inadequate to describe the conditions required for optimum Z. Considerable work is still necessary to relate the thermal and electronic transport — especially the identification of hopping centers — to the composition and crystal structure.

This work was done by Charles Wood of Caltech for **NASA's Jet Propulsion Laboratory**. *To obtain a copy of the report, "Boron Carbides as High Temperature Thermoelectric Materials," Circle 149 on the TSP Request Card.*
NPO-16887

Composites That Exceed Superalloys in Rupture Strength

Ceramic-fiber-reinforced iron alloys show promise as turbine parts for intermediate-temperature service.

Composites made of iron-base alloys reinforced with fibers of silicon carbide or with boron carbide coated boron fibers have stress-rupture strengths at a temperature of 870 °C superior to those of the strongest cast superalloys, according to a report. The report describes a study of the suitability of metal-matrix composites reinforced with low-density fibers for use at intermediate temperatures in gas turbines. Holding the service temperature to 870 °C or less is intended to limit the reactions between filaments and matrices that have thwarted use of these composites at high temperatures (above 1,000 °C). The intermediate-temperature composites could

reduce the weights of turbine blades by 40 percent and would increase the life expectancies of the blades.

In the study, a relatively-low-temperature fabrication process — hollow-cathode sputtering — was developed. The process produces single-filament composites by depositing the iron-base alloys on B_4C coated B fibers and SiC fibers. The temperature of the filaments did not exceed 700 °C during the deposition, and scanning-electron micrographs showed no evidence of chemical reactions between the filaments and the deposited matrix metals.

The 1,000-hour rupture strength at 870 °C projected for a composite filament consisting of 50 percent (by volume) of B_4C coated B fiber and a coat of iron-base alloy is 66 ksi (455 MPa) — 30 percent greater than that of single-crystal CMSX-2 superalloy. Even more impressive, the ratio of the rupture strength to the density under the same conditions is twice that of CMSX-2.

This work was done by Donald W. Petrasek of **Lewis Research Center**. *Further information may be found in NASA TM-87223[X87-10108/NSP], "Compatibility and Strength of Iron Alloy-Coated SiC and B_4C-Boron Fibers at 870 °C."*

Copies may be purchased [prepayment required] from the National Technical Information Service, Springfield, Virginia 22161, Telephone No. (703) 487-4650. Rush orders may be placed for an extra fee by calling (800) 336-4700. *LEW-14594*

Thermal Response of Composite Insulation

An engineering model gives useful predictions.

A pair of reports presents theoretical and experimental analyses of the thermal responses of multiple-component, lightweight, porous, ceramic insulators. Although the particular materials examined were destined for use in the Space Shuttle thermal protection system, the test methods and heat-transfer theory will be useful to chemical, metallurgical, and ceramic engineers who need to calculate the transient thermal responses of refractory composites.

The bulk materials studied were mixtures known as fibrous refractory composite insulation (FRCI), consisting mostly of oriented silica and aluminoborosilicate fibers. A wide range of properties can be obtained by varying the proportions of the different types of fibers; for example, the addition of alumina reduces the shrinkage at high temperature, but it also reduces the tensile strength. An integrated insulating tile with low shrinkage at high temperatures might be made by bonding an alumina-enhanced layer to the front surface of a block of FRCI.

The thermal responses of the composite insulators were calculated from an engineering model described in detail in one of the reports. In the model, interlocking walls of fibers form cubic pores. The pore size, effective fiber diameter, and other model parameters are defined, using governing equations, from the composition and the physical and mechanical properties of the corresponding real composite material. The weak and strong directions of the composite are determined by tensile-strength measurements. In the model, the number of fibers under load within the walls of the model in a given direction is set proportional to the strength in that direction. It is important to incorporate this anisotropy into the model because the thermal conductivity is higher in the strong direction than in the weak direction.

The effective thermal conductivity is calculated as a weighted sum of solid, gaseous, and radiant components. The weighting parameters of the sum take into account the rule of mixtures and the corrections for the variations in fiber bonding and optical properties of each composite.

Insulator samples were assembled into flat-face, 40°-half-angle cones and were instrumented with thermocouples at various depths. To simulate a spacecraft reentry heat pulse, the cores were exposed to arc-heated airjets for 300 s, followed by cooling for 600 s in a vacuum of 190 μm Hg (25 Pa). The engineering-model prediction of temperature as a function of time agreed closely with the thermocouple measurements.

This work was done by David A. Stewart, Daniel B. Leiser, and Marnell Smith of **Ames Research Center** *and Paul Kolodziej of Informatics, Inc. To obtain copies of the reports, "Thermal Response of Integral Multicomponent Composite Thermal Protection Systems" and "Characterization of Thermal Conductivity for Fibrous Refractory Composite Insulations," Circle 76 on the TSP Request Card.*

Inquiries concerning rights for the commercial use of this invention should be addressed to the Patent Counsel, Ames Research Center [see page 12]. Refer to ARC-11680

Steels for Rolling-Element Bearings

Bearing lives have been increased by attention to details of processing and applications.

A NASA technical memorandum discusses the selection of steels for long-life rolling-element bearings. Improvements in the manufacture of steels have made it possible to increase bearing lives by a factor of 100 over those available in the year 1940. To exploit this potential for long life in a particular application, it is necessary to integrate considerations of the effects of manufacturing processes on performance into the selection of the bearing steel.

After a brief review of advances in manufacturing, the report discusses the effect of the cleanliness of the bearing material on fatigue in a rolling element. One mode of fatigue is due to nonmetallic inclusions that act as stress concentrators. Under repeated cyclic stress, incipient cracks emanate from such inclusions, enlarging into a network of cracks that form a fatigue spall or pit. To increase the reliability or load-bearing capacity of the rolling element, the concentration of undesired impurities can be reduced through such manufacturing processes as vacuum melting (to remove gases) and remelting (to remove solid impurities) and by ultrasonic inspection to detect inclusions.

The fatigue life is affected profoundly by the hardness of the bearing material, which in turn is affected by conditions in service and by the heat treatment, composition, and other characteristics of manufacture. The life of a system of rolling elements can be predicted as a function of the operating temperature and of the hardness of the particular material at room temperature. Other hardness considerations that affect fatigue lives include the relative hardnesses of balls and races and differences in hardness among different balls running around the same race. In general, for a bearing that must operate at high temperature, care should be taken to match the hardnesses of the rolling elements and raceways while maintaining the highest hardness of all components.

Carbides that do not go completely into solution during austenitizing affect fatigue lives. Called "residual carbides," they appear to act as nucleation sites for incipient fatigue failure. An empirical carbide factor gives a reasonable prediction of the relative life under identical conditions of material hardness and lubrication mode.

Fatigue lives can be increased by control of the fibrous pattern of flow of material during forging. For example, when the fibers are along a race, the fatigue life is greater than when the fibers run across the race.

A compressive residual stress at the depth of the maximum shearing stress can decrease the maximum shearing stress. Thus, the lives of bearings can be increased by prestressing. For example, a ball-bearing inner race can be prestressed by initially running the bearing during a prescribed number of cycles at a specified load.

The effects of retained austenite are complicated. Retained austenite is generally associated with hardness, but it can also transform to martensite and cause dimensional instability.

Finally, the report discusses the fracture toughnesses of through-hardened and case-hardened materials. The fracture toughness of a steel is inversely proportional to the carbon content and to the hardness. The fracture toughness can be increased by the addition of nickel.

This work was done by Erwin V. Zaretsky of **Lewis Research Center**. *Further information may be found in NASA TM-88881 [N87-11993/NSP], "Selection of Rolling-Element Bearing Steels for Long-Life Application."*

Copies may be purchased [prepayment required] from the National Technical Information Service, Springfield, Virginia 22161, Telephone No. (703) 487-4650. Rush orders may be placed for an extra fee by calling (800) 336-4700.
LEW-14546

Solidification-Rate Effects in MAR-M-246 + Hf Alloy

Under slower solidification, the primary-dendrite-arm spacing increases.

A report discusses experiments on the influence of solidification rates on the crystallographic orientation and mechanical properties of the superalloy MAR-M-246 + Hf. Specimens were grown in a directional-solidification furnace, visually examined (by photography after polishing and etching) for microstructure, and stretched to failure in a tensile-testing machine. Back-reflection Laue x-ray photographs were taken to determine growth orientations.

The single-crystal samples all lay within 45° of the (001) orientation. The anisotropy of directionally solidified specimens was shown by the change in the shape of tensile-tested samples from round to oval. Single-crystal samples did not distort as much as directionally solidified polycrystalline samples.

The spacing of the primary dendrite arms was plotted as a function of the solidification rates at which they were formed, and the data were fitted to several different equations. The data and equations appear to agree qualitatively with those of previous investigators in that the spacing decreases with increasing solidification rate in directionally solidified superalloys.

The major factors influencing the mechanical properties in directionally solidified and single-crystal samples were found to be the preferred (001) orientation and the solidification rate. Slower rates allowed the dendrites to form in uniform patterns and facilitated growth near the (001) orientation, with some samples forming single crystals.

This work was done by David Hamilton of **Marshall Space Flight Center**. *Further information may be found in NASA TM-82558 [N84-14290/NSP], "Solidification Rate Influence on Orientation and Mechanical Properties of MAR-M-246 + Hf."*

Copies may be purchased [prepayment required] from the National Technical Information Service, Springfield, Virginia 22161, Telephone No. (703) 487-4650. Rush orders may be placed for an extra fee by calling (800) 336-4700. The report is also available on microfiche at no charge. To obtain a microfiche copy, Circle 74 on the TSP Request Card.
MFS-27057

Rheological Tests of Shear-Thickening-Polymer Solutions

A vibrational method avoids thickening during measurement.

A report describes measurements of the viscoelastic properties of FM-9, a polymer being considered as an antimisting agent for jet fuel. The purpose of the agent is to prevent the formation of a flammable fuel mist during an aircraft crash.

FM-9 has unusual rheological properties. Its viscosity increases sharply when it is subjected to a shear rate above a critical value. The material quickly forms a gel but reverts to its original consistency after the shearing ceases (a characteristic known as antithixotropic behavior).

The report covers a study of FM-9 in jet fuel under small oscillating shear deformations. This kind of shear was chosen in the belief that the disturbance to the polymer chain would be too small to provoke an interchain association process and consequent gelling. The linear viscoelastic response of the antimisting polymer/fuel solution could then be measured and compared with that of other dilute polymer solutions. Conventional testing apparatuses, in contrast, tend to cause gelling and make measurements at or above the critical shear rate difficult or impossible.

Measurements were made in a multiple-lumped-resonator apparatus over the frequency range from 103 to 6,100 Hz at polymer concentrations from 2.42 to 5.22 g/L and temperatures from 1 to 35 °C. Solutions were compared with and without a carrier — a mixture of low-molecular-weight glycol and an amine — that aids the mixing of the polymer with the fuel.

As expected, there was no antithixotropic behavior under small oscillatory deformations, and values could be determined for the number-average maximum relaxation time as a function of temperature, concentration, and presence of a carrier. The number-average molecular weight could also be determined. The results are consistent with the hypothesis that when the molecules are extended by high shear rates, intramolecular forces break down and intermolecular forces develop, causing the observed increase in viscosity and eventual gelation.

This work was done by Robert F. Landel, Soren Hvidt, and John D. Ferry of Caltech for **NASA's Jet Propulsion Laboratory**. *To obtain a copy of the report, "Oscillatory Measurements of Linear Viscoelastic Properties of Shear-Thickening Polymer Solutions," Circle 117 on the TSP Request Card.*
NPO-16778

Mechanical Properties of Large Sodium Iodide Crystals

For the first time, data on large thallium-doped samples are available.

A report presents data on mechanical properties of large crystals of thallium-doped sodium iodide [NaI(Tl)]. Previously, only data on small crystals were available. However, information was needed on large crystals so that a NaI(Tl) gamma-ray scintillator 20 in. in diameter and 0.5 in. thick (50.8 by 1.27 cm) could be built.

Accordingly, five specimens in the shape of circular flat plates were subjected to mechanical tests. The specimens, although not single-crystal, were composed of large multicrystals. A test fixture in a dry box applied a uniform pressure load across the surface of each specimen.

The report presents the test results for each specimen as plots of differential pressure versus center displacement and differential pressure versus stress at the center. It also tabulates the raw data.

The specimens were found to be plastic and to have a higher ultimate strength than expected. Although they were loaded to develop a stress of 500 lb/in.^{2} (3.5 MPa), only one specimen — an extremely hydrated one — failed. Specimens with many grain boundaries were less plastic, and therefore developed less permanent deformation, than those with fewer gain boundaries.

The test program also developed a procedure for screening candidate crystals for the gamma-ray sensor: specimens that acquire permanent deformations in excess of 0.0025 in. (0.064 mm) during the mechanical test are to be ranked as unacceptable. The procedure should eliminate potentially weak crystals before they are installed and should ensure that material yielding will be kept to a minimum.

This work was done by Henry M. Lee of **Marshall Space Flight Center**. *Further information may be found in NASA TM-86518 [N86-17187/NSP], "Mechanical Testing of Large Thallium Doped Sodium Iodide Single Crystals."*

Copies may be purchased [prepayment required] from the National Technical Information Service, Springfield, Virginia 22161, Telephone No. (703) 487-4650. Rush orders may be placed for an extra fee by calling (800) 336-4700. The report is also available on microfiche at no charge. To obtain a microfiche copy, Circle 160 on the TSP Request Card.
MFS-28158

Circle Reader Action No. 453

Computer Programs

COSMIC: Transferring NASA Software

COSMIC, NASA's Computer Software Management and Information Center, distributes software developed with NASA funding to industry, other government agencies and academia.

COSMIC's inventory is updated regularly; new programs are reported in *Tech Briefs*. For additional information on any of the programs described here, circle the appropriate TSP number.

If you don't find a program in this issue that meets your needs, call COSMIC directly for a free review of programs in your area of interest. You can also purchase the 1986 *COSMIC Software Catalog*, containing descriptions and ordering information for available software.

COSMIC is part of NASA's Technology Utilization Network.

COSMIC® — *John A. Gibson, Director*, (404) 542-3265
Computer Services Annex, University of Georgia, Athens, GA 30602

Computer Programs

These programs may be obtained at a very reasonable cost from COSMIC, a facility sponsored by NASA to make computer programs available to the public. For information on program price, size, and availability, circle the reference number on the TSP and COSMIC Request Card in this issue.

Electronic Systems

Bibliography on Multiprocessors and Distributed Processing

This computerized data base yields citations, indexes, and cross-references.

Multiprocessors and distributed processing are undergoing increased scientific scrutiny for many reasons. It is more and more difficult to keep track of the existing research in these fields. The Multiprocessor and Distributed Processing Bibliography package consists of a large machine-readable bibliographic data base, which in addition to the usual keyword searches, can be used for producing citations, indexes, and cross-references.

The data base is compiled from smaller existing multiprocessing bibliographies and from tables of contents from journals and significant conferences. There are approximately 4,000 entries, covering such topics as parallel and vector processing, networks, supercomputers, fault-tolerant computers, and cellular automata. Each entry is represented by up to 21 fields, including keywords, author, referencing book or journal title, volume and page number, and date and city of publication.

The data base contains UNIX® "refer"-formatted ASCII data and can be implemented on any computer running under the UNIX® operating system. It is easily convertible to other operating systems. The data base requires approximately one megabyte of secondary storage. This bibliography was compiled in 1985.

This program was written by Eugene N. Miya of **Ames Research Center**. *For further information, Circle 96 on the TSP Request Card.*
ARC-11568

Machinery

Computer Code for Turbocompounded Adiabatic Diesel Engine

Transfers of heat and work are analyzed.

A computer simulation has been developed to study the advantages of increased exhaust enthalpy in an adiabatic turbocompounded diesel engine. The subsystems of this conceptual engine include the compressor, reciprocator, turbocharger turbine, compounded turbine, ducting, and heat exchangers. The focus of the simulation of the total system is to define the transfers of mass and energy, including the release and transfer of heat and the transfer of work in each subsystem, and the relationship among the subsystems.

The computer code is written in FORTRAN IV language and was developed on a VAX 11-750 computer. The required inputs include the rate of flow of fuel, the speed of the engine, the temperature or structure of the engine wall, and the size and shape of the engine. The results include the cylinder pressure and temperature, the equivalence ratio, the manifold pressure and temperature, and the turbocharger speed (compressor and turbine), all as functions of the crank angle. Other results include the brake specific fuel consumption, brake horsepower, mean effective pressure, thermal efficiency, volumetric efficiency, and information on the transfer of heat.

The four-stroke diesel cycle is treated as a sequence of continuous processes: intake, compression, combustion (including expansion), and exhaust. Throughout the cycle, the cylinder is treated as a variable-volume plenum spatially uniform in pressure. The contents of the cylinder are represented as one continuous medium by defining an average equivalence ratio and temperature in the cylinder at all times. The properties of the gases are obtained by assuming ideal-gas behavior. Below a temperature of 1,000 K, the contents of the cylinder are treated as a homogeneous, nonreacting mixture of ideal gases. Above 1,000 K, the properties of the gases in the cylinder are calculated to allow for chemical dissociation by assuming that burned gases are in equilibrium, by the use of an approximate calculation method based on the combustion of hydrocarbons in air.

The reciprocator engine model calculates the state variables in one master cylinder of a multicylinder engine. Other cylinders are assumed to vary as echoes of the master cylinder, shifted by the appropriate phase angles. The equations of quasi-steady, adiabatic, one-dimensional flow are used to predict flows of mass past the valves. The manifolds are divided so that the effect of each cylinder can be incorporated in the model. Each section of manifold is treated as a plenum, the pressure and temperature histories of which are determined by solution of the equations of state of the manifold. The rapid mixing of gases in each section of manifold is assumed. The engine model couples with the compressor and heat-exchanger models at the inlet manifold and with the turbocharger turbine model at the exhaust manifold.

The compression process is defined to include the ignition-delay period. The total delay in ignition is related to the mean temperature and pressure of the gas in the cylinder during the delay by an empirical Arrhenius expression. Combustion is modeled as a uniformly-distributed heat-release process. The rate of release of heat is assumed to be proportional to the rate of burning of fuel, which is modeled empirically. Because the diesel combustion process comprises a premixed and a diffusion-controlled combustion mechanism, Watson's fuel-burning-rate correlation is used.

The transfer of heat is included in all the engine processes. Convective heat transfer is modeled by the use of engine correlations based on turbulent flow in pipes. A

Interactive math with your IBM/XT/AT

IAS
INTERACTIVE ANALYSIS SYSTEM

Over 40 preprogrammed functions are grouped into 7 menus for direct selection.

Powerful math options such as differentiate, integrate and FFT are executed in a couple of seconds with simple menu picks.

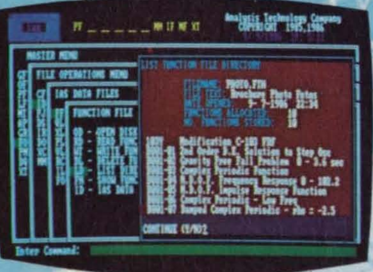

You can list data, edit, operate on, plot and store to disk. The function file directory allows easy access to stored data.

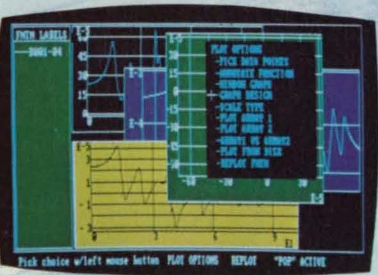

Select plot options in pop-up window using MOUSE or keyboard.

From the NASA Johnson Space Center environment comes breadth and depth of math functionality you've not seen on a Personal Computer.

Now, you have IAS, a main frame grade advanced menu driven system at a price accessable to everyone.

- Your choice: mouse, FNTN key, arrow key cursor pick, or type two-character commands
- New lookahead window and stacked menus with command trail
- More ways to generate math functions
  - Pick preprogrammed functions directly from menu
  - Keyboard x-y data entry
  - Type algebraic equations
  - Differential Equations. 1st, 2nd and 3rd order.
- Interpolation
- Curve fitting
- EQN, parameter and variable tables
- Extensive operations on functions, including FFT, differentiation, integration
- The other guys are eating their hearts out over IAS plot capability. No hoops to jump through, either.
- Matrix analysis
- Wireframe object eigenvector animation (vibration simulation)
- Breakthrough: User menu puts your program inside IAS
- External data interface menu
- Special picks for SDRC I-DEAS, Univ. of Cincinnati Universal Files and Lotus 1-2-3.
- EE's: Build your data acquisition system inside IAS
- Menu driven file management
- DOS command menu
- IBM XT/AT. 512K. 8087. CGA or EGA. Screen copy.
- 30 day moneyback guarantee

$149.00

VISA master charge

ATC ANALYSIS TECHNOLOGY COMPANY
3914 Miami Road
Cincinnati, Ohio 45227

(513) 561-1100

Pick desired colors directly from color bar.

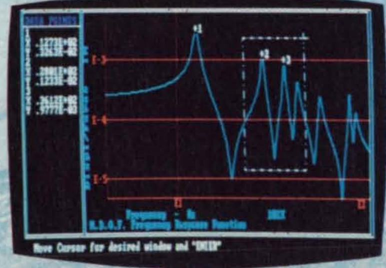

Rubber-banding box zooms on data you wish to magnify. Use MOUSE or keyboard.

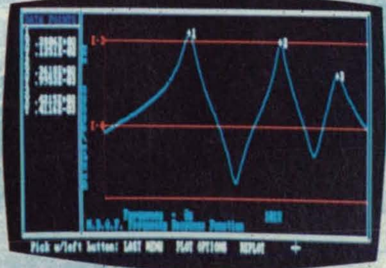

Redisplayed data from zoom box. Data points are cursored for x-y values.

Circle Reader Action No. 546

mean-turbulent-kinetic-energy model is used to obtain the characteristic velocity and length required in the engine correlations. Radiative heat transfer is included during combustion. The inside temperature of the piston, cylinder head, and cylinder liner can be specified or calculated from details of the wall material. An empirical model of friction is used to convert the indicated engine performance quantities to brake performance quantities. Inside manifold wall temperatures are either specified or calculated. Empirical correlations are used to calculate the transfer of heat and the loss of pressure in the manifold.

The performance of turbomachinery is defined by maps that interrelate the efficiency, the pressure ratio, the rate of flow of mass, and the shaft speed for each component. The turbomachinery maps are input parameters. The model includes provisions for off-design performance of the turbomachinery and for scaling when the reciprocator is operated uncooled or as an adiabatic engine. The turbocharger turbine and compressor speeds are equal. The power-turbine speed is determined by the reciprocator engine speed through the ratio of the gears that connect them. The model gives the option of including or not including the power turbine.

This program was written by D. N. Assanis and J. B. Heywood of Massachusetts Institute of Technology for **Lewis Research Center**. *For further information, Circle 159 on the TSP Request Card. LEW-14403*

Mathematics and Information Sciences

Magnetic-Tape Utilities Computer Program

Access to magnetic-tape drives is simplified.

The Fast Magnetic Tape Utility package (MTUTILS/TUTIL) is a collection of subroutines for DEC VAX/VMS computers designed to simplify access to magnetic-tape drives. These routines use standard FORTRAN argument binding and are simpler than the corresponding system service calls. There are two sets of routines: one enables basic tape operations; the other enables certain operations to be performed on a sequence of tape drives. This enables manipulation of sets of data that are too large to be held on a single magnetic tape. The TUTIL program is a user-friendly, menu-driven program that employs the MTUTILS package to process tapes interactively.

MTUTILS routines are provided to activate from one to four tape drives (including all requisite operations like mount and assign input/output channel and the setup of a descriptor for the drives for use with other MTUTILS routines) and to read or write records, skip files or records (forward or reverse), write end-of-file (EOF) marks, search for end of volume (EOV), rewind or unload a tape, request an asynchronous reading, writing, or rewinding operation, and wait for completion of an asynchronous request.

Each command takes the form of a FORTRAN subroutine call or a Pascal procedure call with such appropriate parameters as descriptors, buffers, byte counts, error flags, and others. Extensive error-checking facilities are provided, including an option for automatic printout of complete diagnostic messages.

The TUTIL program interactively supports all the aforementioned functions in addition to printing out a profile of tape contents, printing record contents in hexadecimal/decimal/American National Standard Code for Information Interchange (ASCII) bytes/words/long words, copying arbitrarily-large disk files (with minimum record lengths of 14 bytes) onto magnetic tapes and back, and comparing disk files with tape files. TUTIL supports the wild-card specification of disk files and logging of profiles, record dumps, comparisons of

files, and other output to a disk file. Two on-line help libraries and an optional Pascal environment file are provided with this package.

MTUTILS/TUTIL is written in FORTRAN 77 for batch or interactive execution and has been implemented on a DEC VAX 11/780 computer operating under VMS 4.X with a central-memory requirement of approximately 96K of 8-bit bytes. The program was developed in 1986.

This program was written by N. E. Olson and R. F. Jurgens of Caltech for **NASA's Jet Propulsion Laboratory**. *For further information, Circle 63 on the TSP Request Card.*
NPO-17190

Hybrid Applications of Artificial Intelligence

This computer language couples symbolic processing with compiled-language functions and data structures.

STAR (Simple Tool for Automated Reasoning) is an interactive, interpreted programming language for the development and operation of artificial-intelligence (AI) application systems. STAR provides an environment for integrating traditional AI symbolic processing with functions and data structures defined in such compiled languages as C, FORTRAN, and PASCAL. A need for this type of integration arises in a number of application areas of AI, including the interpretation of numerical sensor data, the construction of intelligent user interfaces to existing compiled software packages, and the coupling of AI techniques with numerical simulation techniques and control-systems software.

A semantic network is used to organize data in STAR, and programming is accomplished through the definition of symbolic functions or through the definition of sets of production rules. The symbolic-processing environment of STAR may be extended by linking the interpreter together with functions defined in conventional compiled languages, and these external functions may interact with STAR through function calls in either direction and through the exchange of references to arbitrary data structures.

Typically, references to data structures defined in the compiled languages are inserted within various data structures of STAR and vice versa, forming a hybrid knowledge base of interconnected symbolic and nonsymbolic information. Through the use of special utility functions accompanying the STAR interpreter, external compiled functions are able to perform basic operations on STAR data structures. Higher-level operations may be carried out remotely through calls from the external compiled functions to various functions in STAR. The hybrid knowledge base may thus be obtained and processed in general by either side of the application.

The STAR language was created at NASA's Jet Propulsion Laboratory in the course of an expert-system project for the geological interpretation of imaging-spectrometer data. The resultant system, called SPECTRUM, uses STAR to couple a controlling layer of symbolic processing with a set of compiled routines for the analysis of these data.

The STAR interpreter is written in the C language and is currently available in a UNIX version (NPO-16832) for the Sun Microsystems 2/170 workstation and a VMS version (NPO-16965) for the VAX-11/780 computer. The interpreter operates interactively and has a memory requirement of approximately 200K bytes, excluding all application-dependent symbolic definitions and external compiled functions and data structures. The total memory allocation for an application system based in STAR is limited only by the host operating system. This program was developed in 1985.

This program was written by Gary C. Borchardt of Caltech for **NASA's Jet Propulsion Laboratory**. *For further information, Circle 20 on the TSP Request Card.*
NPO-16965 and NPO-16832

Mechanics

Hardware, Techniques, and Processes

Books and Reports

Vortex Suppressors Reduce Probe Vibrations

A lightweight addition to the probe reduces cyclical stress aerodynamically.

Marshall Space Flight Center, Alabama

The life expectancy of an instrumentation probe for high-speed flow is increased by the addition of helical strakes to the cylindrical shield that surrounds the probe. The strakes disrupt the vortex shedding that normally occurs in fast flows around a cylindrical body (see figure).

At a sufficiently high flow, vortexes are shed by the probe shield at the resonant vibrational frequency of the probe, and the vortex shedding drives the vibrations. The vibrational forces are transmitted to the mounting base and internal components of the probe. Eventually, the repetitive stresses cause fatigue and failure.

In the case shown in the figure, strakes were added, the probe and shield were shortened, and the root diameter of the probe was increased. This redesign increased the fundamental frequency from 1,550 to 2,030 Hz and decreased the maximum stress in the probe from 60.4 kpsi (416 MPa) to 8.5 kpsi (58.6 MPa).

This work was done by Arthur J. Hill of Rockwell International Corp. for **Marshall Space Flight Center**. *For further information, Circle 136 on the TSP Request Card. MFS-29199*

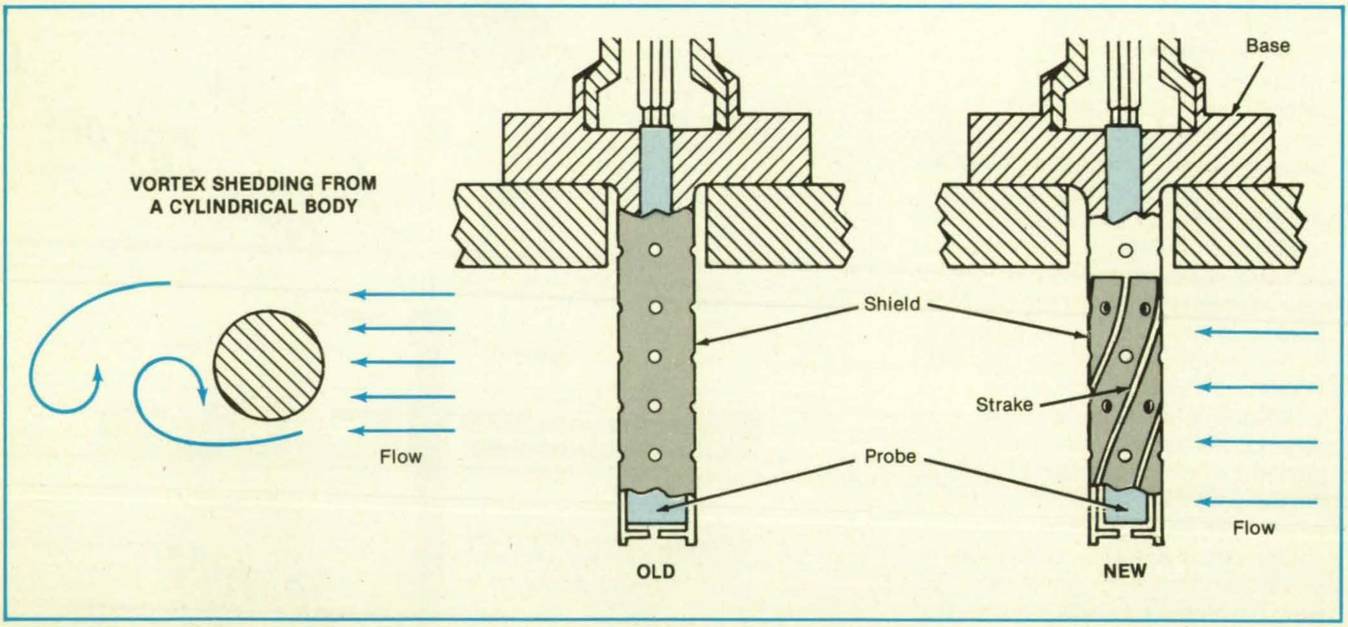

Helical Strakes on the Probe Shield suppress vortex shedding to reduce vibrational stress and thereby prolong life. In this case, the strakes are wound half a turn in 1.31 in. (3.33 cm).

Calculating Rotor/Stator Interactions

Numerical simulations are based on Euler equations and patched grids.

Ames Research Center, Moffett Field, California

The analysis procedure and the associated computer code use the Euler equations of fluid motion and patched coordinate grids to simulate the fluid flow about a rotor airfoil that moves with respect to a stator airfoil. The procedure should prove useful in studies of interactions between rotors and stators in turbines, propellers and nacelles on airplanes, and rotors and fuselages on helicopters.

To obtain a finite-difference solution of the Euler equations, it is necessary to have a computational grid that conforms to the airfoil surfaces. Because the rotor moves with respect to the stator, it is impractical to use a single grid: instead, one grid is fixed to the rotor while another is fixed to the stator. The two grids are patched together and slide past each other along a boundary. The finite-difference equations that transfer information between the grids must be numerically stable, spatially and temporally accurate, conservative (so as not to distort flow discontinuities), and easi-

ly applicable in generalized coordinates. These information-transfer equations have been developed as a part of the study.

The patched-grid technique was applied to a two-dimensional analog of the rotor/stator problem (see figure). The Euler equations for unsteady motion in two dimensions were solved by the Osher integration scheme in conjunction with an implicit relaxation approach. This scheme is accurate to second order in space and time and is total-variation-diminishing in each spatial direction.

Periodic boundary conditions were imposed on the upper and lower boundaries of both zones. Freestream conditions were imposed on the left boundary of zone 1, and supersonic exit-boundary conditions were imposed on the right boundary of zone 2. An implicit, zonal-boundary condition was used at the boundary between the two zones.

About 250 integration steps were required for each cycle, one cycle being the time required for the upper boundary of the rotor zone to move from its current position to the position occupied by the lower boundary of the rotor zone at the present time. The calculation was begun with both airfoils stationary during the first 50 integration steps. Then the rotor airfoil was allowed to move downward at a speed of mach 0.1. After about 3 cycles the initial transients were eliminated, and the solution became periodic. The movements of the pressure contours depict a shock "buzz" phenomenon in which the leading-edge shock of the right airfoil periodically attaches to, and detaches from, the airfoil.

As the figure shows, the pressure contours of the solution are continuous across the patch boundary; even the slopes of the contours are continuous. This is attributed to the conservative zonal-boundary scheme and the manner in which the continuity of dependent variables is enforced across the boundary. The captured shocks in the solution are almost free of spurious numerical oscillation because of the total-variation-diminishing nature of the integration scheme.

This work was done by Man Mohan Rai of **Ames Research Center**. *Further information may be found in NASA TM-86821 [N86-17014/NSP], "A Simulation of Rotor-Stator Interaction Using the Euler Equations and Patched Grids."*

Copies may be purchased [prepayment required] from the National Technical Information Service, Springfield, Virginia 22161, Telephone No. (703) 487-4650. Rush orders may be placed for an extra fee by calling (800) 336-4700.

Inquiries concerning rights for the commercial use of this invention should be addressed to the Patent Counsel, Ames Research Center [see page 12]. Refer to ARC-11724.

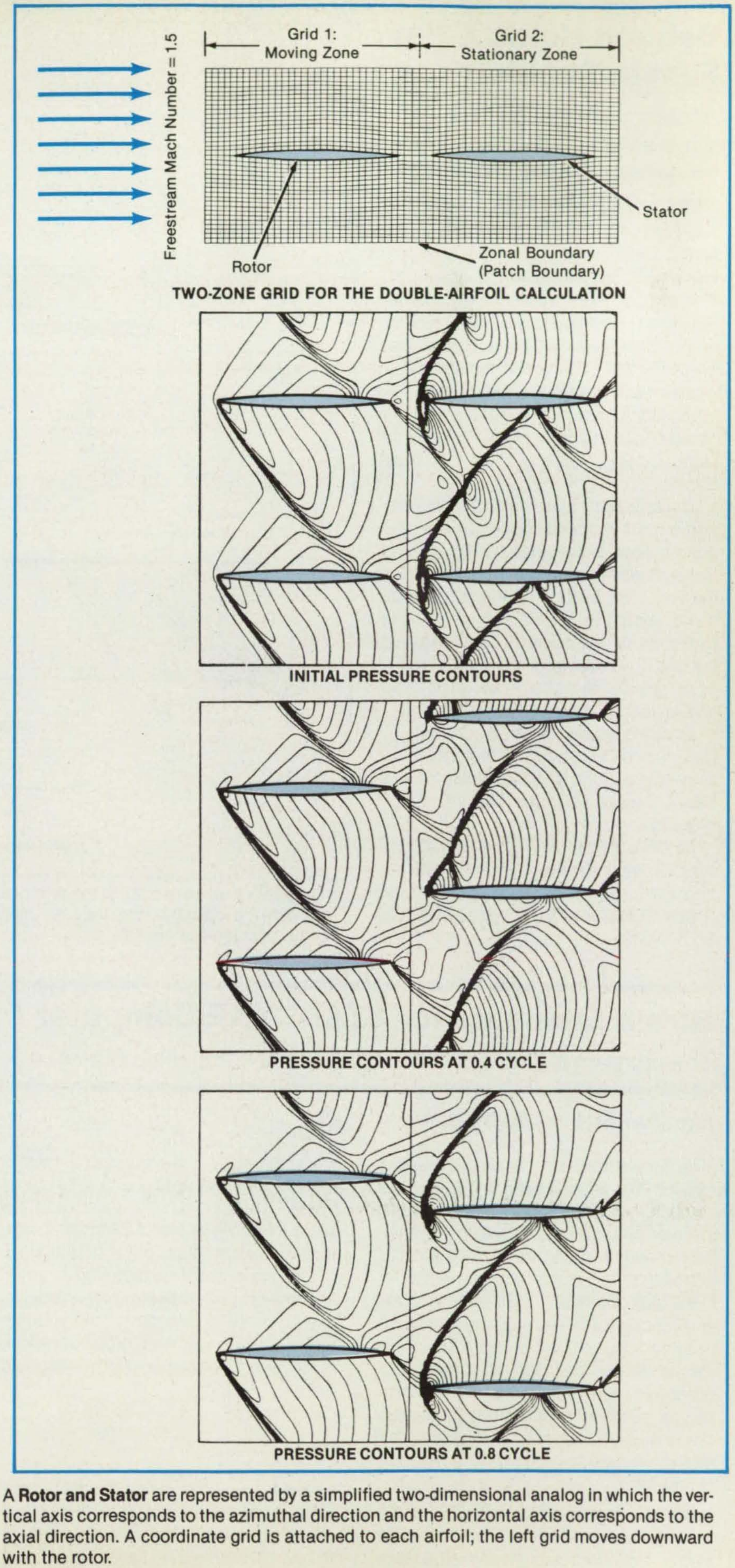

A **Rotor and Stator** are represented by a simplified two-dimensional analog in which the vertical axis corresponds to the azimuthal direction and the horizontal axis corresponds to the axial direction. A coordinate grid is attached to each airfoil; the left grid moves downward with the rotor.

Balloon Holds X-Ray Film in Position

Accuracy of position is increased.

Marshall Space Flight Center, Alabama

A simple pneumatic apparatus holds x-ray film against the inside wall of a tube or cavity. By assuring intimate contact between the wall and the film, the apparatus locates the film precisely: such precision is necessary for depth-of-defect calculations based on the image parallax produced by using different positions for the x-ray source.

The apparatus consists of a small hose with a hand-operated airpump at one end and a balloon at the other (see figure). The film is placed at the desired location near the wall. The balloon is inserted and inflated next to the film, expanding within the tube or cavity until it pushes the film against the wall. The balloon can be covered with a nylon sock to reduce the risk of bursting and to contain debris in case of a burst.

This work was done by Joseph C. Bezaire and Claudio Alonso of Rockwell International Corp. for **Marshall Space Flight Center**. *No further documentation is available.*

Inquiries concerning rights for the commercial use of this invention should be addressed to the Patent Counsel, Marshall Space Flight Center [see page 12]. Refer to MFS-29239.

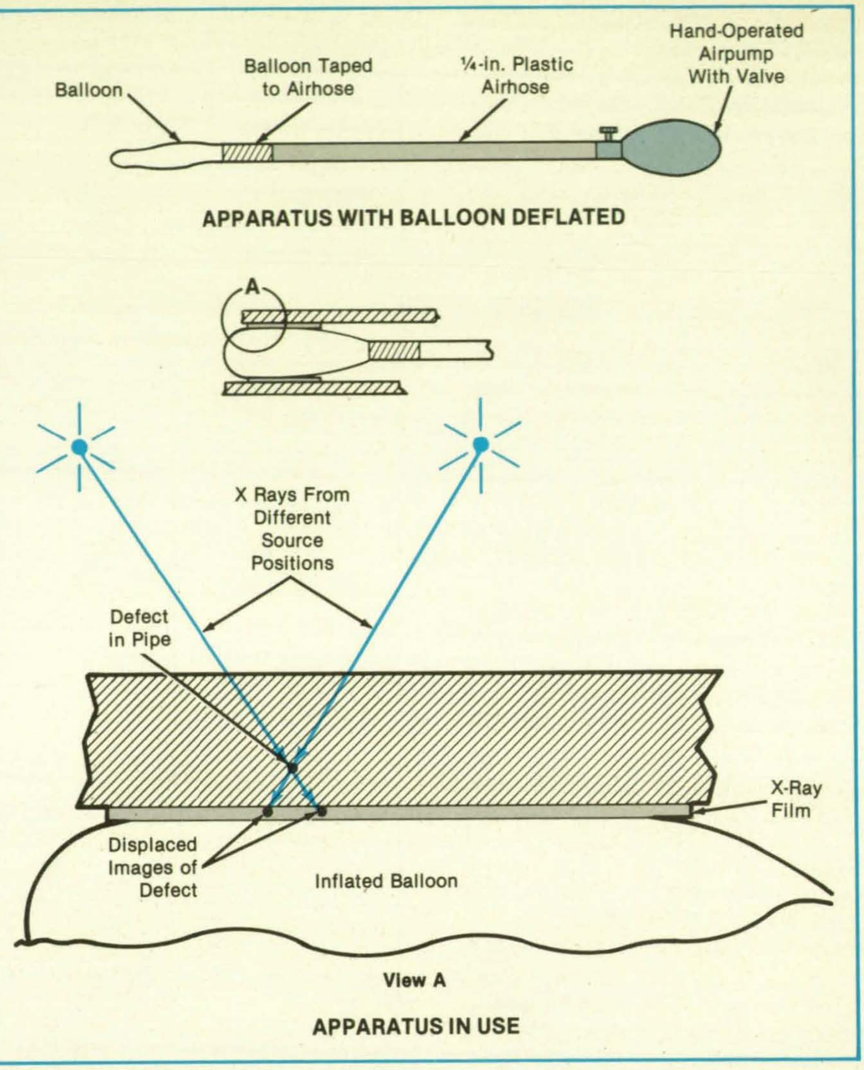

A **Balloon Is Expanded** against the confines of a cavity to push an x-ray film against the inner wall. With the assurance that the x-ray image is formed at the wall, the position of the defect can be calculated accurately.

Strain Elements for STARDYNE Computer Program

The program is "tricked" into calculation of compatible strains.

Marshall Space Flight Center, Alabama

A simple mathematical substitution causes the STARDYNE finite-element computer program to put out compatible static or dynamic strains for the elements. Such strains may be helpful in the effort to correlate strain-gauge data with finite-element mathematical models, where strain as a function of time is required in calculations of fatigue. In the problem for which the substitution was devised, it had previously been impossible to calculate compatible dynamic strains from measured random-vibration stresses because of the loss of phase information in the random-stress data.

The mathematical substitution works only for quadrilateral plates. On each plate element for which output is desired, a dummy strain plate is superimposed: mathematically, the two plates occupy the same space. The dummy plate must have the same thickness as that of the original plate to yield correct values of bending strain.

The properties of the orthotropic material of the original plate are mathematically altered by the substitution of the parameters of elasticity and density of the fictitious strain plate. These strain-plate parameters are

$$E_1 = E_2 = G = 1.00$$
$$\nu_1 = \nu_2 = 0.000001$$
$$\text{density} = 0$$

where E_1 and E_2 are the moduli of elasticity along the perpendicular x_1 and x_2 directions, respectively, and ν_1 and ν_2 are the Poisson's ratios in the x_1 and x_2 directions, respectively. (Although the desired value of ν_1 and ν_2 is zero, the use of zero causes the STARDYNE program to substitute a default value of 0.3.) The remaining STARDYNE entries are not altered.

The STARDYNE program computes compressive and tensile stresses σ_{11} and σ_{22}, where the first subscript on each σ denotes the direction perpendicular to the face of an element on which the stress is specified, and the second subscript denotes the direction of the stress. The stresses σ_{ij} are related to the corresponding strains by

$$\begin{pmatrix} \sigma_{11} \\ \sigma_{22} \\ \sigma_{12} \end{pmatrix} = \begin{pmatrix} E_1/(1-\nu_1\nu_2) & \nu_2 E_1/(1-\nu_1\nu_2) & 0 \\ \nu_1 E_2/(1-\nu_1\nu_2) & E_2/(1-\nu_1\nu_2) & 0 \\ 0 & 0 & G \end{pmatrix} \begin{pmatrix} \varepsilon_{11} \\ \varepsilon_{22} \\ \varepsilon_{12} \end{pmatrix}$$

The strains do not appear explicitly in

the STARDYNE output. However, the use of the fictitious strain-plate values converts this equation to

$$\begin{pmatrix} \sigma_{11} \\ \sigma_{22} \\ \sigma_{12} \end{pmatrix} = \begin{pmatrix} \epsilon_{11} \\ \epsilon_{22} \\ \epsilon_{12} \end{pmatrix}$$

that is, each of the output stresses for a dummy element is equal to a number proportional to the compatible strain in the corresponding element of the original plate.

This work was done by Dale O. Cipra and Richard Ehrgott of Rockwell International Corp. for **Marshall Space Flight Center**. *For further information, Circle 57 on the TSP Request Card.*
MFS-29271

Rotary Fluid Coupling

Stacked modules serve eight lines.

Lyndon B. Johnson Space Center, Houston, Texas

A rotary coupling for heat-transfer fluid contains four lines for vapor and four corresponding liquid-return lines. Unlike hose-type rotary couplings, this one allows unlimited rotation and does not have to be rewound to prevent damage to hoses.

The coupling (see figure) includes a stationary housing, consisting of four stacked modules, and an inner rotating shaft. Each module of the housing includes a vapor inlet and a liquid outlet. These inlets and outlets are connected to circumferential channels equipped with sliding rotary seals that press against the shaft.

The shaft contains a cluster of eight tubes connected to ports that are aligned axially with the corresponding circumferential channels in the housing. In each fluid circuit, vapor from the stationary side enters the housing module through an inlet and travels around the shaft in the circumferential channel until it reaches the port. The vapor then enters the corresponding tube in the shaft and travels to a radiator or other heat exchanger on the rotating side. The return liquid travels through another tube in the shaft until it reaches the port that faces the channel for liquid in the housing. The liquid travels around the shaft in this channel until it reaches the outlet, then continues toward a heat source or pump on the stationary side.

Bearings on the sides and at one end maintain the concentricity and axial alignment of the shaft and housing. An endcap prevents leakage from the housing at one end. The seals are pressure assisted and self-lubricating. Secondary seals are provided for redundant protection against

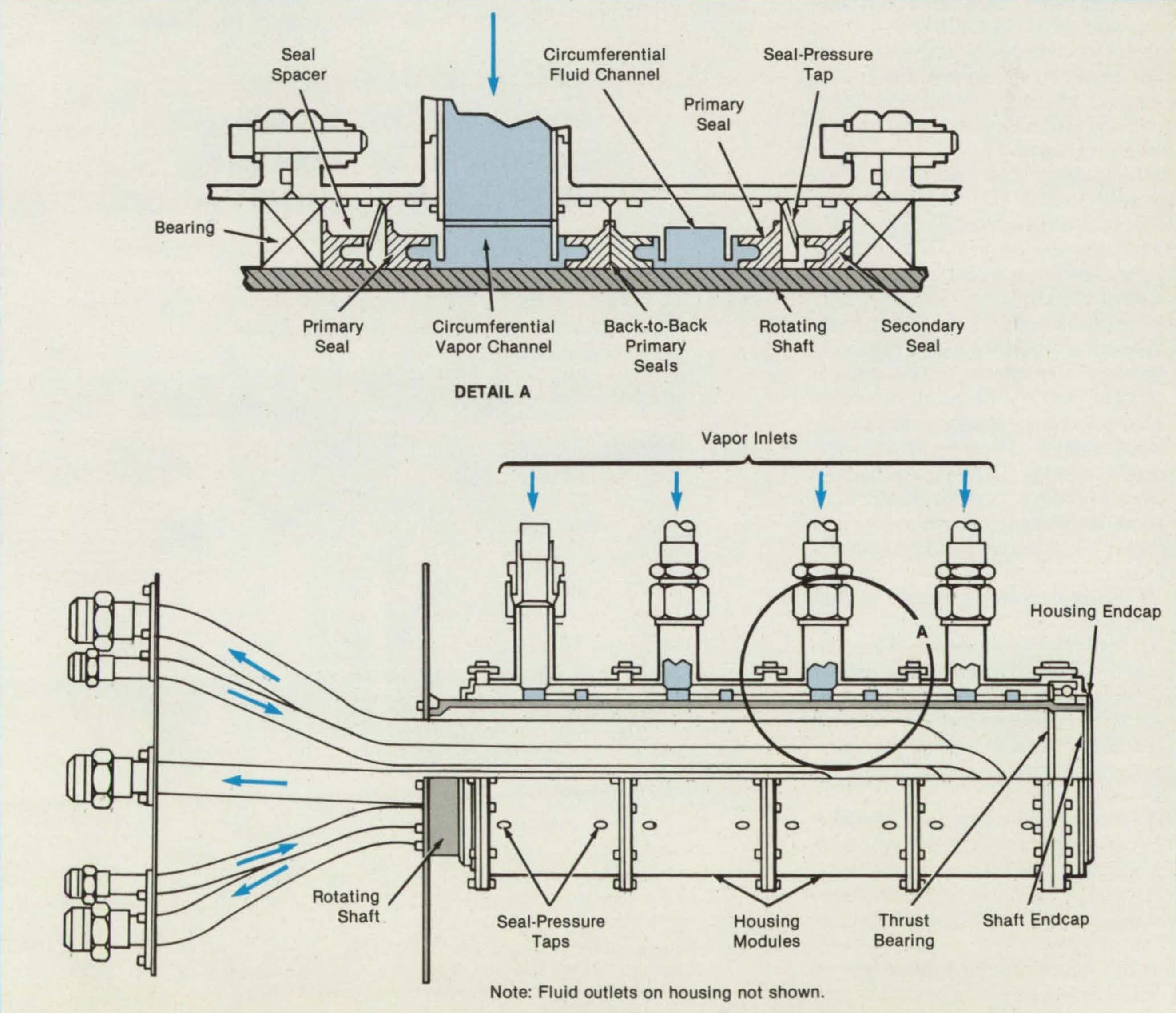

Fluid Is Coupled with minimal leakage between a stationary housing and an inner rotating shaft.

leakage from and between fluid paths. Leakage between the primary and secondary seals can be monitored and removed through pressure taps.

This work was done by Ron Zentner, Gregg D. Rhodes, and Douglas W. Thoreson of the Boeing Co. for **Johnson Space Center**. *No further documentation is available.* MSC-21215

Books and Reports

These reports, studies, handbooks are available from NASA as Technical Support Packages (TSP's) when a Request Card number is cited; otherwise they are available from the National Technical Information Service.

Computational Fluid Dynamics in Rotary-Wing Aerodynamics

Emerging techniques appear vital to progress in the rotary-wing-airplane industry.

A report reviews current trends in the field of helicopter-rotor aerodynamics. Selected test cases are used to demonstrate that current research in computational fluid dynamics (CFD) is vital to the analysis and design of advanced rotorcraft: experimental work in this area is extremely difficult, and the accepted precision being well below that of the fixed-wing-aircraft industry.

The following observations concerning the role of CFD in rotor-aerodynamic research are highlighted:

- Helicopter aerodynamic CFD is on the verge of becoming a significant force in industrial practice.
- More attention should be paid to linear lifting-surface theory, which unifies aerodynamics and acoustics in the simplest possible manner. The basic technology and algorithms are already available to the industry. Lifting-surface theory should be used to develop automated optimization procedures within its range of validity.
- Panel methods are relatively mature and should be incorporated into preliminary analyses of design and performance, by the use of available high-speed processors.
- The finite-difference approach to the analysis of high-speed rotors is slowly gaining acceptance in industry. In the next 5 years, computer codes based on potential flow will be coupled to a variety of available wake models for the analysis of performance and loads.
- The emerging Euler codes will be capable of capturing wakes if certain numerical problems induced by coarse grids can be resolved by the use of high-speed supercomputers that possess very large core memories.
- In the future, full Reynolds-averaged Navier-Stokes solvers will be used for rotor analysis. Such solutions for fixed-wing aircraft are just now beginning to appear in the literature.

The development, validation, and acceptance of a new generation of computer algorithms will also be a cohesive force within the industry. The development of efficient tools of CFD will require cooperation among industry and government laboratories, with each component having a major well-defined role in the effort. Industrial laboratories have the responsibility for validating the codes and applying them to specific company products. Government laboratories are responsible for the transfer of technology, for the development of advanced computational hardware, and for the development of more-generally-applicable algorithms. Both sectors must also work closely with the academic community in generating the new ideas and concepts that will ultimately feed into industrial practice. The process must also be flexible enough to allow all communication channels to be as open as possible.

This work was done by Sanford S. Davis and I-Chung Chang of **Ames Research Center**. *To obtain a copy of the report, "The Critical Role of Computational Fluid*

Dynamics in Rotary-Wing Aerodynamics," Circle 40 on the TSP Request Card.

Inquiries concerning rights for the commercial use of this invention should be addressed to the Patent Counsel, Ames Research Center [see page 12]. Refer to ARC-11748.

Experimental Test of Aerodynamic Computer Program

Linear potential-flow theory is applied to an advanced air plane design.

A report discusses the use of the PANAIR computer program to predict the airflow about an advanced fighter aircraft. The predictions are compared with measurements about a scale model of the aircraft in a wind tunnel at mach numbers of 0.6, 0.9, and 1.2 and at angles-of-attack from 0 to 10°.

PANAIR uses linear potential-flow theory to predict the subsonic or supersonic airflow about a body of arbitrary shape. It is based on the Prandtl-Glauert equation, which assumes that local flow velocities do not differ greatly from the freestream velocity. Therefore, PANAIR can be expected to give accurate solutions for cases in which linear flow predominates. The advanced aircraft in question is highly complex, and the investigation was done to determine how well PANAIR would predict the aerodynamics of the particular complicated geometry.

The design features a canard closely coupled to swept wings, an engine with a large inlet on each side of the fuselage, and an outrigger pod under each wing. Although the design also calls for four deflecting exhaust nozzles, the PANAIR calculations were conducted in the zero-deflection, cruise mode only. The aircraft definition was specified in terms of successive cross sections, and a computer-aided design system was utilized to generate the PANAIR model.

The user need only specify one side of the aircraft geometry when running zero sideslip cases such as those in the current study. PANAIR accounts for the symmetry about the longitudinal midplane. In the PANAIR model, the right side of the geometry has 990 source/doublet panels, 184 doublet wake panels for subsonic flow, and 243 doublet wake panels for supersonic flow. The impermeable surface is modeled by applying appropriate boundary conditions to the panels, which model the solid surface. PANAIR does not account for the model support in the wind tunnel; this may contribute to differences between PANAIR results and wind-tunnel data.

The flow-through model used in the wind-tunnel tests is approximated in the PANAIR model via the boundary conditions applied to the panels at the inlet and exit planes.

PANAIR does not solve for the shape and position of a wake from a lifting surface; these must be specified by the user for the particular model. In the numerical simulations, the position of the canard wake relative to the freestream had a large effect on the results. Canard wakes parallel to the freestream yielded results closer to experimental data than did canard wakes that remained fixed relative to the aircraft throughout the range of angles-of-attack.

Four supersonic and two subsonic nozzle-exit flow conditions were studied. The best supersonic results were obtained using networks of panels at the nozzle-exit planes and wakes off the nozzles. The best subsonic results were obtained with networks of panels but without wakes off the nozzles.

This work was done by M. D. Madson and L. L. Erickson of **Ames Research Center**. *To obtain a copy of the report, "Application of PANAIR to an Advanced Supersonic Fighter/Attack Aircraft," Circle 54 on the TSP Request Card.*

Inquiries concerning rights for the commercial use of this invention should be addressed to the Patent Counsel, Ames Research Center [see page 12]. Refer to ARC-11733.

Machinery

Zero-Deadband Ball Bearings

Axial motion of the shaft is accommodated but limited.

Marshall Space Flight Center, Alabama

Proposed supports for ball bearings would press the outer races against the balls without radial clearance (deadband). The bearing supports would thus eliminate the nonlinear spring response in the support assembly, which adversely affects the dynamics of the rotor, especially in the case of such high-speed machines as turbopumps.

In the new supports (see figure), the races are held by diaphragms or other axially flexible springs. The springs are preloaded axially in opposite directions so that the outer races are preloaded against the balls, which in turn press against the inner races rigidly clamped to the rotor. The need for diametral clearance between the outer bearing race and the bearing supports — ordinarily required to accommodate axial motion of one race relative to the other — is eliminated.

If a pair of bearings is needed at each end of the rotor, the outer race of the additional bearing at each end can be supported separately by a similar diaphragm or spring in series with the first spring. Alternatively, all of the bearings can be supported by radially stiff and axially flexible springs mounted on the frame extending from the outer-race supports. Both arrangements allow for the axial motion of the rotor without the usual diametral clearance between the outer and inner races.

Separate axial-preload springs are not needed. So that the bearings are not loosened by large axial motions of the rotor, the axial movement of the rotor can be limited by hard stops.

This work was done by Michael J. Hine of Rockwell International Corp. for **Marshall Space Flight Center**. *No further documentation is available.*
MFS-29146

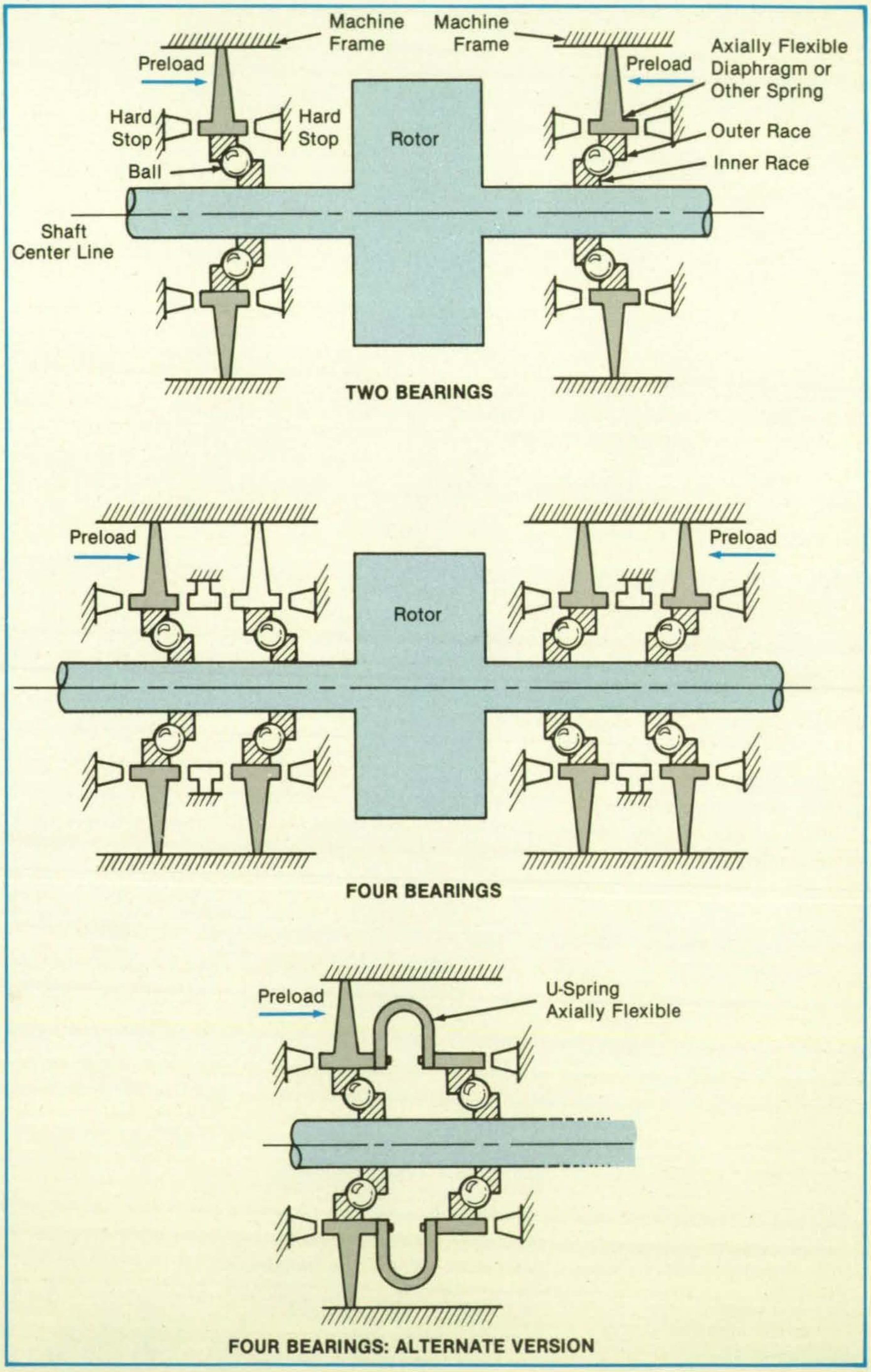

Diaphragmlike Axially Flexible Springs eliminate deadband and the consequent nonlinear radial vibrational response of the rotor. If the shaft needs two bearings at each end, they can be supported independently or connected in series by a U-spring. Mechanical stops limit the axial travel of the shaft.

WILL YOUR WORK LEAVE A LASTING IMPRESSION?

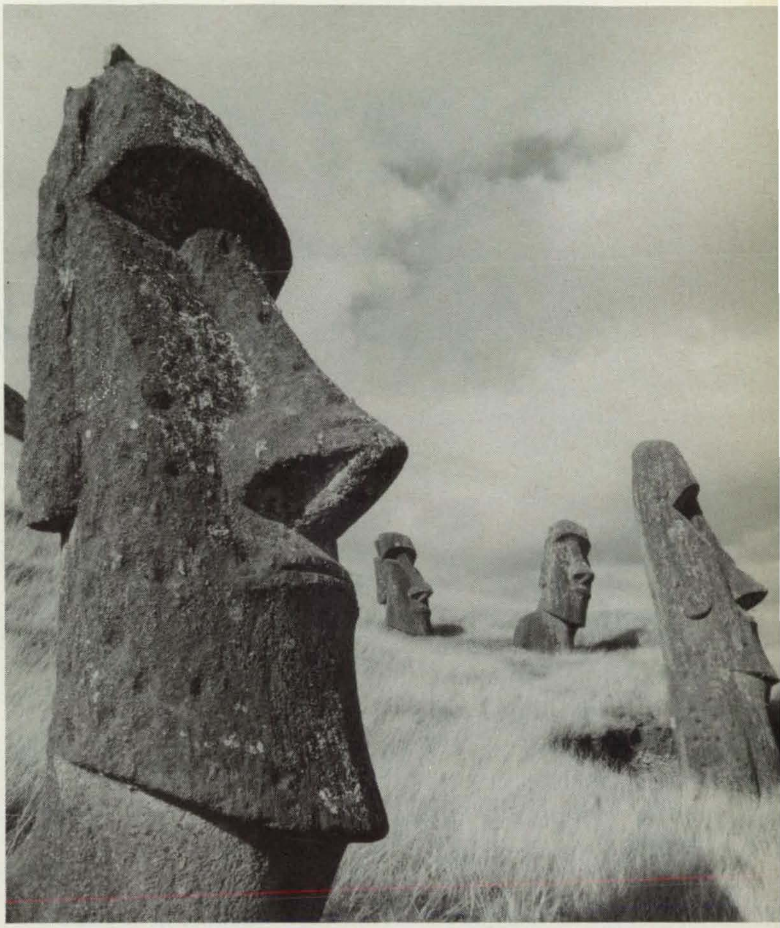

European seafarers landing on Easter Island at the beginning of the 18th century were awestruck by the hundreds of colossal statues laying scattered throughout the island. These giant carved monoliths, weighing close to fifty tons and standing up to sixty-six feet high, are puzzling scholars and explorers even today.

How did these statues come to be? Were they created by "space gods" as the natives believed? Were they left by intelligent beings from outer space? Or are they the only remnants of a highly advanced people whose entire civilization has since been destroyed?

Who was capable of engineering such fantastic images?

The enigma that is Easter Island has not yet been explained. It persists as a reminder of the infinite possibilities on earth and in space.

At General Dynamics Space Systems Division you will be encouraged to seize the challenges of the unknown and to create the technologies to explore them. You will have the opportunity, as did the anonymous sculptors of Easter Island, to create what is thought to be impossible and to leave a lasting impression for those who follow.

We currently have opportunities available for individuals with a technical degree or the equivalent combination of formal education and related experience. Government or aerospace industry background is preferred.

If you have experience in one or more of the areas listed below, please send your resume to: Professional Staffing, GENERAL DYNAMICS SPACE SYSTEMS DIVISION, MZ C2-7143-I154, P.O. Box 85990, San Diego, CA 92138. (Opportunities also exist in Huntsville, AL and Harlingen, TX.)

STRUCTURAL DESIGN
- Tank Structures
- Adapters
- Fairings
- Materials & Processes
- Pre-Design
- Liaison

FLUID SYSTEMS DESIGN
- Pneumatic
- Hydraulic
- Propulsion
- Cryogenics

THERMAL/FLUIDS ANALYSIS
- Systems Modeling
- Space Environments
- Propulsion
- Cryogenics

AVIONICS
- EMI/EMC
- Electrical Power
- Instrumentation
- RF Systems
- Parts Engineering
- Harness Design/Installation
- Liaison
- Analog/Digital Circuit Design
- Avionics Systems
- Mechanical Packaging
- Control Systems
- Guidance & Navigation

SYSTEMS
- Systems Requirements
- Systems Safety

DYNAMICS/ANALYSIS
- Launch Vehicle Transient Load
- Environmental Dynamics
- Acoustics
- Jettison Trajectory
- IRAD & CRAD
- CAE

STRESS ANALYSIS
- Hand Analysis
- Finite Element Modeling
- Structural Test Support
- CAE
- Methods

TEST & EVALUATION

GENERAL DYNAMICS

Space Systems Division

Equal Opportunity Employer/Principals Only

Circle Reader Action No. 417

Emergency-Evacuation Cart

A proposed vehicle would ease escape from areas inaccessible to or dangerous for ambulances.

John F. Kennedy Space Center, Florida

A proposed cart is designed to remove an injured worker from the vicinity of a hazardous chemical spill. The self-propelled cart would enable a rescuer to move the victim of an industrial accident quickly away from toxic, flammable, explosive, corrosive, carcinogenic, asphyxiating, or extremely cold liquids. The cart is intended for use where it is too dangerous for ambulances and other vehicles to approach the accident site.

Under control of the rescuer, the cart would carry the incapacitated victim for a distance of 3,000 ft (about 1 km) on pavement at speeds ranging up to 20 mi/h (about 9 m/s). The cart could also travel up to about 200 ft (60 m) on sand, and similar distances on rough terrain. The victim would ride in a semireclining position (see figure) to ameliorate the effects of exposure to hypergolic liquids, which can cause pneumonia. Facemasks and a compressed-air tank would furnish breathing air for 30 minutes to both the victim and the rescuer. The vehicle could accommodate victims with or without protective clothing; a protective blanket could be stored on the cart in case it is needed.

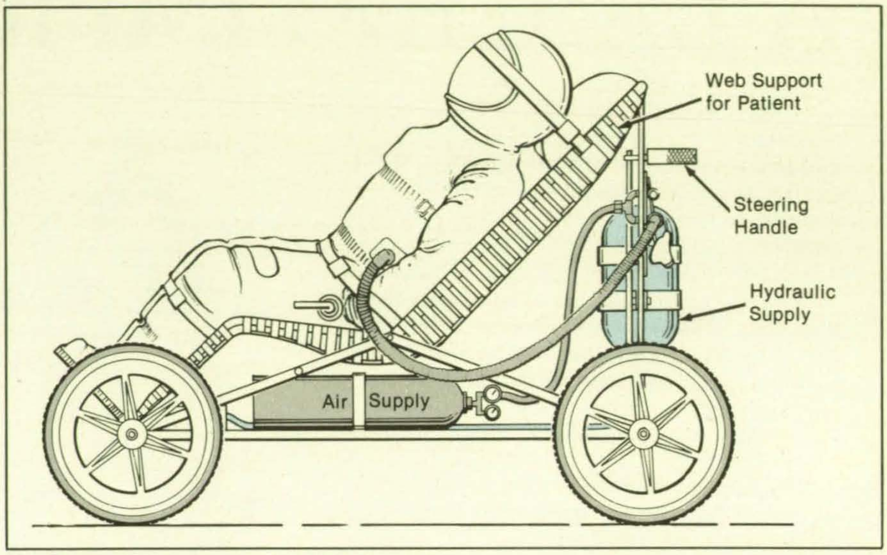

The **Rescue Cart**, constructed of high-strength tubing, would ride on bicycle wheels with balloon tires. The rescuer would steer the cart with a handle at the rear. The estimated mass of the fully equipped vehicle is 650 lb (295 kg).

Pressurized hydraulic fluid would drive the cart. Unlike an electric motor or internal combustion engine, the hydraulic motor would generate no sparks or heat that could cause a fire or explosion. The cart could be stored ready for use for 2 years or more. In an emergency, the rescuer would simply break a seal on the cart and start using it.

This work was done by Otto H. Fedor and Lester J. Owens of ***Kennedy Space Center****. For further information, Circle 133 on the TSP Request Card.*

This invention has been patented by NASA (U.S. Patent No. 4,646,860). Inquiries concerning nonexclusive or exclusive license for its commercial development should be addressed to the Patent Counsel, Kennedy Space Center [see page 12]. Refer to KSC-11282.

Books and Reports

These reports, studies, handbooks are available from NASA as Technical Support Packages (TSP's) when a Request Card number is cited; otherwise they are available from the National Technical Information Service.

Gear Handbook

Topics range from early history to advanced design.

A reference publication that integrates the results of 15 years of NASA-related gear research has been compiled to form a complete design synthesis using the latest analytical methods, materials, and lubrication analysis and techniques. The introductory section provides background information separating the early history of gearing and the beginning of modern gear technology. Section 2 describes the types and geometry of gears, including information on proper gear selection. Section 3 covers the processing and manufacture of gears. This section includes a comprehensive treatise on gear materials and metallurgical processing variables as well. Stresses and deflections of gear teeth are treated in Section 4.

Life-prediction methods are presented in Section 5 together with sample problems. Gear lubrication and the application of lubricants to improve gear operation, life, and reliability are given in Section 6. This section includes additives as well as elastohydrodynamic effects. Section 7 provides methodology and equations for the prediction of power loss. The optimal design of spur-gear mesh, including sizing for torque and life, is presented in Section 8. The final section deals with gear-transmission concepts. The information in this section can be combined with the information from previous sections to form a design synthesis for mechanical transmissions.

This work was done by John J. Coy, Dennis P. Townsend and Erwin V. Zaretsky of ***Lewis Research Center****. Further information may be found in NASA Reference Publication 1152 [N86-14612/NSP] (AVSCOM Technical Report 84-C-15), "Gearing."*

Copies may be purchased [prepayment required] from the National Technical Information Service, Springfield, Virginia 22161, Telephone No. (703) 487-4650. Rush orders may be placed for an extra fee by calling (800) 336-4700.
LEW-14489

Study of Helicopter-Tail-Rotor Noise

Impulsive noise and blade loads in blade/vortex interactions are discussed.

A report describes the findings of an experiment in the generation of impulsive noise and fluctuating blade loads by a helicopter tail rotor interacting with the vortexes from the main rotor. The experiment used a model rotor and an isolated vortex and was designed to isolate the blade/vortex interaction (BVI) noise from other types of rotor noise.

It was found that BVI produces impulsive noise, which radiates primarily ahead of the blade. The interaction away from the blade tip demonstrated the dipole character of BVI radiation. More-

over, the direction of minimum noise radiation, previously found to be in the plane of the blade, was found to be shifted considerably downstream. The shift is believed to be due to unsteady drag radiation caused by the stronger BVI's in the present study.

For BVI close to the rotor tip, the three-dimensional relief effect reduced the intensity of the interaction, despite the larger BVI angle and higher local mach number. The radiation pattern was also more complex because of diffraction at, and pressure communication around, the tip.

Fluctuating blade pressures measured near the leading edge displayed impulsive features due to BVI. Away from the tip, the peak-to-peak amplitude of fluctuating pressure on the suction side of the blade was larger than that on the pressure side. However, this trend was reversed near the blade tip. Furthermore, the peak-to-peak amplitude of the fluctuating pressure on the pressure side near the tip was consistently the largest of all measured blade pressures for all conditions tested.

This work was done by Ali R. Ahmadi of Bolt Beranek and Newman Inc., for **Ames Research Center**. *Further information may be found in NASA CR-177338 [N85-23376/NSP], "An Experimental Investigation of the Chopping of Helicopter Main Rotor Tip Vortices by the Tail Rotor."*

Copies may be purchased [prepayment required] from the National Technical Information Service, Springfield, Virginia 22161, Telephone No. (703) 487-4650. Rush orders can be placed for an extra fee by calling (800) 336-4700.

Inquiries concerning rights for the commercial use of this invention should be addressed to the Patent Counsel, Ames Research Center [see page 12]. Refer to ARC-11677.

Interference Fits and Roller-Bearing Fatigue

Factors affecting life and stress are analyzed.

A technical memorandum describes studies of the effects of interference fits on the fatigue lives of roller bearings. With the advent of higher-speed aircraft turbojet engines, engine manufacturers began experiencing shorter bearing life than could be accounted for by conventional analysis, material and metallurgical variables, and manufacturing processes. As a result, aircraft users and engine manufacturers have borne the high costs of warranty replacements.

By trial-and-error methods, interference fits between the bearing rings and mainshafts have been adjusted, resulting in increased bearing lives. However, the reason for this improvement was not readily apparent. An analysis was performed to determine the effects of inner-ring speeds and press fits on roller-bearing fatigue lives. The effects of the resultant hoop and radial stresses on the principal stresses were considered.

The maximum shear stresses below the Hertzian contact were determined for different conditions of inner-ring speed and load and were applied to a conventional roller-bearing analysis. The effect of the mean stress was determined through a Goodman-diagram approach. It was found that hoop stresses caused by press fits and centrifugal forces can reduce bearing lives by as much as 90 percent. The use of a Goodman diagram resulted in a prediction of a life reduction of 20 to 30 percent. The depth of the maximum shear stress remained virtually unchanged.

This work was done by Harold H. Coe and Erwin V. Zaretsky of **Lewis Research Center**. *Further information may be found in NASA TM-87165 [N86-19616/NSP], "Effect of Interference Fits on Roller Bearing Fatigue Life."*

Copies may be purchased [prepayment required] from the National Technical Information Service, Springfield, Virginia 22161, Telephone No. (703) 487-4650. Rush orders may be placed for an extra fee by calling (800) 336-4700. LEW-14490

Testing Parabolic-Dish Concentrators

Experience at a solar-energy test site is described.

A report describes test equipment and tests at the Parabolic Dish Test Site at Edwards Air Force Base in California. The site was established in 1978 for testing point-focusing solar concentrators operating at temperatures above 600 °F (315 °C). It was used for six years to evaluate parabolic-dish concentrators, receivers, power-conversion units, and solar/fossil-fuel hybrid units. The report describes the evolution of the test program at the site, lists the experiments conducted there in chronological order, and summarizes the experimental data.

The site was used to check the performances of newly designed subsystems and components, to conduct tests to analyze the effect of independent variables on performance, and to develop rapid optical testing techniques of parabolic-dish concentrators.

The concentrators at the site included the following:

- A precursor concentrator simulating a portion of a parabolic concentrator, used to measure mirror performance and evaluate alignment techniques;
- An electricity-generating-concentrator power module with a two-axis Sun tracker developed by the industry;
- Two test-bed concentrators, 11 m in diameter; and
- A low cost concentrator designed for mass production.

Prior to the tests performed at the site, trackers and concentrators were mechanically checked. The mirror segments were aligned, and solar-tracking errors, mirror-surface reflectances, and moonlight focal-point locations were measured. Radiation fluxes were mapped in the focal zones, and thermal performances of receivers were measured by cold-water calorimeters. Systems were proof tested and leak tested. Performances of power conversion modules were measured.

This work was done by M. Kudret Selcuk of Caltech for **NASA's Jet Propulsion Laboratory**. *Further information may be found in DOE/JPL-1060-84 [N85-28447/NSP], "Parabolic Dish Test Site: History and Operating Experience."*

Copies may be purchased [prepayment required] from the National Technical Information Service, Springfield, Virginia 22161, Telephone No. (703) 487-4650. Rush orders may be placed for an extra fee by calling (800) 336-4700.
NPO-16848

Transfer Lubrication for Cryogenic Bearings

Bronze-filled PTFE cages promise to extend lives of ball bearings.

A report presents an evaluation of bronze-filled polytetrafluoroethylene (PTFE), known as Salox M (or equivalent), as the cage material for ball bearings in high-pressure turbopumps for liquid oxygen. The material was evaluated as a potentially longer-lived replacement for glass-filled PTFE known as Armalon (or equivalent). The cage transfers PTFE to the balls to form a solid lubricant film. However, glass fibers in the glass-filled material tend to interfere with the transfer.

The evaluation addressed the following questions:

- Will the bronze-filled PTFE transfer a film at cryogenic temperatures?
- What is the wear rate of bronze-filled PTFE in comparison with the glass-filled PTFE?
- Does the bronze-filled material cause less deleterious ball wear than the glass-filled PTFE?
- Is transfer enhanced at some value of the ball-surface roughness?
- Can the bronze-filled material be fabricated in an acceptable cage configuration?

A series of experiments was conducted to answer the questions. The experiments involved block-on-ring tests (the block was the filled PTFE, and the ring was through-hardened 440C steel) and high-speed traction tests of two 440C steel disks, in which one disk was rubbed with a filled PTFE block to generate a film. Posttest visual observations were made of the condition of the steel, and measurements were made of wear of the block and of the traction between the disks.

Both the bronze-filled and glass-filled PTFE transferred PTFE to the steel at cryogenic temperatures. Bronze is also transferred from the bronze-filled material. The bronze-filled PTFE wore slightly more than the glass-filled PTFE. However, the bronze-filled material was clearly less abrasive to the steel than was the glass-filled material. Smooth ball surfaces were found to accept PTFE adequately. The wear rate did not change significantly when the surface roughness was increased from 0.025 μm to 0.1 μm. With greater roughness, however, the wear rate increased.

Two cage-design concepts were developed: one involves a metal-reinforced cage of bronze-filled PTFE; the other calls for bronze-filled PTFE inserts in a metal structure.

This work was done by S. A. Barber, J. W. Kannel, and K. F. Dufrane of Battelle for **Marshall Space Flight Center**. *To obtain a copy of the report, "Evaluation of Transfer Films of Salox M on 440C for HPOTP Bearing Cage Applications," Circle 8 on the TSP Request Card. MFS-27167*

Flexible Docking Tunnel

A flexible tunnel would reduce the risk of damage to spacecraft.

A brief report proposes the use of a flexible tunnel to provide "soft docking" between a Space Shuttle Orbiter and the space station during resupply visits. Soft docking would reduce the risks of structural damage to either spacecraft during docking maneuvers, provide an adaptable docking interface, and avoid jarring sensitive material-processing experiments in the space station. After docking, the tunnel would be pressurized to enable the exchange of people and cargo between the two spacecraft.

To date, only "hard-docking" procedures have been used with spacecraft. Most have used a pin-and-cone principle, according to which a probe on one spacecraft slides into a drogue cone on the other spacecraft, triggering a latching process. Despite features designed to lessen the impact of the two spacecraft, it has been estimated that hard docking of the Orbiter to the space station would result in a 3-mm displacement of the space station from its normal path.

One end of the docking tunnel would be permanently attached to the space station. If the docking end of the tunnel were designed to link with the Orbiter airlock, rather than to the docking module now being contemplated, then the module (which would occupy 12 percent of the payload-bay length and 6 percent of the payload weight capacity) would not be required.

The alignment process required prior to docking could be based on a system of light-emitting diodes surrounding the mating section on the Orbiter, operating in conjuction with sensors in corresponding positions around the opening at the free end of the tunnel. Sealing of the tunnel to the Orbiter could be achieved by a rotating mount at the end of the tunnel, by the use of pressure differentials, or by mechanical hatches.

This work was done by Roger Michaud, Ladonna Miller, and Kathy Albright of General Electric Co. for **Johnson Space Center**. *To obtain a copy of the report, "Flexible Docking Tunnel," Circle 85 on the TSP Request Card. MSC-21226*

Recursive Dynamic Equations for Two Robot Arms in a Closed Chain

Filtering and smoothing algorithms solve forward dynamics for closed chain systems.

A paper discusses the use of difference equations from Kalman filtering and Bryson-Frazier smoothing to solve the equations of forward dynamics of a closed chain of robot-arm links. By "forward dynamics" is meant the computation of the linear and angular accelerations of the joints between the links, given a set of applied or prescribed joint torques. The paper lays the foundation for the potential use of filtering and smoothing techniques in the dynamics of robots and in the design of controls for robots.

The problem involves a mechanical system of N rigid links connected together by $N+1$ rotary joints; the two ends of the chain (joint 0 and joint $N+1$) are located at fixed points on an immovable base. Joints 0 and $N+1$ lie at the bases of the left and right robot arms, respectively, and one of the intermediate links represents the object handled by the two arms.

As in a previous paper on the recursive dynamics of a single robot arm, the author introduces the concept of spatial force on a link by defining the six-dimensional vector that represents the torques and forces on the link. Similarly, the spatial acceleration is defined as the six-dimensional vector representative of the linear and angular accelerations of the link. The spatial inertia is defined as a six-by-six matrix that specifies the mass and moments of inertia of the link, and the spatial interval is defined as the ordinary three-dimensional vector from the inner to the outer joint of the link.

In this matrix/vector form, the equations of motion for each joint are combined into a linear difference equation that enables the spatial force at an inner joint to be calculated from the spatial force at an outer joint and the spatial acceleration of the link. The difference equation is similar in form to equations that describe the evolution of state-space systems in discrete time steps; here, the spatial force plays the role of the state, while the link spatial interval plays the role usually reserved for the discrete time step.

The kinematic equations are combined into a difference equation for the spatial accelerations as functions of the joint accelerations. The spatial accelerations play the role of costates that are typical in optimal-control and estimation problems. The costate equation gives the spatial acceleration of a link at its outer joint, given the acceleration of its inner joint. The combination of state and costate equations defines a two-point boundary-value problem, with the boundary condition that the costates vanish at the bases of the two arms because the bases do not move.

One forward-dynamical solution of the boundary-value problem is based on the use of the Bryson-Frazier smoother twice: first to solve the problem with fixed/free boundary conditions and then to correct the first solution to match the true fixed/fixed conditions. The filtering recursions involve prediction and correction corresponding to that of a Kalman filter with no measurement noise. After the first smoothing process, the fixed boundary condition of the base of the left arm is not matched. However, the condition is matched in the second smoothing process, which is a forward and backward recursion that gives the spatial and joint accelerations, using the results of the first process as inputs.

In an alternative solution, the roles of the states and costates are reversed to enable better matching of the boundary conditions. It is not necessary to use the smoothing procedure twice, but there is a penalty in a slight increase in the complexity of the recursive equations.

This work was done by Guillermo Rodriguez of Caltech for **NASA's Jet Propulsion Laboratory**. *To obtain a copy of the report, "Recursive Forward Dynamics for Two Robot Arms in a Closed Chain," Circle 35 on the TSP Request Card. NPO-17072*

Fabrication Technology

Hardware, Techniques, and Processes

Preassembly of Insulating Tiles

A mesh backing carries ceramic tiles to ease installation and prevent damage.

Lyndon B. Johnson Space Center, Houston, Texas

A concept for preassembling high-temperature insulating tiles speeds and simplifies installation and repair and reduces damage from handling. Moreover, the preassembly concept would facilitate the placement of tiles on gently contoured surfaces as well as on flat ones. The concept resembles that for preassembled kitchen and bathroom tiles. Applications might include boilers, kilns, and furnaces.

The tiles would be bonded with a silicone adhesive to a nylon mesh backing, chosen for light weight and high resistance to strain. The tiles would be hexagonal so that a sheet of them on the backing could nearly conform to a curved surface. For example, preassembled 2.5-in. (6.35-cm) hexagons of 0.5-in.- (1.27-cm)-thick ceramic would readily conform to a surface having a 3-ft (0.9-m) radius of curvature, and probably even to a surface of 1-ft (0.3-m) radius. Smaller radii may be accommodated by smaller hexagonal tiles.

The specific backing mesh would be chosen according to the requirements of specific applications. For the Space Shuttle service for which the concept was developed, the primary purpose of the backing was to maintain the assigned configuration of the preassembled tiles, with minimal influence on the supporting structure.

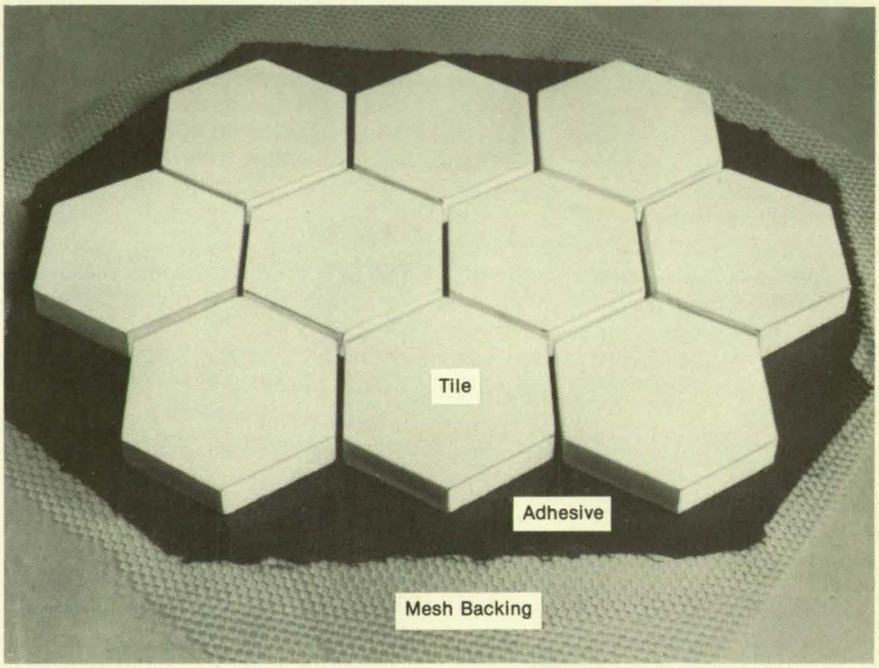

Tiles Are Bonded to nylon mesh with a room-temperature-vulcanizing silicon rubber. The spacing between tiles is 0.03 in. (0.76 mm).

Once the tiles have been bonded to it, the backing carries them through such final processing steps as drying, sintering, coating by spraying or dipping, and computer-controlled machining to final thickness. Through all, preassembly on the backing will reduce the cost of processing as compared with that of the handling of individual tiles. Tile preassemblies can be emplaced in a "cut-and-paste" operation similar to that of commercially available tiles for the home.

This work was done by Y. D. Izu, E. N. Yoshioka, and T. Rosario of Lockheed Missiles and Space Co. for **Johnson Space Center**. *For further information, Circle 67 on the TSP Request Card.*
MSC-21204

Anodization as a Repair Technique

A thin, hard oxide layer can be added to an aluminum part.

Lyndon B. Johnson Space Center, Houston, Texas

Surfaces on an aluminum part that are worn out of tolerance by no more than 0.004 in. (0.1 mm) often can be repaired by anodizing to build up aluminum oxide layers. The oxide layers are very hard and can be ground to the desired final dimensions.

Over the past two years this technique has been used to salvage a number of machined fittings with close-tolerance holes that were oversize or "egg-shaped." It is expected that the technique will become a standard repair procedure.

Although the chemistry is different, the new repair technique is conceptually similar to the use of surface plating to restore worn surfaces on steel parts; for example, hard chromium plating on engine crankshafts. Unlike plated metal, the anodized layer is an integral part of the surface and hence not subject to peeling or separation during thermal or structural loading. Also, unlike plating, anodization does not require the preparatory removal of material from the surface to be treated.

This work was done by Roy E. Groff, Robert D. Maloney, and Robert W. Reeser of Martin Marietta Corp. for **Johnson Space Center**. *No further documentation is available.*
MSC-21177

Electrostatic Liquid-Drop-Levitation System

Charged drops up to 4 mm in diameter remain spherical during levitation.

NASA's Jet Propulsion Laboratory, Pasadena, California

An electrostatic levitator has levitated drops of liquid up to 4 mm in diameter while maintaining spherical drop shapes. The stable levitation of spherical drops will be valuable in experiments involving supercooling, solidification, and crystal growth.

Previously, only smaller drops had been electrostatically levitated without significant distortion; comparably large drops had been levitated by acoustic and airflow techniques, but only with distortions of drop shapes away from spherical.

Before the drop is formed, a vertical electric field is applied between the levitator electrodes. The drop to be levitated is formed by a small nozzle located near the lower electrode in the levitator (see figure). The nozzle is connected to a reservoir of the liquid through a valve or a syringe pump, which controls the flow rate and the final volume of the drop.

The electric field charges the drop by induction and helps to support the drop against gravitation. To launch the drop, a much larger electric field is applied momentarily. Once the drop is free of the nozzle, its vertical position between the electrodes is actively controlled by varying the applied electric field under microprocessor control.

This work was done by Won Kyu Rhim, Sang Kun Chung, Michael T. Hyson, and Daniel D. Elleman of Caltech for **NASA's Jet Propulsion Laboratory**. *For further information, Circle 21 on the TSP Request Card.* *NPO-16823*

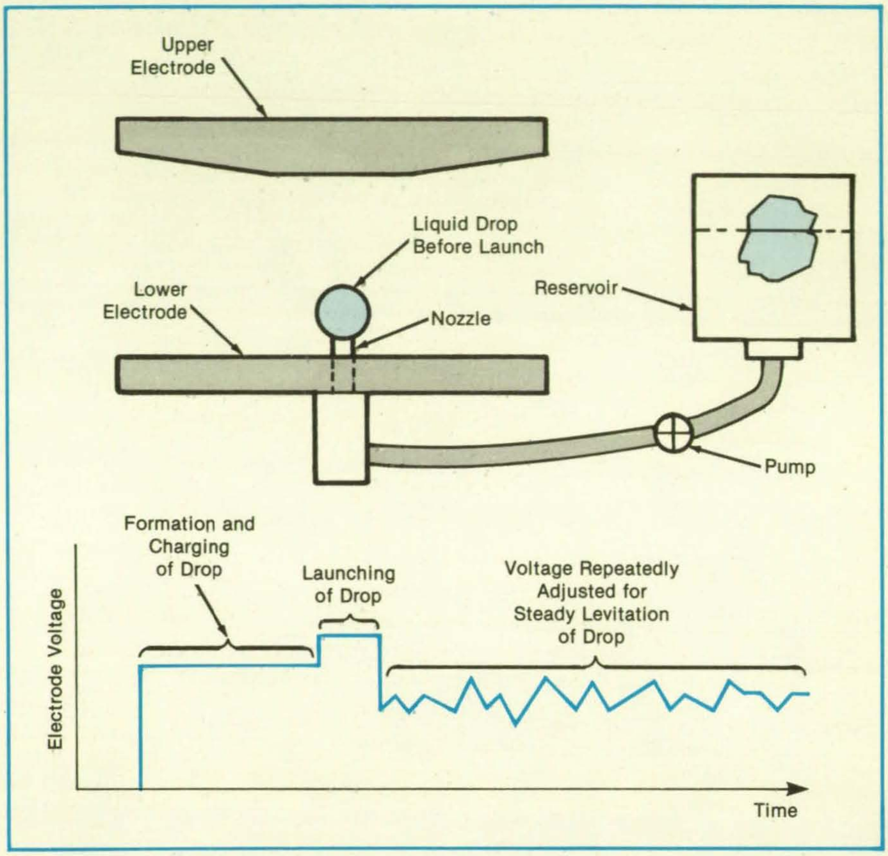

The **Drop To Be Levitated** is formed on the nozzle. The graph indicates how the field between the plates of the levitator changes during the formation and levitation of a drop.

Electron Beam "Writes" Silicon on Sapphire

Micron-wide lines are formed.

Ames Research Center, Moffett Field, California

A method of growing silicon on a sapphire substrate uses a beam of electrons to aid the growth of the semiconductor material. The silicon forms as an epitaxial film in precisely localized areas in micron-wide lines. The method therefore is a promising fabrication method for fast, densely-packed integrated circuits.

The conventional way of growing epitaxial films of silicon on silicon or sapphire is by the chemical-vapor deposition (CVD) of silane at essentially atmospheric pressure (1.013×10^5 Pa) in a reactor at a temperature of 700 to 1,000 °C. Silicon precipitates from the silane vapor, uniformly coating the entire sapphire substrate.

The new process depends upon the effect of substrate cleanliness on CVD at silane pressures considerably below at-

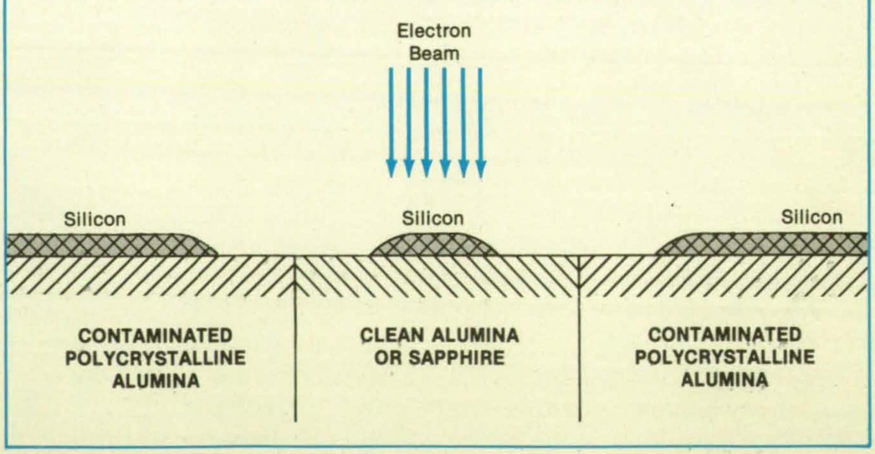

Silicon Is Deposited preferentially in contaminated substrate zones and in a clean zone irradiated by an electron beam. The electron beam, like the surface contamination, appears to stimulate the decomposition of the silane atmosphere.

mospheric. Silicon grows preferentially on contaminated polycrystalline alumina or on contaminated single alumina crystals of various orientations and crystalline phases. Deposition is suppressed, however, on clean substrates. The presence of an electron beam on a clean area reestablishes growth at essentially the same rate that is experienced on contaminated areas without the electron beam.

In the new process, a clean sapphire substrate is prepared by electron-beam flash heating of an amorphous-alumina film to 1,250 °C. (It may also be possible to clean the alumina without recrystallization to sapphire by heating for several minutes or hours to temperatures between 1,000 and 1,250 °C.) The substrate is placed in a silane atmosphere of 0.001 to 100 Pa and heated to 900 to 1,000 °C. A 100-keV, 1-mA/cm^2 electron beam is directed at the sapphire substrate in the requisite pattern. A silicon film forms wherever the beam strikes (see figure). The thickness of the silicon deposit grows at a rate of the order of several nanometers per minute.

This work was done by Klaus Heinemann of Stanford University for **Ames Research Center**. *No further documentation is available.*

Inquiries concerning rights for the commercial use of this invention should be addressed to Patent Counsel, Ames Research Center [see page 12]. Refer to ARC-11411.

Ceramic Welding-Torch Extension

A simple attachment extends a torch to difficult-to-reach joints.

Marshall Space Flight Center, Alabama

An extension for a welding-torch gascup enables a welder to reach joints through openings that are otherwise too narrow or deep. With its critical part made of a machinable ceramic, the extension can readily be cut to the required size and shape but will not short-circuit the welding arc.

The extension consists of the following three parts (see figure):

1. An externally threaded bushing fits into a standard gascup so that it protrudes from the end of the cup. The bushing can be made of metal or machinable ceramic.
2. An internally threaded torch extender screws onto the protruding bushing. The extender is made of machinable ceramic that provides electrical insulation from the arc.
3. A gasket seats between the gascup and a shoulder on the extender. The gasket provides a gas-tight seal. It can be made of polytetrafluoroethylene or other heat-resistance gasket material.

Unlike extenders fabricated from steel, the ceramic extender does not have to be plasma-spray-coated with a refractory insulating material. It is therefore immune to the flaking and chipping that plague coated-steel extenders. Flaking and chipping expose bare metal to arcing and create debris, either of which can ruin a weld.

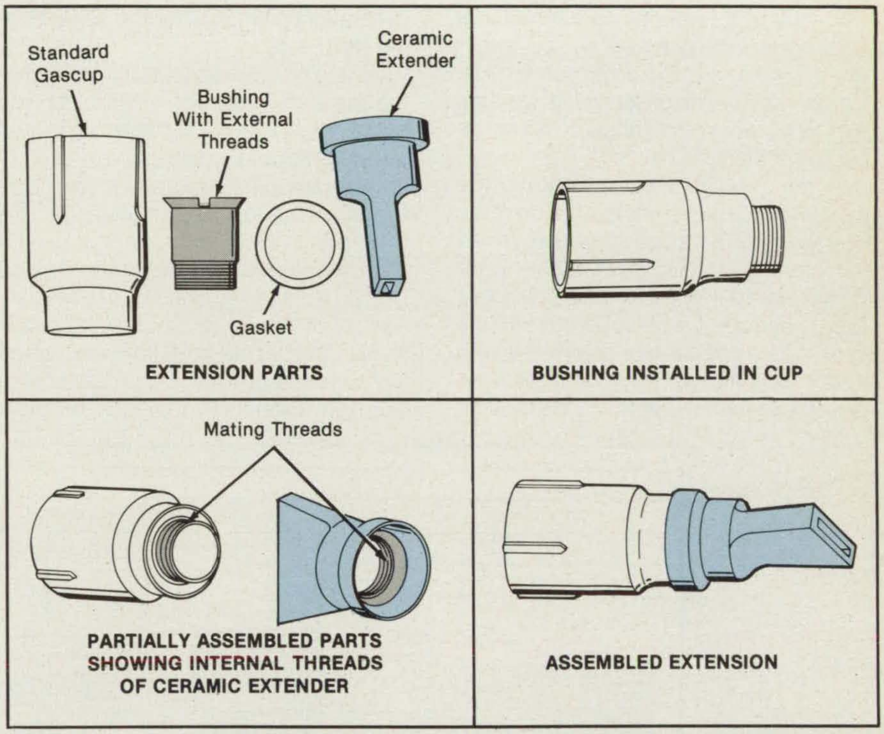

The **Bushing, Gasket, and Extender** mate with the gascup to form the extension assembly. The extender is designed and fabricated to suit a particular job.

This work was done by Stephen S. Gordon of Rockwell International Corp. for **Marshall Space Flight Center**. *No further documentation is available.*

Inquiries concerning rights for the commercial use of this invention should be addressed to the Patent Counsel, Marshall Space Flight Center [see page 12]. Refer to MFS-29252.

Checking Nickel Plate for Porosity

A porosity test goes for a free ride with a cryogenic adhesion test.

Marshall Space Flight Center, Alabama

Porosity in nickel plating on thermally insulated components can be readily detected as a side effect of an adhesion test for the plating. The combined adhesion/porosity test makes it unnecessary to subject the plated layer to a tedious, time-consuming inspection through a magnifying glass or microscope.

The adhesion of the nickel plating is checked by immersing the plated, thermally insulated part in liquid nitrogen, then withdrawing it and examining it for separation of the plated layer. A side effect of the immersion is that as soon as the part is removed from the cryogenic bath and for several minutes afterward, outgassing occurs at pores in the form of small gas jets. At each pore, the jet causes a rapid buildup of white frost that can be seen easily with the unaided eye.

The frosted areas can be marked so that the pores can be found after the frost disappears. A plating stylus can then be used for local repair of the nickel layer.

This work was done by Michael D. Roberts of Rockwell International Corp. for **Marshall Space Flight Center**. *No further documentation is available.*
MFS-29246

Image Control in Automatic Welding Vision System

The orientation and brightness are varied to suit welding conditions.

Marshall Space Flight Center, Alabama

An image controller for a welding vision system maintains a fixed orientation of the view presented to a video camera regardless of the motion of the welding torch. The controller presents a view in which the unwelded joint, the weld pool, and the weld bead always appear from top to bottom in the video picture. The constant orientation simplifies analysis of the weld image by the computer that operates the welding robot.

In addition, the image controller regulates the level of light entering the camera. Since the light level can vary widely, depending on welding current and the length of the welding arc, the controller ensures that the light used to generate the video image stays within the range of linear response of the camera.

In the welding head, the image of the weld is formed on the end of a bundle of optical fibers, as described in "Robotic Vision for Welding" (MFS-27119), *NASA Tech Briefs*, Vol. 10, No. 5 (September/October 1986), page 121. The fibers carry the image to an optics-and-camera unit (see figure) on the robot frame. The light from the output end of the fiber-optic bundle passes through an iris, the opening of which is adjusted by a servomechanism to regulate the light level. The vision-system computer sends commands to the servomechanism according to the level of the video-camera output.

Leaving the iris, the light passes through a Dove prism — one that when rotated, rotates the image twice as much. A servomechanism drives the prism so that the required top-to-bottom orientation of the weld image is maintained. Again, the computer generates commands for the servo from the video data.

An analog video signal is used to display the image on a television monitor. Portions of the image in two adjustable "windows" are also digitized: one window is used to acquire data in the region of the weld joint; the other is used to acquire data from the weld pool. Within each window, picture elements along a scan line can be skipped or scan lines can be skipped to reduce the amount of data to be processed. Frames (at the standard rate of 30 frames/s) can be skipped to assure that image data are not acquired faster than they can be processed. The additional exposure time made available by the skipped frames can be exploited to brighten the image, if necessary, by integrating the image brightness in the camera over more than one frame period. Image processing is described more fully in the companion article, "Processing Welding Images for Robot Control" (MFS-26036) in this issue of *NASA Tech Briefs.*

This work was done by Richard W. Richardson of Ohio State University for **Marshall Space Flight Center**. *For further information, Circle 103 on the TSP Request Card.*

In accordance with Public Law 96-517, the contractor has elected to retain title to this invention. Inquiries concerning rights for its commercial use should be addressed to

Ohio State University
Attn. Professor R. W. Richardson
1314 Kinnear Road
Columbus, OH 43212.

Refer to MFS-26035, volume and number of this NASA Tech Briefs *issue, and page number.*

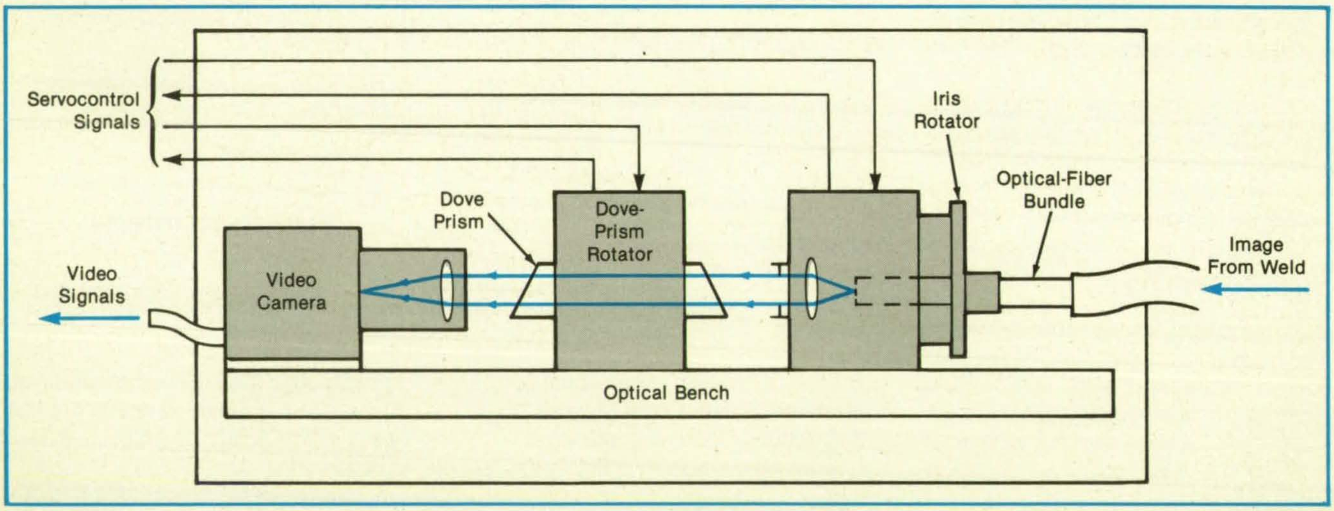

Commands From the Vision-System Computer drive servomotors on the iris and the Dove prism, providing the proper light level and image orientation (see inset) for the video camera. The optical-fiber bundle carries a view of the weld area as viewed along the axis of the welding electrode.

Processing Welding Images for Robot Control

Image data from two distinct windows are used to locate weld features.

Marshall Space Flight Center, Alabama

A video-image analyzer isolates elements of an arc-welding scene into two distinct windows. The analyzer is part of the vision system described briefly in the companion article, "Image Control in Automatic Welding Vision System" (MFS-26035) in this issue of *NASA Tech Briefs*. The analyzer examines images of the weld as it is being made and sends control signals to a welding robot according to what it "sees."

The analyzer creates windows around the unwelded joint and around the weld pool (Figure 1). By focusing attention on these crucial parts of the weld, the analyz-

er has to process only a small number of the 60,512 picture elements in the image, ignoring irrelevant parts of the image. This reduces the requirement for memory and increases the processing speed. The windows can be moved and changed in size to encompass key features, either automatically by the vision-system computer or manually by an operator. The analyzer handles data from the windows separately and in parallel to speed processing further.

A separate computer board acquires the digitized data from each window. Each board accepts up to 4,064 bytes of 8-bit parallel data per image frame, the exact number of bytes depending on the window size. The boards are programmed by internal registers to pick up only the data from picture elements in designated rows and columns in a window to reduce further the processing load.

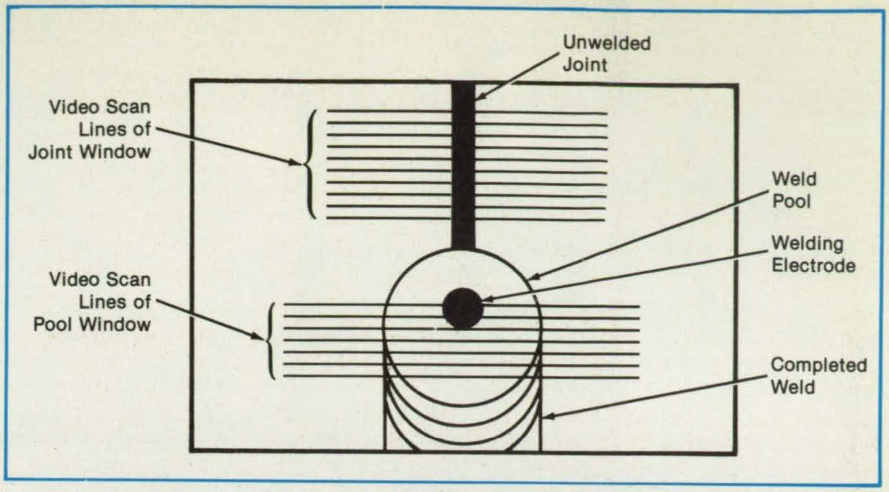

Figure 1. **Horizontal Video Lines Define Windows** for viewing the unwelded joint and the weld pool, respectively. Data from the picture elements outside the windows are not processed.

The video camera presents a new image frame every one-thirtieth second. Because the analyzer usually requires more than one-thirtieth second to process the window data, the data-acquisition boards can skip frames. During the skipped frames, the analyzer can catch up on processing the data it already has. The number of frames to be skipped is chosen manually. If not enough frames are skipped, the system displays an error message, indicating to the operator that more frames must be blanked out. Ordinarily, from 2 to 30 frames must be skipped to allow enough processing time.

Frame skipping is also used to exploit the inject/inhibit-gate feature of the video camera. For example, picture elements in the upper window might be allowed to accumulate light during a period extending over an active frame and one or more blanked frames, whereas those in the lower window might be allowed to accumulate light during only one frame. Thus, the window containing the image of the unwelded joint, which is not as bright as the image of the weld pool, can be given a longer exposure period.

After the windows of video data are obtained, subroutines are called to do the two basic steps in image processing:

1. Systematic analysis of each window to identify local features and
2. Identification of closely spaced groups of local features corresponding to welding features of interest — in particular, to the left and right edges of the weld pool and left and right edges and centerline of the unwelded joint.

Each horizontal line of video data in a window is represented by a sequence of binary numbers in the computer memory. The binary numbers are proportional to the amount of light falling on each successive picture element. The variation of brightness within each horizontal line is examined to find locations with predetermined characteristics — the local features. If such local features appear at about the same position in successive horizontal lines, forming a cluster of local features (Figure 2), it is likely that the edge of a pool or joint feature is indicated.

The product of image processing of a set of upper and lower windows is a sequence of up to 10 numbers, which are passed to the welding controller. The numbers represent the left, right, and middle locations of the joint and the left and right locations of the pool edge, as well as a confidence level for each. The controller decides whether the confidence level is high enough and whether to act on the information by sending appropriate control signals that affect the path of the welding heat, the weld-wire feed, and the welding current.

This work was done by Richard W. Richardson of Ohio State University for **Marshall Space Flight Center**. *For further information, Circle 103 on the TSP Re-*

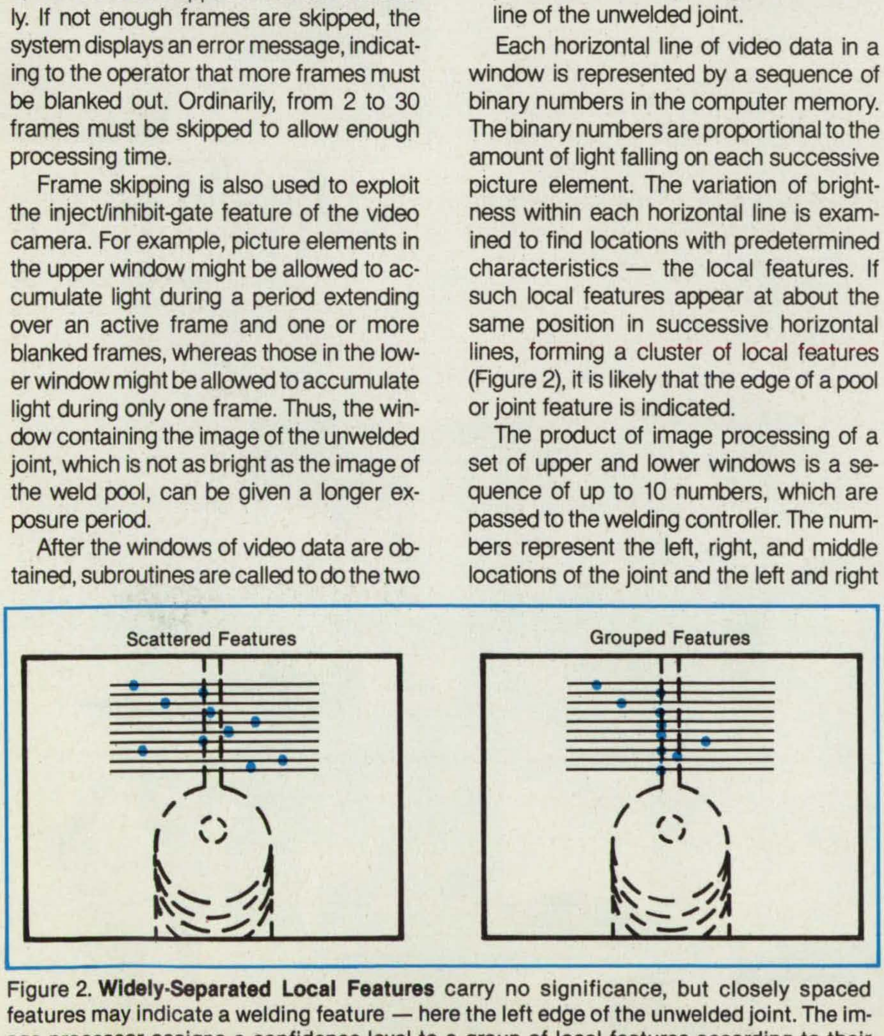

Figure 2. **Widely-Separated Local Features** carry no significance, but closely spaced features may indicate a welding feature — here the left edge of the unwelded joint. The image processor assigns a confidence level to a group of local features according to their spacing and pattern.

MOVE UP TO A NEW LINE

FROM HOUSTON INSTRUMENT

Prepare to be impressed. Meet the new line of high-performance plotters from Houston Instrument.™ HI's sleek new DMP-60 series is designed to impress even the most demanding CAD professional.

Discover unprecedented flexibility—blended with ultra-fine resolution, speed, and software compatibility. Benefit from HI's rigorous standards for quality, reliability, and service. All at prices starting from $4,695.*

Watch the DMP-60 series double as a scanner with HI's unique SCAN-CAD™ option. Quickly produce multicolored drawings when you use the Multi-Pen adaptor. Plot several originals—without tying up your PC when you add HI's buffer expansion board.

Select media as small as 8½″×11″ or as large as 36″×48″. Load either DM/PL™ or HP-GL 758X-compatible software. Then watch as your plotter quickly produces a drawing polished to a precise resolution of 5 ten-thousandths of an inch. Smile when you see smoothly formed circles, curves, and lettering.

Explore HI's host of support programs including an overnight plotter-replacement service. And then relax, knowing that HI's new plotters rest on 27 years of engineering excellence.

Move up. To a fine, new line. From Houston Instrument. Begin by calling 1-800-444-3425 or 512-835-0900 or writing Houston Instrument, 8500 Cameron Road, Austin, TX 78753.

*U.S. suggested retail price.

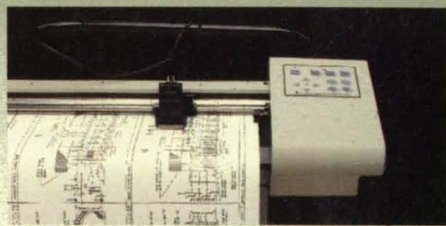

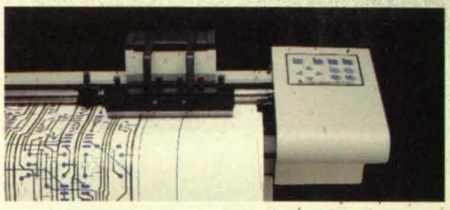

HOUSTON INSTRUMENT
A DIVISION OF AMETEK

Houston Instrument, SCAN-CAD, and DM/PL are trademarks of AMETEK, Inc.

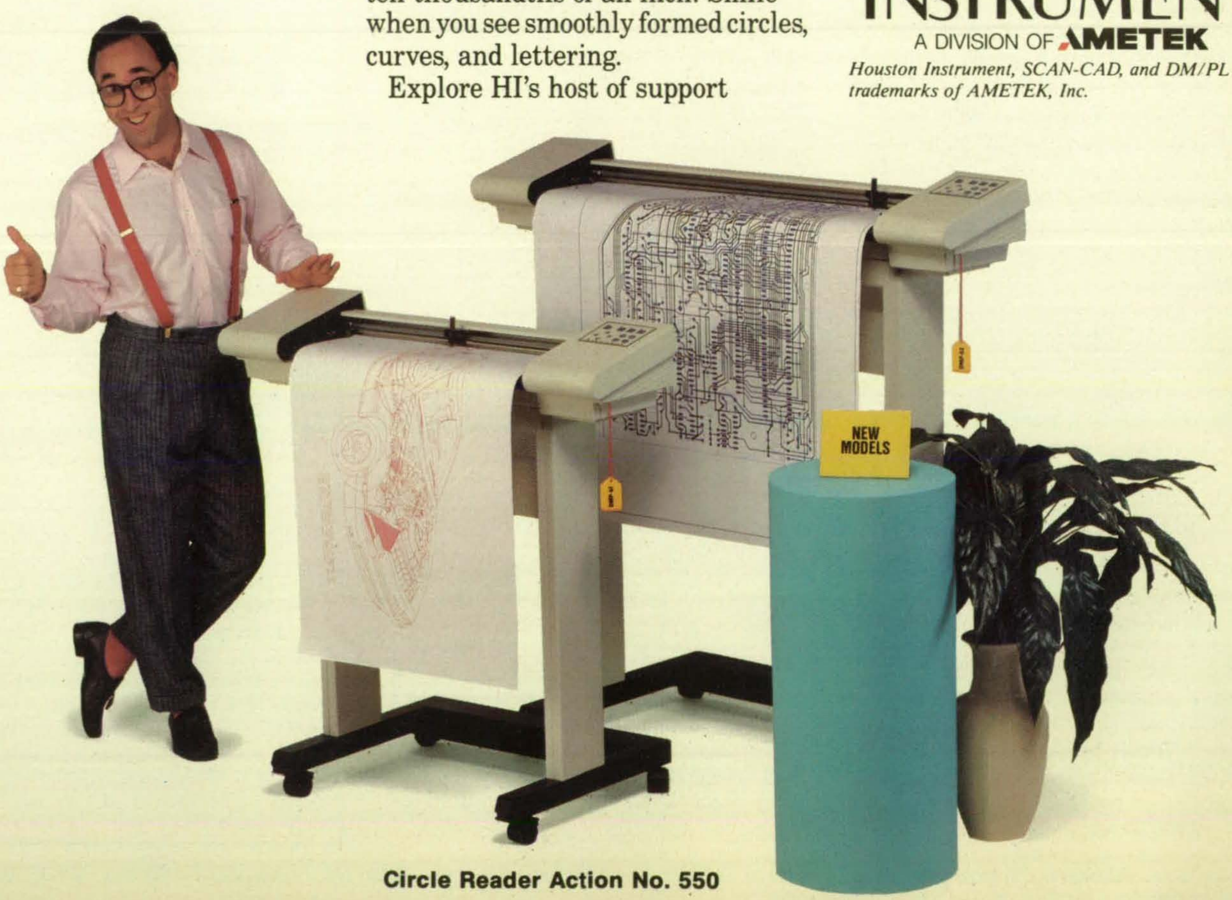

Circle Reader Action No. 550

quest Card.

In accordance with Public Law 96-517, the contractor has elected to retain title to this invention. Inquiries concerning rights for its commercial use should be addressed to

Ohio State University
Attn. Professor R. W. Richardson
1314 Kinnear Road
Columbus, OH 43212.

Refer to MFS-26036, volume and number of this NASA Tech Briefs *issue, and page number.*

Plasma Spraying of Dense, Rough Bond Coats

A modified plasma torch sprays coarse powders.

Lewis Research Center, Cleveland, Ohio

Dense metallic coatings with surface roughnesses of at least 400 μin. (10 μm) can now be prepared. Heretofore, low-pressure-plasma spraying has been used to produce dense, oxidation-resistant bond coats for thermal-barrier coating systems. The disadvantage of this method is that it is difficult to melt coarse metal particles completely during the short times they spend in the high-velocity, low-pressure plasma effluent. Thus, it is generally necessary to use starting powders that have particle sizes less than 44 μm. However, bond-coat roughness sufficient for the attachment of ceramic layers is difficult to obtain from fine starting powders.

A simple modification of the plasma torch facilitates the spraying of coarse powders. The shape of the nozzle is changed to obtain a decrease in the velocity of the gas and a consequent increase in the time the particles spend in the flame before impact on the substrate. The increased residence time allows melting of the coarser powders, the spraying of which results in rougher bond surfaces.

This work was done by Robert A. Miller and Brian J. Edmonds of **Lewis Research Center** *and George W. Leissler of Sverdrup Technology, Inc. No further documentation is available.*
LEW-14526

Computer-Graphical Simulation of Robotic Welding

Limitations on equipment can be investigated in advance to prevent expensive mistakes.

Marshall Space Flight Center, Alabama

The computer program ROBOSIM, developed by NASA to simulate the operations of robots, has been applied to the preliminary design of a robotic arc-welding operation. When the simulation program is run alone or with a robotic program supplied by the user, the output of the computer is a picture of the welding operation that can indicate such potential problems as collisions between the robot and other objects, the inability of the welding head to reach some weld locations, and the impossibility of maintaining the correct orientation or velocity of the welding head or the workpiece during some operations. By performing the simulation before a welding operation, the user can also prevent damage to an expensive workpiece or injury to workers.

The simulated robotic welder has six degrees of freedom and operates on a workpiece mounted on a two-degrees-of-freedom positioner (see figure). The control algorithms of the robot and positioner have to satisfy the special requirements of arc welding, the most important of which are the following:

- The workpiece should be held in an orientation (called the "downhand position") in which gravitation holds the molten metal in the weld pool and aids the fusion process; in practice, this often means making the workpiece surface at the weld joint as horizontal as possible.
- The speed of the torch relative to the workpiece should be held constant to heat the weld at a constant rate.
- The torch has to track the weld joint accurately despite thermal distortions and other dimensional inaccuracies in the workpiece and equipment.

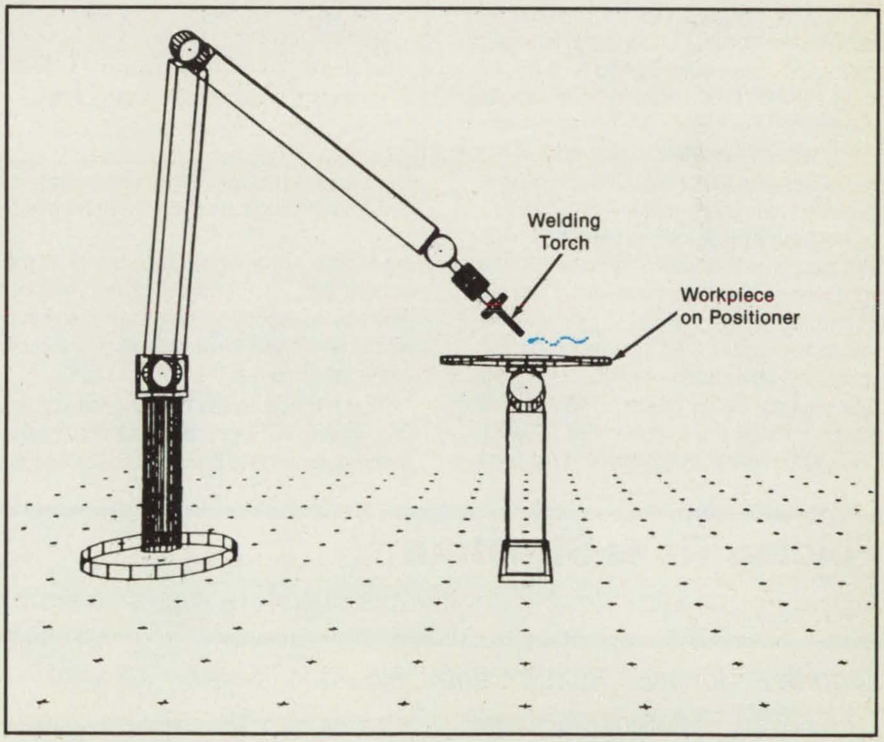

A **Computer Makes a Drawing** of a robotic welder and a workpiece on a positioning table. Such a numerical simulation can be used to perform rapid, safe experiments in computer-aided design or manufacturing.

A transformation algorithm based on the geometric relationships among the robot joints, torch, workpiece, and positioner helps to satisfy the first two requirements. This algorithm enables the robot and positioner to be "taught" by manually positioning and orienting the torch relative to the workpiece at successive, closely spaced points along the weld path. During "teaching," it is not nec-

essary to maintain the downhand position.

The algorithm reorients the torch and the workpiece with respect to the horizontal and vertical axes of the workspace to maintain both the desired weld path and the downhand position. It computes the kinematic transformation matrix for the robot joints, the velocity of the torch, and the velocities of the positioner axes to ensure (or attempt to ensure) that the weld is performed in the downhand position and that the weld travel speed is constant. Because the downhand position may not be achievable in all programmed welds, the simulation can be valuable in quickly identifying and correcting the weld design, without the cost of a failed weld, or the loss of time in a practice run without welding current.

This work was done by Ken Fernandez and George Cook of the Society of Manufacturing Engineers for **Marshall Space Flight Center**. *For further information, Circle 6 on the TSP Request Card. MFS-28199*

Micromachining of Silicon

Diffusion and preferential etching make new structures possible.

Lewis Research Center, Cleveland, Ohio

The etching rates of alloys and heavily-doped semiconductor materials can be significantly higher than that of a lightly doped semiconductor if the proper etching system is used. This selectivity can be used to etch regions of a semiconductor preferentially while not etching other unmasked regions. When this selective etching is used with laser-induced-diffusion techniques, it will be possible to make structures that cannot be made at present. Thus, it will be possible to produce well-defined structures in and through a wafer while not damaging existing structures on the wafer. Since these structures are patterned on the front surface of the wafer by the use of conventional microelectronic techniques, it will be possible to make these structures well aligned to such existing front-surface patterns or structures as integrated circuits.

The figure illustrates an example of the type of process described. The top left part shows an aluminum pattern deposited on the front surface of a silicon wafer. The top right part shows infrared radiation from a high-power CO_2 laser incident on the silicon wafer from the back side. Because silicon is transparent to infrared radiation while Al/Si absorbs the radiation, only the Al/Si regions will be heated. The Al/Si will diffuse through the silicon wafer by laser-induced temperature-gradient zone melting with no lateral diffusion, as shown at the bottom left. The removal of the Al/Si regions by a selective etchant will result in a micromachined structure in the silicon wafer, as shown at the bottom right.

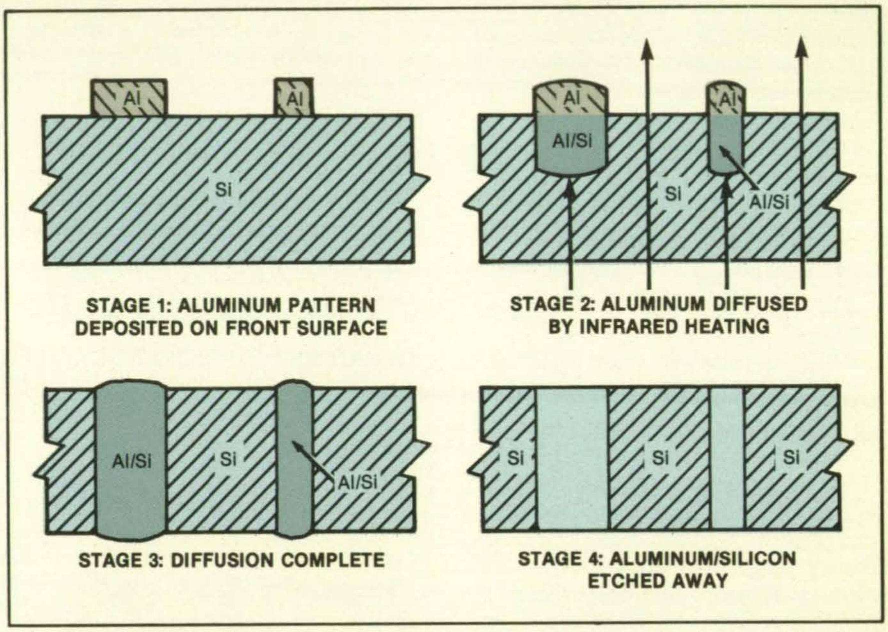

Aluminum Is Diffused into a silicon wafer by selective infrared heating. The resulting aluminum/silicon plugs are then preferentially etched away, leaving small holes in the silicon.

The method would be a significant improvement on the present micromachining techniques used to fabricate structures for sensors and isolation of devices. This technique will make it possible to manufacture smaller devices and structures than those produced by the currently available methods.

This work was done by John E. Dickman of **Lewis Research Center**. *No further documentation is available. LEW-14481*

Folding Truss Structure

A conceptual foldable and deployable structure would be simpler than earlier versions.

Lyndon B. Johnson Space Center, Houston, Texas

A concept for a foldable and deployable truss offers the advantages of strength, rigidity, and mechanical simplicity. Intended for the transportation of structures for assembly in outer space, the concept can readily be adapted to terrestrial transportable structures — scaffolds, cranes, and rows of cubicles, for example.

The conceptual structure consists of a series of boxlike bays with 9-ft (2.7-m) sides. Each box has panels on its top and bottom and two sides. Its two remaining sides are open. The panels are hinged at their connecting edges.

Depending on the available cargo space, from one to five bays can be deployed simultaneously. For deployment, the box is unfolded, and diagonal members are inserted on the panelless sides. A long truss can be made by putting tops and bottoms of a series of boxes together.

For storage or transportation, a deployed box is refolded. If the truss consists of 10 boxes, for example, 5 folded boxes are folded together to the left, and the remaining 5 are folded together to the right, to form a compact module.

The members of the truss could be made of composite materials for light weight. With minor modifications of the hinges, the direction of deployment can be changed to any one of four at each interconnection between bays. The design of utility-distribution lines is simplified because, in comparison with the previous version of the deployable structure, the

new conceptual version features longer rigid sections with fewer connections between them. Other advantanges relative to the previous version include the following:

- Only two, instead of eight, hinged or telescoping struts per bay;
- Only 36, instead of 48, bond joints per bay;
- Less complex fabrication;
- Lighter weight;
- Higher reliability;
- Lower cost; and
- More units in the same cargo space.

This work was done by Aubrey D. Warren of Rockwell International Corp. for **Johnson Space Center**. *No further documentation is available.*
MSC-21255

Orienting Acoustically-Levitated Aspherical Objects

The orientation can be controlled and the asphericity measured.

NASA's Jet Propulsion Laboratory, Pasadena, California

By suitable adjustments of the amplitudes and phases of the three acoustic fields in a three-axis acoustic levitator, the orientation of an aspherical levitated object can be controlled, and the degree of its asphericity can be measured. The orientation-and-measurement technique can be used to manipulate workpieces during containerless processing or to measure the approach to desired asphericity in small objects like targets for laser-fusion experiments.

There are several versions of the technique. In all of them, the workpiece is levitated at the center of a generally rectangular chamber having an acoustic driver on each axis (see Figure 1). The chamber can have unequal axes (each acoustic driver at a different frequency), two equal axes (two drivers at the same frequency), or all axes equal (all drivers at the same frequency).

In the first version, the axes are unequal. The axis of asphericity of the workpiece (for example, the axis of symmetry in the case of a disk) lines up with the strongest of the three acoustic fields. Thus, the workpiece can be aligned along the x, y, or z axis by supplying the most power to the driver on the desired axis.

In the second version, the x and y axes are equal, and their acoustic drivers are locked in phase. The axis of asphericity lines up with the stronger of the z or the net x-y acoustic fields. If the net x-y acoustic field is stronger, then the orientation in the x-y plane is along the vector sum of the x and y acoustic-field flow velocities, the axis of which can be varied by varying the relative strengths of the x and y fields.

In the third version, the chamber is cubical; all three drivers are operated at the same frequency and phase. The axis of asphericity of the workpiece can be oriented along any direction by choosing the relative powers of the drivers to obtain the vector-sum acoustic-flow velocity in the desired direction.

Like the second version, the fourth version calls for equal x and y axes. In this case, the net x-y field is made stronger than the z field, and the x and y fields are driven at equal amplitudes but at a phase difference selected to give a desired amount of torque about the z axis; that is, to rotate the axis of asphericity in the x-y plane about the z axis. The z-axis torque is counteracted by the torque that aligns the axis of asphericity with the net x-y acoustic-flow field. Because the maximum alignment torque occurs at orientations of ±45° with respect to the net x-y acoustic flow, the x-y phase difference can be used to turn the sample to a new orientation within ±45° about the z axis.

The critical x-y phase difference ϕ_c that

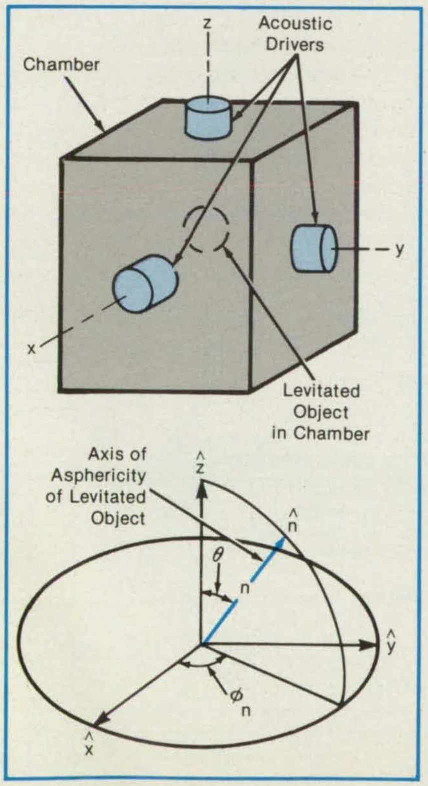

Figure 1. A **Three-Axis Acoustic Levitator** controls the rotation or orientation of a levitated aspherical object with respect to the three principal axes.

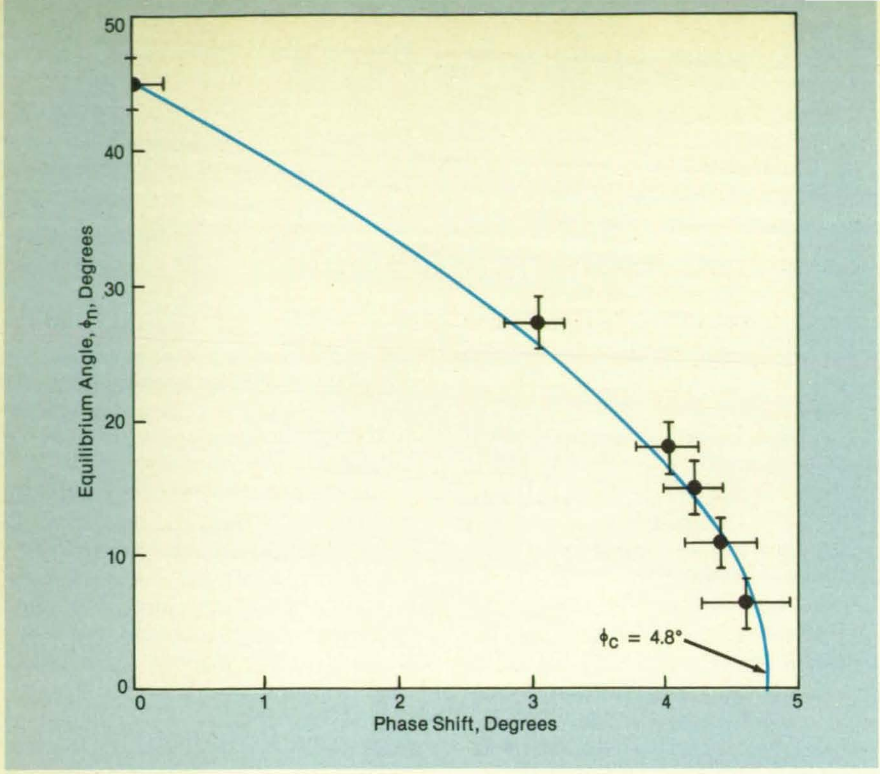

Figure 2. The **Angle of Reorientation** of a levitated aspherical object was measured at various phase differences between two acoustic fields of equal amplitude and frequency. The solid line among the data points represents a simple theory of balance between rotating and aligning acoustical torques.

produces the ±45° reorientation depends on the degree of asphericity and can be used as a measure of the asphericity. At greater phase differences, the workpiece rotates. At lesser phase differences, the reorientation angle is less; one can measure the reorientation angle as a function of the phase difference to determine the degree of asphericity (see Figure 2).

Like the third version, the fifth involves a cubical chamber. In this case, however, many different combinations of phases and/or amplitudes can be selected to orient the axis of asphericity along various directions.

This work was done by Martin B. Barmatz of Caltech for **NASA's Jet Propulsion Laboratory**. *For further information, Circle 23 on the TSP Request Card.*

Inquiries concerning rights for the commercial use of this invention should be addressed to the Patent Counsel, NASA Resident Office-JPL [see page 12]. Refer to NPO-16846.

Periscope for Viewing Weld Penetration

The same device gives a full view and provides shielding.

Marshall Space Flight Center, Alabama

A periscope enables the viewing of a weld joint from inside a cylindrical duct to determine when weld penetration occurs. The periscope supplies a steady stream of inert gas to shield the joint. The device is used to calibrate and evaluate techniques for sensing weld penetration.

The periscope gives a clear perpendicular view of the joint, unlike unaided observations from the end of the duct, which are at a shallow angle. Although observations with a mirror on a stick (like a dentist's instrument) also give a perpendicular view, such a device requires a sliding seal to contain the inert gas and accommodate rotation of the duct during welding. In contrast, the periscope itself supplies the shielding gas without a seal, rotating or otherwise.

The periscope is housed in a tube that is positioned in the duct so that its window opens on the weld joint just below the welding torch (see figure). Inert gas flows through the periscope and out the window, covering the joint. The gas flows out of the duct through the narrow channel between the periscope and the duct wall.

The duct is rotated under the torch by a turntable while the periscope remains fixed. An observer looks through a viewing window, located at the far end of the periscope, into an internal mirror at 45° to the periscope axis. The mirror provides a full view of the joint so that the signs of weld

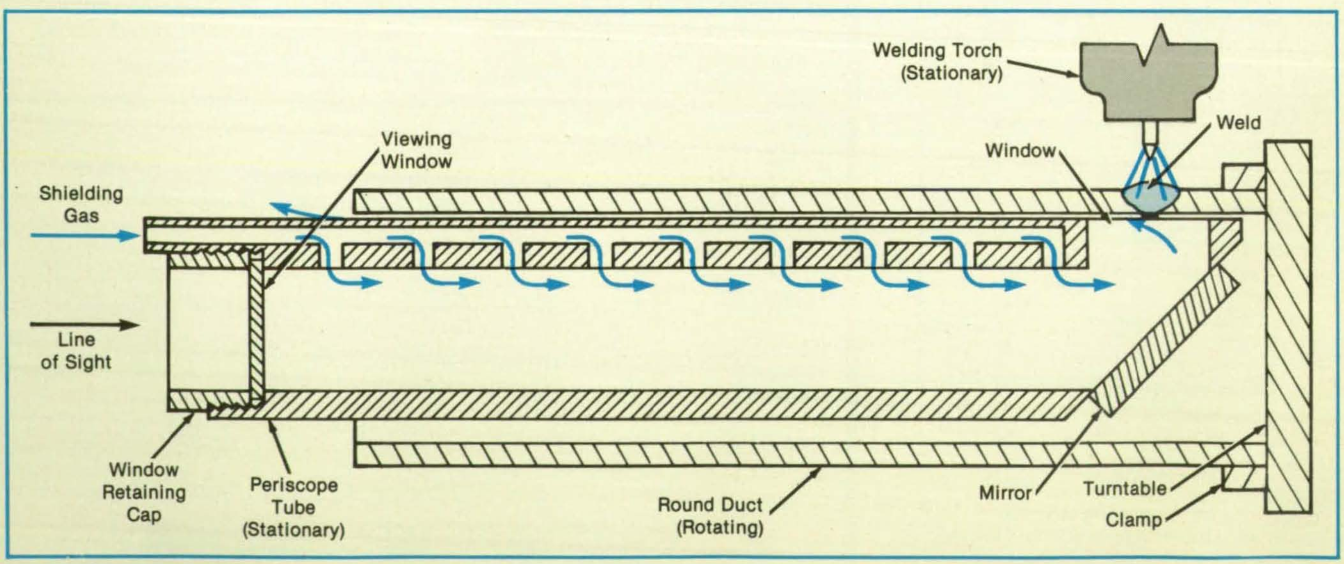

Inert Shielding Gas Flows from a manifold in the periscope. The thin outlet channel provides sufficient back pressure to keep the weld joint blanketed with gas.

penetration are obvious to the observer.

This work was done by Stephen S. Gordon and Jonathan M. Marman of Rockwell International Corp. for **Marshall Space Flight Center**. *No further documentation is available. MFS-29346*

Forming Solar-Cell Junctions by Flash Diffusion

An expedited fabrication process costs less but does not sacrifice cell performance.

NASA's Jet Propulsion Laboratory, Pasadena, California

A modified fabrication process simultaneously forms the front and back junctions of silicon photovoltaic cells. With flash diffusion, junctions can be formed in 10 to 20 seconds instead of 20 to 30 minutes as in conventional one-side-at-a-time thermal diffusion. Cost reductions of 25 to 30 percent are expected with the modified process. Moreover, the devices produced have performance equal to or better than that of cells made by conventional diffusion.

In flash diffusion, a ribbon of silicon (grown by the dendritic-web process) is coated on both sides with liquid dopants, then exposed simultaneously on both sides to a brief pulse of heat from a tungsten/halogen flashlamp. The heat quickly drives the dopants into the silicon, where they form semiconductor junctions about 0.2 λm deep (see figure). The dopants on opposite sides remain isolated from each other; they do not have time to cross-contaminate as they do when simultaneous thermal diffusion is attempted.

In a laboratory demonstration of flash diffusion, liquid dopants were applied to silicon ribbons manually with applicator pads (a meniscus coating machine would be used in production). Both n- and p-type materials were used, in thicknesses of 100 and 130 λm. The ribbons were flashed at 1,100 °C for 10 seconds in an argon atmosphere. About 200 ribbons, representing more than 200 solar cells, were treated.

The best performance was obtained with n-type material, into which a p/n/n$^+$ cells were 14 to 15 percent efficient — at least as good as conventionally diffused cells.

This work was done by Paul Alexander, Jr., of Caltech for **NASA's Jet Propulsion Laboratory** *and Robert B. Campbell of Westinghouse Electric Co. For further information, Circle 28 on the TSP Request Card.*

Inquiries concerning rights for the commercial use of this invention should be addressed to the Patent Counsel, NASA Resident Office-JPL [see page 12]. Refer to NPO-17048.

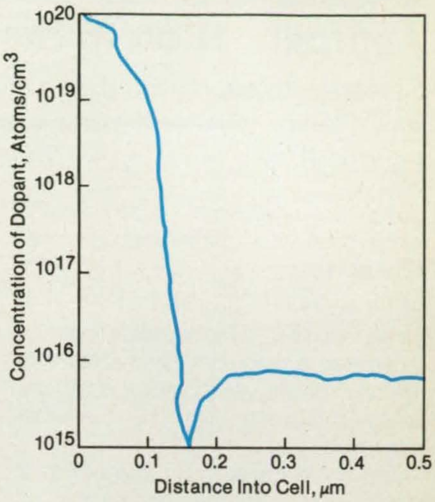

This **p$^+$/n Junction** was formed by flash diffusion of p$^+$ material into an n-type silicon substrate.

Circle Reader Action No. 460

Approximation to the Normal Probability Distribution

Closed-form expressions give *P(x)* and *x(P)*.

Lyndon B. Johnson Space Center, Houston, Texas

A pair of closed-form equations yields approximate values for the normal probability distribution

$$P(x) = (2\pi)^{-1/2} \int_{-\infty}^{x} \exp[-(1/2)t^2]dt$$

and its inverse $x(P)$. The new equations can be entered in many programmable hand-held calculators, yielding quick, easy, and fairly accurate estimates of normal-probability values.

The normal probability distribution is widely used in engineering, medical research, psychology, physics, biology, and other disciplines. There are no exact, closed-form expressions for $P(x)$ and $x(P)$. Although there are several methods of approximation, none of them combines ease of calculation with appreciable accuracy. However, the new equations do both.

The new approximation $P'(x)$ for the exact value $P(x)$ is given by

$$P'(x) = \{1 + \exp[-x(a + bx^2)]\}^{-1}$$

for $x > -1.16$, where $a = (8/\pi)^{1/2}$ and $b = (4-\pi)(2/\pi)^{1/2}(3\pi)^{-1}$. The relative error

$$|\ln[P'(x)/P(x)]|$$

is less than 3.2×10^{-4}, provided that x remains above -1.16. This is an order of magnitude less than the error of the best previous approximation of comparable simplicity, namely

$$P''(x) = \{1 + [1 - \exp(-2x^2/\pi)]^{1/2}\}/2$$

for $x > 0$.

The new approximation for the inverse is given by

$$x(P') = 2A^{1/2}\sinh\{[\sinh^{-1}(BA^{-3/2})]/3\}$$

for $P' > 0.123$, where $A = a/3b$, $B = \{\ln[(P')^{-1} - 1]\}/2b$. Although this approximation is not as simple as that for $P'(x)$, it is still straightforward for a hand-held calculator equipped with the hyperbolic-function capability.

This work was done by John D. Vedder of McDonnell Douglas Corp. for **Johnson Space Center**. *No further documentation is available.* *MSC-21285*

Dynamic Replanning System

Planning software is augmented by software that takes new goals into account.

NASA's Jet Propulsion Laboratory, Pasadena, California

An artificial-intelligence computer program for planning automatically changes its plan when conditions warrant. The system uses planning software called SWITCH, which can be used, for example, to schedule the turning on and off of devices that use electrical power.

With different knowledge bases, SWITCH has made plans involving nonconsumable resources in a simple electric-appliance world and in a simulated military-intelligence-gathering world. An example of a nonconsumable resource is power when only a finite amount of it is available: when a device that uses power is turned on, it reduces the amount of power available for running other devices; when the device is turned off, the power it drew becomes available for other devices. Power has not been consumed, as fuel would be.

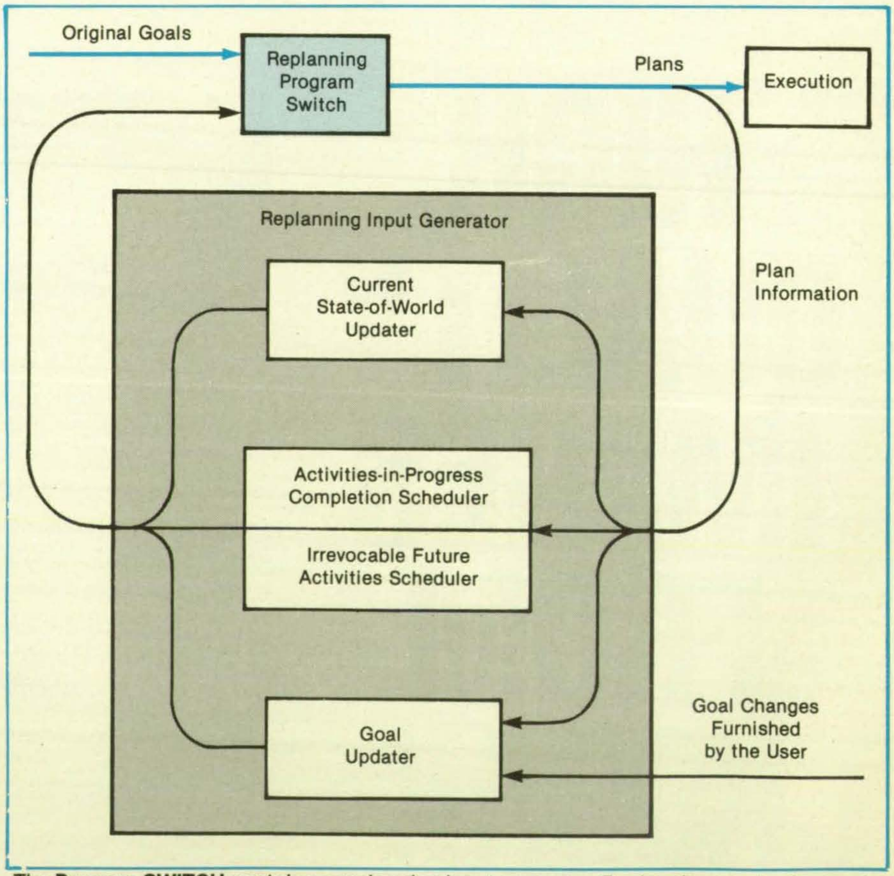

The **Program SWITCH** contains a replanning input generator. Replanning can be done only for situations in which SWITCH has made a plan but the goals have changed; the system still assumes that the original knowledge base is correct, which often is not the case. Future development is aimed at compatibility with changing knowledge bases.

SWITCH does limited replanning in response to unforseen changes in goals. Embedded in it is a replanning input generator that operates between calls to the planner. The generator processes the output of, and previous input to, the planner to generate input for the next call (see figure).

The code that generates replanning input does not attempt to select and preserve the steps in the old plan that probably will not need to be changed. This is because the preserved steps are entered into the new plan in such a way that SWITCH will not be able to change them, and therefore, if a preserved step has to be changed after all, the planner could fail. Instead, the replanning input generator saves only those steps that cannot be changed in any event; for example, steps that are in progress at the start of the new plan and irrevocable activities scheduled to start after the new start time.

The goal portion of the replanning input is not automatically generated, because the user is allowed to make changes in goals that the program cannot predict. The replanning code examines the goals of the existing plan and collects those that have not been fulfilled into a tentative goal list, which it presents to the user for editing.

The developers of the program expect to explore replanning to recover from execution errors and other discrepancies. The discrepancies indicate that some of the assumptions in the old input are inaccurate. The system that generates the new input will have to find the incorrect assumptions within the knowledge base and replace them with corrected versions.

This work was done by Harry J. Porta of Caltech for **NASA's Jet Propulsion Laboratory**. *For further information, Circle 33 on the TSP Request Card.*
NPO-16941

Books and Reports

These reports, studies, handbooks are available from NASA as Technical Support Packages (TSP's) when a Request Card number is cited; otherwise they are available from the National Technical Information Service.

Liquid-Oxygen Expert System

A complicated system is monitored for equipment failures.

A report summarizes the structure, capabilities, and development history of the Liquid-Oxygen Expert System (LES), an artificial-intelligence system designed to detect and diagnose failures in the equipment network that loads liquid oxygen into the external tank of the Space Shuttle before the launching. This system is designed to detect immediately the signs of trouble among the measurements fed into the current Launch Processing System (LPS), so that the more common failures in the complex control and monitoring system can be distinguished from the less common failures in the sensors and other equipment that the instruments monitor. If successful, the LES would keep the LPS from mistakenly delaying or canceling launches.

The LES contains three elements: a knowledge base, a constraint mechanism, and a diagnoser. The knowledge base contains the information that defines and describes the control system. Each component in the control system is represented by a frame in the knowledge base, the ultimate size of which will be approximately 2,000 frames. The knowledge base includes the representations of the connectivity of the electrical, pneumatic, and mechanical components as well as specific characteristics of the individual components and the functional relationship between components.

Malfunctions within the control system cause deviations from the relationships described in the knowledge base and signal a constraint failure. When a constraint failure occurs, the offending measurement is identified, and the diagnosis operation is initiated.

The diagnoser must then determine the single failure within the control system that is the cause of the measurement deviations. The diagnoser performs its task by searching through a space of possible component states to find, if it can, a single bad component or, failing that, a list of possibly bad components.

The search space is pruned by a series of thought experiments that determine the measurement values pertinent to the situation. The generality of this approach makes it possible to centralize the information about the subject control system entirely in the knowledge base and to include only general troubleshooting logic in the software.

The output of the LES is in the form of written reports similar to those produced by system engineers. The LES identifies single-point failures (when it is possible to do so from the input data) and performs as well as an experienced system engineer, while being more consistent and at least an order of magnitude faster.

This work was done by John R. Jamieson, Jr. and Carl I. Delaune of **Kennedy Space Center**. *To obtain a copy of the report, "A Monitor and Diagnosis Program for the Shuttle Liquid Oxygen Loading Operation," Circle 45 on the TSP Request Card.*

Inquiries concerning rights for the commercial use of this invention should be addressed to the Patent Counsel, Kennedy Space Center [see page 12]. Refer to KSC-11332.

Life Sciences

Hardware, Techniques, and Processes

Implanted Blood-Pressure-Measuring Device

Arterial pressure is compared with ambient bodily-fluid pressure.

Goddard Space Flight Center, Greenbelt, Maryland

An implanted apparatus, which would be capable of measuring the blood pressure of a patient, would include a differential-pressure transducer connected to a pressure sensor positioned in a major artery (see figure). An electrical signal that is a function of the differential pressure between the blood-pressure sensor and a reference-pressure sensor is transmitted through the skin of the patient to a recorder or an indicator.

The blood-pressure sensor includes a titanium funnel with an elastomer diaphragm stretched over the funnel mouth and is sutured to the inside of the arterial wall with the diaphragm parallel to the wall. So positioned, the diaphragm makes direct contact with the flowing blood in a manner that minimizes fluid turbulence in the artery.

Also connected to the implanted transducer is a subcutaneous, bulb-type pressure sensor positioned near the arterial sensor but not within a blood vessel. This sensor is used to detect a reference pressure proportional to the ambient pressure within the body.

The blood-pressure sensor and the reference-pressure sensor are each in fluid connection with a corresponding chamber of the differential-pressure transducer. These two adjacent chambers are separated by a flexible wall provided with a pressure-sensing element and with associated electrical connections. The differences in the pressure transmitted to the chambers from the two pressure sensors produce corresponding flexures in the flexible wall, causing the pressure-sensing element to generate the electrical signal that, transmitted through the skin, indicates the blood pressure.

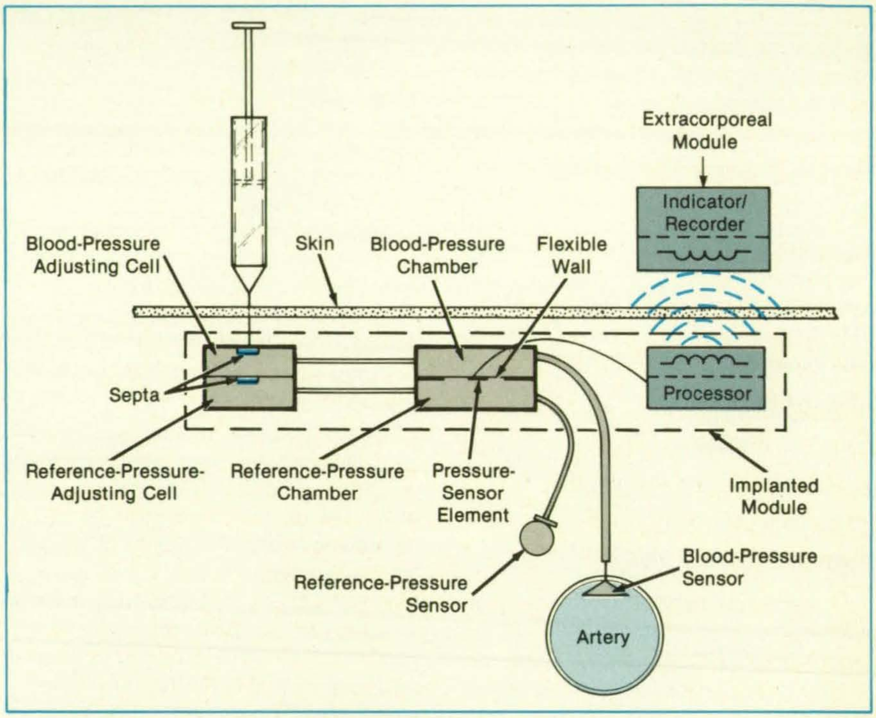

An **Implantable Blood-Pressure-Measuring Device** transmits a signal that is a function of the difference between the arterial pressure and ambient bodily-fluid pressure.

To enable the adjustment of the fluid pressures within the two chambers, each chamber is in fluid connection with a corresponding pressure-adjusting cell. The two adjusting cells are placed one above the other and are separated by a septum. The outer (blood-pressure-adjusting) cell is also provided with a second septum. To adjust the fluid pressure, a noncoring hypodermic needle is used to pierce the top septum to add or subtract fluid to or from the blood-pressure-adjusting cell or to pierce both septa to add or subtract fluid to or from the reference-pressure-adjusting cell.

This work was done by Robert E. Fischell of the Johns Hopkins University, Applied Physics Laboratory, for **Goddard Space Flight Center**. *No further documentation is available.*

This invention is owned by NASA, and a patent application has been filed. Inquiries concerning nonexclusive or exclusive license for its commercial development should be addressed to the Patent Counsel, Goddard Space Flight Center [see page 12]. Refer to GSC-13042.

Biofeedback With Implanted Blood-Pressure Device

A patient is alerted to excessive pressure.

Goddard Space Flight Center, Greenbelt, Maryland

Additional uses have been found for the proposed equipment described in the preceding article, "Implanted Blood-Pressure-Measuring Device" (GSC-13042) in this issue of *NASA Tech Briefs*. Implanted with the device would be electronic circuitry

that measures, interprets, and transmits data via an inductive link through the patient's skin to an external receiver.

The receiver would include an audible alarm generator that is activated when the patient's blood pressure exceeds a predetermined threshold. The alarm would indicate to the patient that he or she should use biofeedback techniques to reduce the blood pressure to a value below which the alarm turns off. Also included in the receiver would be a blood-pressure display, a recorder, or both, for use by the patient or physician.

This work was done by Robert E. Fischell of Johns Hopkins University for **Goddard Space Flight Center**. *No further documentation is available.*
GSC-13043

Heavy-Duty Rescue Straps for Coveralls

Straps enable rescuers to move injured people.

John F. Kennedy Space Center, Florida

A new type of strap on coveralls helps rescuers lift victims of industrial accidents. The new strap is made of heavy twill instead of the thin nylon previously used. The new material, which is 1 in. (2.54 cm) wide and has a breaking strength of 600 lb (2,670 N), is sewn to the coveralls with polyester thread in box "X" stitching. Reinforcing nylon webbing, 1¾ in. (4.4 cm) wide, is sewn with the strap at the attachment points.

Pairs of straps are placed at the back, shoulders, and hips, and a single strap is at the abdomen. They give rescuers a firm grip and enable them to carry the victim vertically or horizontally or by dragging. The bright-blue color of the straps makes them readily visible against white coveralls.

Normally, the straps are held flat against the coverall fabric by hook-and-pile patches. They are therefore less likely to snag on protruding equipment or otherwise impede wearers doing their work. However, the straps can be quickly detached by rescuers when they are needed. The patches replace metal fasteners.

This work was done by Henry M. Waddell of Rockwell International Corp. for **Kennedy Space Center**. *For further information, Circle 120 on the TSP Request Card.*
KSC-11295

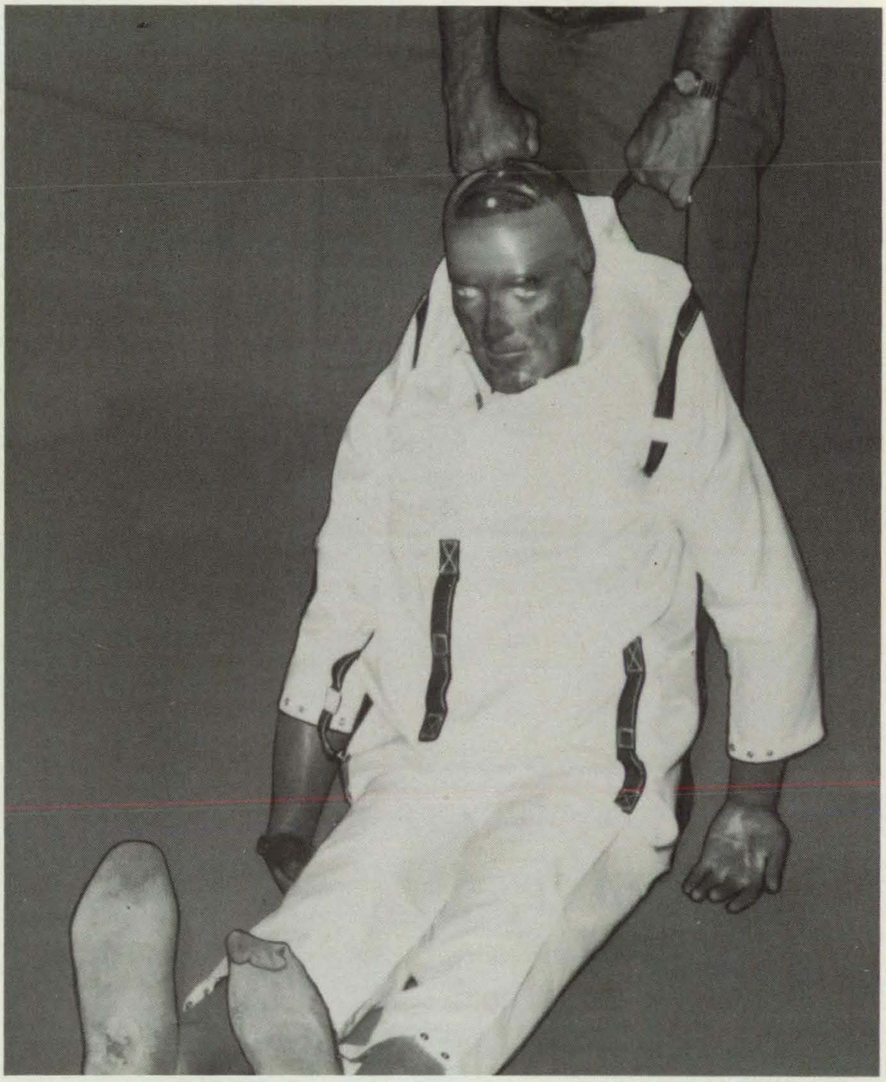

A Dummy Is Used to illustrate one of the many possible ways in which an incapacitated worker can be moved by the heavy-duty straps on coveralls. When they are not being used, the straps are stored flat against the garment.

Screening for Alcohol-Producing Microbes

A dye reaction rapidly identifies alcohol-producing microbial colonies.

NASA's Jet Propulsion Laboratory, Pasadena, California

A method visually detects alcohol-producing micro-organisms, such as yeast and bacteria, and distinguishes them from other microbial colonies that do not produce alcohol. Hundreds of colonies on agar plates can be screened at a time by this nonlethal, alcohol-specific method.

The technique, still being perfected, uses a visual dye linked to the reaction of alcohol dehydrogenase to indicate the presence of alcohol. A change in the color of the dye surrounding a microbial colony readily distinguishes it from other colonies. The method, which should be of interest to the brewing industry, should also be useful for screening mixed microbial populations in environmental samples.

This work was done by Wayne W. Schubert of Caltech for **NASA's Jet Propulsion Laboratory**. *For further information, Circle 16 on the TSP Request Card.*
NPO-15842

New on the Market

Texas Instruments, Dallas, TX, has enhanced the capabilities of its new **symbolic processing** product family with the introduction of Explorer II color systems. The systems feature 16-inch integral color monitors with 1024 x 808 pixel resolution capable of displaying 256 colors simultaneously, from a palette of 16.7 million. The Explorer TI workstation systems are based on TI's high performance Lisp microprocessor, which was designed specifically for AI. **Circle Reader Service Number 599.**

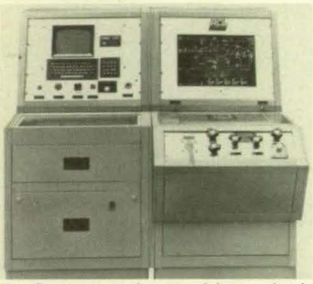

By eliminating the need for multiple test stands, ACL Technologies' Image systems cut capital equipment expenditures and bring unprecedented versatility to **hydraulic servo testing**. Hundreds of different valves, actuators, servos, pumps, motors and controls can be tested on a single Image system test stand by relatively unskilled personnel. An end-to-end computerized self-calibration feature ensures repeated adherence to set accuracy levels. The equipment complies with SAE standards, including ARP490, and is supported by various sizes of hydraulic systems. **Circle Reader Service Number 594.**

A new pamphlet from the Dow Chemical Company discusses the construction features and benefits provided by Chiploc ES and Chiploc DP **electrostatic discharge and dissipative packaging** for sensitive electronic components and assemblies. Chiploc ES bags offer electrostatic shielding and Faraday cage protection with a buried shield in a multiple-layer static dissipative construction. Chiploc DP bags have a single-layer construction that provides static dissipative protection for less sensitive components and assemblies. **Circle Reader Service Number 586.**

Intermetrics has added support for the **68020 microprocessor** to their product line of software development tools. InterTools is an integrated set of cross-compilers, cross-assemblers, source level cross debuggers, and utilities designed specifically for programming embedded microprocessor systems. The InterTools cross-compiler for the 68020 supports the efficient bit manipulation and powerful addressing modes of the 68020. InterTools also provides hardware and software floating points, including mathematical functions. The C and Pascal compilers produce efficient, reentrant ROMable code. **Circle Reader Service Number 587.**

Daedal's new **motion control system**, the MC3000 Programmable Microstep Controller, is designed to control one to four axes of motion. The system includes the indexer, microstepping motor(s) with 2000 to 20,000 step/rev resolution, and the Model MD23 drive. No other components are necessary for operation. The indexer features an easy-to-use membrane keypad, alpha/numeric liquid crystal display, non-volatile memory, and simple menu-driven control programming. **Circle Reader Service Number 582.**

Melles Griot Gas Laser Products announces that their new 0.8 milliwatt Omega series HeNe **plasma tube** (model 05 LHR 006) is an exact form/fit/function equivalent to both the Spectra Physics model SL008-58 and the Uniphase Model 1007. The Melles Griot version of this tube is manufactured on their Omega product line and exhibits operational reliability and long, trouble-free life. The randomly polarized output beam diameter is 0.48 mm; beam divergence is 1.7 mrad. Current draw is 4.0 mA at 1000VDC during operation. **Circle Reader Service Number 588.**

Apollo Lasers, Inc, Chatsworth, CA is offering a new technical data sheet on its Dot/Script Series portable **laser-based marking systems**, designed to eliminate tooling costs for deep image parts marking. The data sheet covers systems descriptions, design principles, applications, features, advantages, system configurations, specifications, options and accessories. **Circle Reader Service Number 595.**

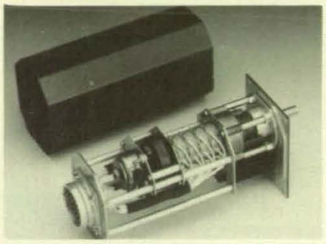

The new 24104 Series **control switch system** from Janco Corp. utilizes modules of QPL switching components, with a built-in solenoid. Designed specifically for the autobrake antiskid system on the Fokker F50 and F100 aircraft, the rotary switch provides multi-position, multi-function characteristics for interfacing with the controlling microcomputer system. The solenoid provides position latching coupled with a momentary return, offering pilots a positive "detent feel" for each selected autobraking control movement. **Circle Reader Service Number 580.**

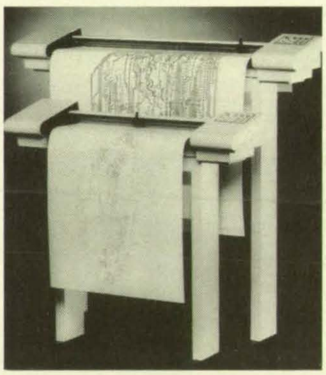

A line of high-performance professional **drafting plotters** has been announced by Houston Instrument, Austin, TX. The DMP-60 series is designed for applications requiring fast pen speed, acceleration, and processing power for fast throughput. The single-pen plotters offer adjustable media size capabilities, handle a variety of English and metric media formats, and can accept add-on accessories. **Circle Reader Service Number 591.**

Magnavox Electronic Systems Company has released a **capabilities brochure** describing the company's experience in the following product areas, as well as a description of their current products: Anti-Submarine Warfare, Airborne Communications, Anti-Jam Communications, C3 Systems and Ada Software Development. **Circle Reader Service Number 584.**

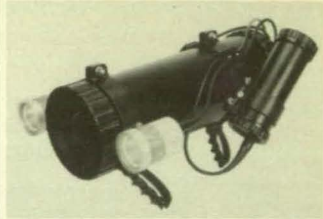

A broadcast quality **CCD camera designed for underwater applications** has been announced by NEC America. The Model SP-3AUW is based on the SP-3A broadcast ENG camera, and is equipped with a variable speed electronic shutter to provide sharp images of high speed objects. Shutter speeds are 1/60, 1/125, 1/250, 1/500, 1/1000 or 1/2000th of a second. The camera provides a resolution of 550 TV lines, and can operate down to 1000 feet. Focus, zoom, iris, shutter and other operations can be controlled up to 1000 feet from the camera head. **Circle Reader Service Number 585.**

McDonnell Douglas has recently updated Stradis, a step-by-step approach to managing and building **information systems**. The enhancement primarily updates the methodology's data modeling procedures to incorporate entity-relationship modeling. Entity-relationship modeling is a top-down approach to data analysis, providing a structural model of the data required to support an information system. It graphically represents the various products, services, places, roles, agreements, events, organizations and concepts on which a company wants to retain data, along with their interrelationships. **Circle Reader Service Number 590.**

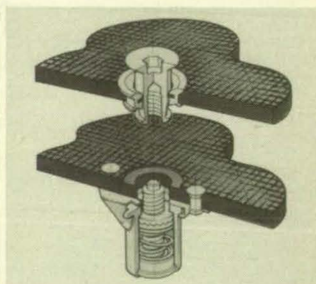

The LiveLock **Structural Panel Fastener**, now available from Rexnord Specialty Fastener Division, Torrance, CA, utilizes several design features that make it an ideal multi-use fastener for composite panels. The LiveLock Fastener's stud nut threads are inside the body, leaving a smooth outer surface that won't promote panel delamination. A stud nut grommet further protects laminate integrity, presents a hard seating surface for the stud, and distributes the fastener load evenly. A retaining ring inside the grommet provides positive stud hold-out retention. A spring-loaded ratchet inside the LiveLock receptacle insures positive locking action and vibration resistance. **Circle Reader Service Number 593.**

Subject Index

Classifieds

Classified advertising rates and specifications are as follows: Set in 6 point light type face, with up to five words at beginning of copy in bold caps. Count box numbers as six words.

50 words or less	$ 180
100 words	$ 250

Check or money order must accompany order to: Classified Advertising Manager, NASA Tech Briefs, Suite 921, 41 East 42nd Street, New York, NY 10017-5391.

Advertiser's Index

*RAC stands for **Reader Action Card.** For further information on these advertisers, please circle the RAC number on the Reader Action Card elsewhere in this issue. This index has been compiled as a service to our readers and advertisers. Every precaution is taken to ensure its accuracy, but the publisher assumes no liability for errors or omissions.

This box contains the world's finest motorized linear positioner. And the test results to prove it.

At Klinger, we go to an incredible amount of trouble to eliminate any eccentricity errors in the motion of our motorized linear stages. In fact, you might think we're a bit excessive, or eccentric, ourselves.

For example, we insist that every Klinger motorized stage be thoroughly tested and calibrated before shipment. These tests can take more than an hour each time.

We test under computer control using a laser interferometric system. Then we print the test results and pack them in the box with every linear stage. We'd like the proud owner of one of our stages to appreciate what a special product he holds in his hands.

We know of no other manufacturer who goes to so much trouble and expense to test their products' precision. Perhaps that's because no other manufacturer goes as far as Klinger to make their products so precise in the first place.

MAKING PERFECT LEAD SCREWS.

The incredible accuracy of a Klinger motorized linear stage begins with the lead screw drive system.

Unlike other companies, Klinger manufacturers its own lead screws. We begin with heat-treated steel and diamond correct the threads so the profile and pitch – the distance of travel per screw revolution – approach perfection. This not only insures accuracy, it reduces wear and backlash. Our unique drive nut is matched to the screw and incorporates an ingenious design for uncoupling any remaining eccentricity in the screw from the moving carriage, reducing wear and improving long-term performance.

KLINGER PRECISION HAS NEVER BEEN SO AFFORDABLE.

Because Klinger engineers and technicians have gone to so much trouble in the design and manufacturing processes, these linear stages will improve the accuracy of any extremely precise application. Including ultra-fast laser systems, optical breadboards, and laser machining of metals, ceramics or semiconductors.

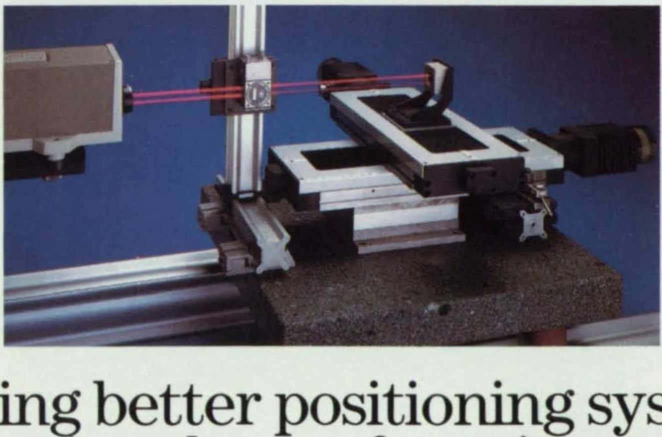

What's more, Klinger will modify any stage to operate in unusual environments. In high magnetic fields, we can use non-magnetic materials and treat surfaces to reduce reflections in laser laboratories. And our stages have demonstrated their accuracy and durability even at liquid Helium temperatures and in high vacuums.

We'll also provide adaptor plates for any Klinger product to accommodate either metric or English mounting holes.

Right now, Klinger products are priced more competitively than at any time in our company's history.

To learn more about the thousands of Klinger micropositioners and systems, send for our free micropositioning handbook. Write or call Klinger Scientific Corporation, 999 Stewart Avenue, Garden City, NY 11530. (516) 745-6800.

KLINGER SCIENTIFIC

Building better positioning systems, piece by perfect piece.

U.S.A. Headquarters: 999 Stewart Avenue, Garden City, NY 11530 (516) 745-6800.
Regional Offices: Northern California (415) 969-0247; Southern California (714) 999-5088. Worldwide distribution network: Contact Micro-Controle, Z.I. de St. Guenault, B.P. 144, 91005 Evry Cedex, France. Tel.33(1)64.97.98.98. FAX 33(1)60.79.45.61.

Circle Reader Action No. 368

NON-DESTRUCTIVE TESTING: NOBODY ELSE OFFERS SO MANY WAYS TO LISTEN.

The extensive use of composite parts in the aerospace industry has created a need for fast, reliable, cost-efficient methods of testing.

As a major user of composites, McDonnell Douglas had reason to become a leader in ultrasonic testing.

We've developed four highly effective, state-of-the-art ultrasonic testing systems for our own needs. These systems are now available to you.

AUSS-IV, our fourth-generation Automated Ultrasonic Scanning System, is a computer-controlled machine and data handling system that automatically checks parts for anomalies.

AUSS-V, presently under development, will add totally new robotic, data imaging, and computer automation dimensions to ultrasonic testing.

ADIS, our Advanced Data Acquisition, Imaging, and Storage System, can update existing inspection units to provide state-of-the-art data acquisition, imaging, and plotting capabilities. Other features include depth measurements, cross sections, and histograms.

And MAUS, our Mobile Automated Ultrasonic Scanner, allows fast, in-place inspection of composite parts. It can scan the surface of compound curvatures without any special attachments.

To find out more about our systems, and how they can help you increase productivity while reducing costs, call or write:
McDonnell Aircraft Company,
Dept. 080, P.O. Box 516,
St. Louis, MO 63166
(314) 232-7454

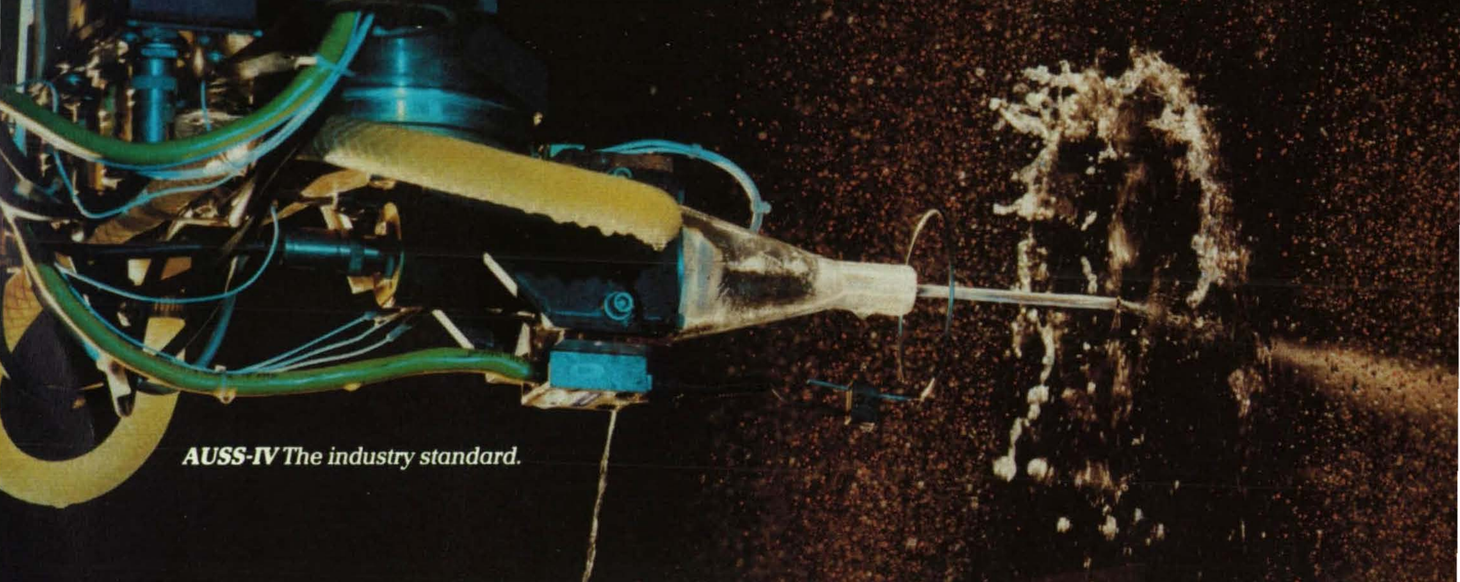

***AUSS-IV** The industry standard.*

***AUSS-V** Adds new dimensions to ultrasonic testing.*

***ADIS** Updates existing inspection units.*

***MAUS** Provides fast, in-place inspection of composite parts.*

MCDONNELL DOUGLAS